

NORTHWESTERN UNIVERSITY

Investigation into the Role of Zinc Regulation in Germline Development in *Caenorhabditis elegans*

A DISSERTATION

SUBMITTED TO THE GRADUATE SCHOOL
IN PARTIAL FULFILLMENT OF THE REQUIREMENTS

for the degree

DOCTOR OF PHILOSOPHY

Field of Interdisciplinary Biological Sciences

By

Adelita D. Mendoza

EVANSTON, ILLINOIS

December 2017

© Copyright by Adelita Dolores Mendoza 2017

All Rights Reserved

ABSTRACT**Investigations into the Role of Zinc Regulation in Germline Development in *Caenorhabditis elegans***

Adelita D. Mendoza

The purpose of the egg is to give rise to offspring in sexually reproducing organisms. Zinc thresholds became connected to egg quality from initial breakthrough discoveries in *M. musculus* which demonstrated that large-scale zinc fluxes occur during meiotic maturation, and these fluxes are required to maintain female egg viability. Numerous reproductive processes are conserved in multiple areas of the phylogenetic tree, thus we hypothesized that large-scale zinc fluxes are a conserved characteristic that is required for female egg viability in the invertebrate *Caenorhabditis elegans*. *C.elegans* are a powerful model system to conduct zinc studies because they possess a simple reproductive system and provide the ability to easily harvest and visualize developing eggs. Initial experiments demonstrated that hermaphrodites cultured under zinc insufficient conditions produced fewer oocytes which resulted in a reduced brood size. Oocytes maturing in vitro under zinc insufficient conditions were unable to extrude the second polar body at the end of Meiosis II, resulting in aberrant pronuclear formation, hyperploidy, spindle defects and abnormal cytokinesis. These combined defects resulted in cell cycle arrest at various time-points between pronuclear migration and the 2-cell mitotic stage. These findings provided the basis for uncovering the presence of zinc fluxes in maturing *C. elegans* oocytes. Utilizing the combined approaches of X-ray Fluorescence Microscopy and fluorescence imaging with the novel zinc sensor ZincBy-1, we discovered that *C. elegans* zygotes exhibit large-scale zinc

fluxes during meiotic progression at stages similar to mouse, with influx occurring after fertilization from Metaphase I to Metaphase II. Efflux occurred from Anaphase II through Pronuclear Fusion, after which point zinc levels remained steady through the 2-cell stage. XFM data of total zinc corresponds to the changing levels highlighted by ZincBy-1. Large-scale zinc fluxes were restricted to zygotes during meiotic progression, as we did not detect this activity during oocyte maturation or in the distal, loop or proximal regions of the spatio-temporal gonad. Furthermore, zinc sequestration at the influx stage induces developmental abnormalities including retraction or retention of the second polar body, hyperploidy, and mitotic spindle defects that ultimately lead to cell cycle arrest. When I tracked zinc movement throughout meiotic maturation, I discovered that labile zinc is first present in the cytoplasm during influx through Metaphase II and then continuously exits the cytoplasm into multiple eggshell layers during efflux from Anaphase II through pronuclear fusion. Combined these results support that the hypothesis that dynamic zinc fluxes are conserved between *C. elegans* and mammals during meiotic maturation. However, key details revealed that zinc regulation in *C. elegans* diverges from *M. musculus*. First, in *C. elegans*, fertilization occurs before zinc influx is initiated, however fertilization does not occur prior to influx in mouse. Second, zinc efflux occurs independently of meiotic arrest in *C. elegans*, unlike mouse where Metaphase II arrest occurs prior to the zinc spark. Collectively, my studies in *C. elegans* have demonstrated that zinc availability strongly impacts oogenesis, proper meiotic spindle assembly and cytokinesis. Zinc fluxes are a key aspect for proper meiotic progression. Zinc influx occurs during a critical developmental window during early meiosis, where zinc ion absorption increases by 470%. Without accrual of adequate zinc during this period, the maturing oocyte cannot properly complete meiosis and is inviable.

ACKNOWLEDGEMENTS

I would first and foremost like to thank my core Thesis advisors, Thomas V. O'Halloran, Teresa K. Woodruff, and Sadie M. Wignall. Tom immediately welcomed me into the lab, recognized my abilities and nurtured me as a budding scientist, despite me being a Biologist in a Chemistry lab. His constructive criticism, and guidance were always available. I also appreciate his strong sense of adventure, and ability to take risks, as this matched my personality as well, and therefore, I didn't get the reins pulled on me too hard. This was a big confidence builder for me. Teresa is such a pillar of the reproductive science community. Through her actions, she became an immediate role model for me, as through her I could see just how far I can fly as a scientist. I am honored that she provided me with practical guidance, and a positive outlook toward my work. SOMEONE THAT IMPORTANT THINKS HIGHLY OF ME. Wow. Sadie is a rising star in her field, and having someone on an upward trajectory certainly takes you with them. I thank Sadie for being a voice of reason in the madness of graduate school, and for making worm science fun. I spent the majority of my time in Tom's lab as the only worm person to study zinc, and without Sadie I wouldn't have a proper worm community at my disposal or known just how rad working with *C. elegans* are! I kept my eye on how Sadie carried herself as young faculty at Northwestern, and I suspect that I will think of her when I (hopefully!) run my own lab one day. In situations I may think, "What would Sadie do?". I affectionately call my three mentors, my TTS, and they ALL believed in me the whole time.

My committee members were all such a great help to me in helping me become a strong and thoughtful scientist, your words of wisdom will always stick with me. Thank you so much Neil Kelleher and Eric Weiss!

As I said before, I am a Biologist in a chemistry lab, which meant I needed to learn more about inorganic chemistry, and related techniques. Enter Team Zinc. Emily Que (now a professor at UT, Drew Nowakowski, Seth Garwin, Amanda Bayer, Manon Isaac, Stephen Allen, and Galyah Boneh all had a hand in helping me grow and challenge how I think about zinc biology. They were all like an extended family to me (with similar dynamics as most real ones!) and I certainly would not be here without them. Thanks for the science and the camaraderie! Aaron Sue, showed up near the end, but it was nice having another worm person in the lab. I think I grew exponentially just from being around him and picking his brain about worm biology. Janelia was a blast, and we'll always have the cafeteria, Jeremy the Blue Heron and Louie the crazy crayfish. I think combined, we were the weirdest entity the lab has ever seen. Plus, there were the Game of Thrones conversations we had in the office! Eric Wagner, you too!! So much fun! So many fan theories and hypothesis! I will miss you two when season 8 rolls around. To the rest of the lab, thank you for sitting through and contributing during my group meetings and celebrating with me when I published my first paper. That was a doozy! So many wonderful events happened to the lab members during my time. Engagements, weddings, births and various accolades- I am so happy to have been with you all for these events. Did I ever say that I was glad the gefilte fish was retired? I am. Both of the O'Halloran lab coordinators have also been tremendous in helping me. Before Jenna Ter Molen left to New York she always had chocolate on her desk, was very good at keeping track of Tom, and checking my grammar. Now Sandy Siepka works in a similar

capacity and has offered a tremendous amount of advice and time spent helping me prepare documents and helping me finish my Ph.D. She is a boss-lady.

I need to thank the Wignall lab for their role in shaping my growth. The students in her lab are class acts, and so good at what they do and are very enthusiastic about their research. Thank you specifically, to Ian Wolf, Tim Mullen and to former Wignall lab members Chrissy Muscat and Mike Tran for training me while I was a neophyte second year.

Thank you to my collaborators at Argonne National Laboratory, Stefan Vogt, Olga Antipova, and former staff Sophie Charlotte Gleber and David Vine. Before I began working with them my knowledge about X-Ray physics was ZERO, and now I am happy to say that I am a Biologist with working knowledge about how X-rays tell us how much metals are in cells. They are all brilliant individuals and I am in awe of all of them.

Thank you to staff at the Northwestern University Facilities, specifically Jessica Hornick at BIF and Keith MacRenaris at QBIC. Jessica is so friendly and extremely knowledgeable about fluorescence microscopy and she taught me so much about how to make beautiful images.

Thanks for repeatedly reminding me to turn the key to turn on the microscope! Keith is a fun guy who knows a lot about ICP-MS, which was great because I knew nothing about this technique or how to do the calculations for it when I started at Northwestern. Thanks for your help, kiddo.

I am also grateful to have been a part of multiple communities at Northwestern. The reproductive science community was really special, and learning about the diverse array of studies involved in reproduction was mind-blowing. The faculty are all top-notch researchers and I am deeply appreciative that you attended my own talks, and provided feedback for my work, in particular Kelly Mayo and Francesca Duncan. The worm community at Northwestern is so collegial, I

knew I could count in specific members from other labs to assist me with my experiments, including Renee Brielman and Sue Fox from the Morimoto lab, and Eric Andersen.

I have been fortunate to be a member of the SACNAS community and the Chicago contingency has been amazing! Thank you, Traci for finding me at SACNAS, and encouraging me to apply to Northwestern, and for further support after I was accepted as the Associate Director of IBiS and later is our SACNAS chapter advisor. You made it so easy and natural for me to be present at Northwestern early on and that was so important for my success. Thank you, Toni Gutierrez for being my next SACNAS advisor and mentor and for listening to me talk about how tricky it can be as a Latinx scientist. I also would like to thank all of my friends and mentors from the other SACNAS chapters in Chicago including Jesús Pando, Pam Geddes, Joe Hibdon, Lucia Rothman-Denes, and Jorge Cantú. Their very presence as Ph.D. holders in their respective fields, demonstrates to me every day that I belong in science, that I can make my mark in my chosen field and that I will be celebrated for who I am as a brown-faced woman.

In my final months at Northwestern I have been frequently reflecting on how my childhood experiences influenced my approach to research. Therefore, I have to thank two of my earliest mentors and role-models from childhood, Dr. Tammy Maldonado and Dr. Levi Crespín. Through their mentorship as my instructors they taught me lessons about discipline, self-control and how to push through challenging times. They normalized for me that Latinos can be Ph.D. holders from an early age.

I need to thank my family who prepared me for a life of hard work and discipline. They never let me quit anything in my life, and always pushed me to be a high achiever and to never give up or make excuses. They ingrained in me early a strong work ethic, and a strong knowledge about the challenges I would face growing up as a brown girl, and that I would always have to jump

through many hoops to get what I want in life. It has served me well in graduate school. I also would like to thank my in-laws who always ask about my work and my progress and who have supported me since I met my husband. Even the small things matter to me. Finally, I would like to thank my husband, Victor who has watched me develop through nearly all of graduate school. He has seen the challenges, the failures, and the successes. No matter where I was at, or how I felt, he always made sure that I knew in my heart that he loved me and that I deserve everything I dreamed of and more.

TABLE OF CONTENTS

ABSTRACT	3
ACKNOWLEDGEMENTS	5
TABLE OF CONTENTS	10
LIST OF FIGURES AND MOVIES	13
LIST OF TABLES	21
CHAPTER 1: GENERAL INTRODUCTION	22
Oocyte Maturation in Metazoans: A Comparison	24
Prophase I Arrest	24
Meiotic Progression	25
Metaphase II arrest & Cell Cycle Re-entry	26
Activation	26
Zinc is a Regulator of Oocyte Maturation in Metazoans	27
Maturing eggs in Metazoans undergo zinc fluxes	27
Manipulating zinc levels in maturing oocytes disrupts normal meiotic progression	29
Zinc availability impacts major transition stages during oocyte maturation	31
Current Proposed Models for zinc regulation of oocyte maturation in mouse	32
Caenorhabditis elegans: A Robust Model System for understanding the role of	33

Zinc fluxes in oocyte-to-embryo transitions	
<i>C.elegans</i> hermaphrodite germline is organized within the spatio-temporal gonad	34
Early Oocyte Maturation in <i>C. elegans</i>	34
Meiotic Divisions- Late Stage Prophase I through Meiosis II	36
Transition from Meiosis to Mitosis	38
Eggshell establishment in <i>C. elegans</i>	38
Scope of Thesis	39
CHAPTER 2: ZINC AVAILABILITY DURNG GERMLINE DEVELOPMENT	43
IMPACTS OOCYTE DEVELOPMENT	
Abstract	43
Introduction	44
Methods and Materials	46
Results	53
Discussion	61
CHAPTER 3: ZINC FLUXES REGULATE MEIOTIC PROGRESSION IN	67
MATURING <i>C. ELEGANS</i> OOCYTES	
Abstract	68
Introduction	69
Methods & Materials	72
Results	79
Discussion	91
CHAPTER 4: GENERAL DISCUSSION	100

REFERENCES	119	12
APPENDIX A: SUPPLEMENTARY FIGURES FOR ZINC AVAILABILITY DURNG GERMLINE DEVELOPMENT IMPACTS OOCYTE DEVELOPMENT	130	
APPENDIX B: SUPPLEMENTARY FIGURES FOR ZINC FLUXES REGULATE MEIOTIC PROGRESSION IN MATURING <i>C. ELEGANS</i> OOCYTES	138	
APPENDIX C: FUTURE DIRECTIONS	150	
TABLES	152	
CURRICULUM VITAE	156	

LIST OF FIGURES, AND MOVIES

Figure 1.1 *C. elegans* are hermaphrodites and males

Figure 1.2 *C. elegans* reproduction: Oocyte maturation & fertilization

Figure 2.1A Schematic of animals cultured under control and zinc insufficient conditions

Figure 2.1B TPEN impacts brood size development

Figure 2.1C Brood size reduction by TPEN is dose dependent

Figure 2.2A Reduced brood size by TPEN is rescued by zinc

Figure 2.2B Brood size is not impacted by the copper chelator ammonium tetrathiolmolybdate

Figure 2.2C Brood size is not impacted by the copper chelated Neocuproine

Figure 2.3A Zinc insufficiency impacts oocyte production

Figure 2.3B Fluorescence images of oocytes in the gonad in control and TPEN conditions

Figure 2.4A Brood size is reduced when oocytes are zinc insufficient, and not sperm- mating hermaphrodites with males

Figure 2.4B Brood size is reduced when oocytes are zinc insufficient, and not sperm- mating feminized worms with males

Figure 2.5A Zinc insufficiency does not impact sperm production in males

Figure 2.5B DAPI staining of sperm in control and ZI conditions

Figure 2.6A Normal spindle morphology during meiotic progression in controls

Figure 2.6B Prolonged zinc insufficiency induces spindle defects in isolated zygotes during meiotic progression

Figure 3.1A ZincBy-1 fluorescence distribution in Metaphase I, Metaphase II and 2-Cell stage zygotes

Figure 3.1B XFM maps of Fe, Cu and Zn in maturing *C. elegans* oocytes

Figure 3.1C Total atom counts for Fe, Cu and Zn during oocyte maturation

Figure 3.2A Brightfield and XFM maps of isolated gonads in control (NGM-C) and TPEN treated (NGM-TPEN) gonads

Figure 3.2B Total atom counts for Fe, Cu and Zn in isolated gonads

Figure 3.2C Brightfield and XFM maps of oocytes

Figure 3.2D Total atom counts for Fe, Cu and Zn in oocytes

Figure 3.2E ZincBy-1 fluorescence intensity in oocytes imaged *in vivo*

Figure 3.2F Normalized fluorescence quantification of oocytes imaged *in vivo*

Figure 3.3A ZincBy-1 fluorescence distribution during meiotic progression

Figure 3.3B ZincBy-1 fluorescence intensity/volume during meiotic progression

Figure 3.3C ZincBy-1 fluorescence images of Prometaphase II versus 2-cell stage zygotes

Figure 3.3D Gray scale fluorescence intensity comparison of cytoplasm in Prometaphase II versus 2-cell stage zygotes

Figure 3.4A A model comparison of zinc fluxes in *C. elegans* and *M. musculus*

Figure 3.4B A model demonstrating the fate of zygotes exposed to zinc insufficiency long-term

Figure 3.4C Proposed pathway for ejected zinc in *C. elegans*

**APPENDIX A: SUPPLEMENTARY IMAGES: ZINC AVAILABILITY DURING
GERMLINE DEVELOPMENT IMPACTS OOCYTE DEVELOPMENT**

A.1 Percentage of hatched embryos in control versus ZI conditions

A.2 Eating behavior in control versus ZI conditions

A.3 Percent of worms eating on control versus ZI plates

A.4 Brood size in worms grown on plates with TPEN/DMSO or TPEN/MeOH

A.5 Sperm counts in hermaphrodites in control versus ZI growing conditions

A.6A Brightfield images of GFP::tubulin & GFP::H2B histone in control versus ZI embryos with inappropriate cytoplasmic pinching around the second polar body

A.6B Fluorescence images of GFP::tubulin & GFP::H2B histone in control versus ZI embryos with inappropriate cytoplasmic pinching around the second polar body

A.7A Brightfield and fluorescence images of control embryos at pronuclear migration

A.7B Brightfield and fluorescence images of GFP::tubulin & GFP::H2B histone in zinc insufficient embryos with inappropriate cytoplasmic pinching

A.7C Brightfield and fluorescence images of GFP::tubulin & GFP::H2B histone in zinc insufficient embryos with inappropriate cytoplasmic pinching

A.8.1A Movie of meiotic progression in GFP controls from TII to pronuclear meeting

A.8.1B Movie of meiotic progression in GFP controls from pronuclear meeting to 2-cell

A.8.1C Movie of meiotic progression in GFP ZI zygote from Prometaphase II to Anaphase II

A.8.1D Movie of meiotic progression in GFP ZI zygote from Anaphase II to 2-cell with extra pronucleus

A.9.1A Movie of meiotic progression in GFP controls from Anaphase I to pronuclear formation

A.9.1B Movie of meiotic progression in GFP controls from pronuclear formation to 2-cell

A.9.1C Movie of meiotic progression in Brightfield controls from Anaphase I to pronuclear formation

A.9.1D Movie of meiotic progression in Brightfield controls from pronuclear formation to 2-cell

A.9.2A Movie of meiotic progression in GFP ZI zygote in pronuclear formation with abnormal cytoplasmic pinching near the polar body

A.9.2B Movie of meiotic progression in GFP ZI zygotes in pronuclear formation to pronuclear meeting with abnormal cytoplasmic pinching near the polar body

A.9.2C Movie of meiotic progression in GFP ZI zygotes in pronuclear meeting to 2-cell with abnormal cytoplasmic pinching near the polar body

A.9.2D Movie of meiotic progression in Brightfield ZI zygotes in pronuclear formation with abnormal cytoplasmic pinching near the polar body

A.9.2E Movie of meiotic progression in Brightfield ZI zygotes in pronuclear formation to pronuclear meeting with abnormal cytoplasmic pinching near the polar body

A.9.2F Movie of meiotic progression in Brightfield ZI zygotes in pronuclear meeting to 2-cell with abnormal cytoplasmic pinching near the polar body

A.10.1A Movie of meiotic progression in GFP control zygotes

A.10.1B Movie of meiotic progression in GFP control zygotes from pronuclear migration pronuclear meeting

A.10.1C Movie of meiotic progression in GFP control zygotes from pronuclear meeting to 2-cell

A.10.1D Movie of meiotic progression in Brightfield control zygotes

A.10.1E Movie of meiotic progression in Brightfield control zygotes from pronuclear migration pronuclear meeting

A.10.1F Movie of meiotic progression in Brightfield control zygotes from pronuclear meeting to 2-cell

A.10.2A Movie of meiotic progression in GFP ZI zygotes from AI to PMII

A.10.2B Movie of meiotic progression in GFP ZI zygotes from PII to AI

A.10.2C Movie of meiotic progression in GFP ZI zygotes from abnormal AII arrest and abnormal cytoplasmic pinching

A.10.2D Movie of meiotic progression in Brightfield ZI zygotes from AI to PMII

A.10.2E Movie of meiotic progression in Brightfield ZI zygotes from PII to AII

A.10.2F Movie of meiotic progression in Brightfield ZI zygotes from abnormal AII arrest

**APPENDIX B: SUPPLEMENTARY IMAGES: ZINC FLUXES REGULATE MEIOTIC
PROGRESSION IN MATURING *C. ELEGANS* OOCYTES**

- B.1** Validation of zinc binding to ZincBy-1 in isolated oocytes
- B.2A** Ratios of Fe/P during oocyte maturation
- B.2B** Ratios of Cu/P during oocyte maturation
- B.2C** Ratios of Zn/P during oocyte maturation
- B.3A** Ratios of Fe/S during oocyte maturation
- B.3B** Ratios of Cu/S during oocyte maturation
- B.C** Ratios of Zn/S during oocyte maturation
- B.4A** XFM map of an isolated gonad in TPEN treated animals
- B.4B** Gonad size comparison between control and TPEN treated animals
- B.5** Total Fe, Cu, and Zn per gonad region
- B.6A** Ratios of Fe to P and S from gonads in control and TPEN treated animals
- B.6B** Ratios of Cu to P and S from gonads in control and TPEN treated animals
- B.6C** Ratios of Zn to P and S from gonads in control and TPEN treated animals
- B.7A** Total Fe iron per gonad regions in control and TPEN treated animals
- B.7B** Total Cu iron per gonad regions in control and TPEN treated animals
- B.7C** Total Zn iron per gonad regions in control and TPEN treated animals
- B.8A** Total Fe/ROI in oocytes
- B.8B** Total Cu/ROI in oocytes
- B.8C** Total Zn/ROI in oocytes
- B.9A** Total Fe, Cu and Zn to P ratios in oocytes

B.9B Total Fe, Cu and Zn to S ratios in oocytes

B.10 Validation of zinc binding to ZincBy-1 in isolated gonads

B.11A *In vivo* Brightfield and fluorescence images of ZincBy-1 in oocytes

B.11B ZincBy-1 fluorescence % in oocytes

B.12A Movie of ZincBy-1 fluorescence during oocyte maturation from Metaphase I to 2-cell

B.12B Movie of GFP::tubulin and GFP::H2B fluorescence during oocyte maturation from Metaphase I to 2-cell

B.12C Movie of merged ZincBy-1 and GFP::tubulin and GFP::H2B fluorescence during oocyte maturation from Metaphase I to 2-cell

B.13A Movie of ZincBy-1 fluorescence during mitotic divisions from the 2-cell to 8-cell stage

B.13B Movie of GFP::tubulin and GFP::H2B fluorescence during mitotic divisions from the 2-cell to 8-cell stage

B.13C Movie of merged ZincBy-1 and GFP::tubulin and GFP::H2B fluorescence during mitotic divisions from the 2-cell to 8-cell stage

B.14 Movie of ZincBy-1 accumulation in the eggshell region

B.15 Movie of ZincBy-1 fluorescence during meiotic progression post-buffer rinse

APPENDIX C: FUTURE DIRECTIONS FIGURES

C.1 Predicted zinc finger sites within the MRCK-1 protein sequence

LIST OF TABLES

T2.1 Fe, Cu and Zn content of NGM plates

T3.1 Total P, Fe, Cu and Zn content during oocyte maturation

T3.2 Total P, Fe, Cu and Zn content in oocytes

T3.3 Percent increase of zinc influx in metazoans

CHAPTER 1
GENERAL INTRODUCTION

The egg is specialized cell type whose purpose is to give rise to progeny in sexually reproducing organisms. The production of a healthy, viable egg requires temporal coordination of a number of conserved molecular processes and cell signaling pathways.

This Thesis introduces zinc as a regulator of proper germline formation, and the oocyte to embryo transition in the invertebrate, *Caenorhabditis elegans*. Large scale movements of zinc during meiotic progression have recently been shown to be essential for the maturation of mammalian oocytes into viable eggs. Other types of zinc fluxes have also been shown to be required for a fertilized mammalian egg to complete meiosis and progress into a viable embryo. *C.elegans* serves as an ideal model system for understanding the molecular mechanism by which these zinc fluxes control the meiotic cell cycle.

In this thesis, I first characterize several of the features of these regulatory zinc fluxes that are conserved during oocyte maturation. I have also found several mechanistic features of zinc regulation that differ from other metazoans. My central hypothesis is that *C. elegans* zygotes utilize large-scale zinc fluxes to advance meiotic progression during oocyte maturation, and like mammalian systems, perturbing zinc availability at specific stages in the cell cycle will render the oocytes inviable. In this Chapter, I will review the state of zinc ion regulation in the maturing egg in other metazoans, and in the *C. elegans* germline. I will then summarize my findings on the roles of zinc availability on oocyte formation, and then briefly outline how zinc fluxes during the oocyte to embryo transition. In this Chapter I will provide an overview of the established roles of zinc fluxes in egg biology and frame the findings of my dissertation research in the context of several of the open questions in the field concerning the mechanism of meiotic cell cycle control. Finally, I will speculate on candidate mechanistic players that rely on zinc availability in regulating oocyte maturation in *C. elegans*.

Oocyte Maturation in Metazoans: A comparison

Prophase I arrest

In all animals, oocytes undergo a prolonged Prophase I arrest. During this period, the oocyte accumulates maternal factors, such as mRNAs, subcellular organelles, and macromolecules (1). Arrest spans months in *M. musculus*, or decades in humans (2). Mammalian oocytes maintain Prophase I arrest in part, by low levels of Maturation Promoting Factor (MPF, which consists of Cdk1 and Cyclin B). Both the APC/C and Cdh1(APC^{cdh1}), maintain low MPF levels by reducing cyclin B levels. Cyclic adenosine 3', 5'-monophosphate (cAMP) also contributes to maintaining low MPF levels via activation of protein kinase A (PKA). PKA phosphorylates and activates Wee1, which in turn inactivates Cdc25, a Cdk1 activator (3, 4). Mediators of Prophase I arrest in *X. laevis*, is controversial, as it was initially proposed that progesterone inhibits adenylate cyclase, which lowered cAMP levels, therefore repressing PKA. However, there are conflicting reports on the timing and extent of decreasing cAMP levels, and whether decreasing cAMP levels actually induces Prophase I release (5).

In *C. elegans*, Prophase I arrest is partially maintained by an antagonistic relationship between *lin-41* (abnormal cell LINEage), and *oma-1/2* (Oocyte Maturation defective) signaling. *Lin-41* encodes a Ring finger-B Box-Coiled coil, and is a member of the NHL family of proteins. LIN-41 levels are elevated in the loop region of the gonad and signaling diminishes closer to the spermatheca. *Lin-41* depletion by RNAi induces premature release from Prophase I arrest in the 1 oocyte (6), demonstrating that it is a key factor in maintaining arrest. Prophase I exit is permitted upon MSP (major sperm protein), OMA-1 and OMA-2 signaling upstream from wee-

1.3, a known CDK-1 inhibitor. Combined, these signaling activities prevent premature oocyte maturation and M phase entry (6)

Meiotic progression

Oocyte maturation begins when the oocyte is released from Prophase I in response to a hormonal stimulus: methyladenine in starfish, progesterone in *Xenopus laevis*, luteinizing hormone (LH) in *M. musculus*, and Major Sperm Protein in *C. elegans* (3). MPF activation initiates meiotic progression in most animals. Active MPF phosphorylates downstream targets, which leads to nuclear envelope/germinal vesicle breakdown (NEBD/GVBD), chromosome condensation, and meiotic spindle assembly. The response to LH involves signaling between the oocyte and the surrounding somatic support cells (7). Initiation of meiotic progression results from a.) LH reduction of cAMP via reduction of cGMP signaling in granulosa cells, and b.) inducing gap junction closure between neighboring somatic support cells. Closing gap junctions prevents cGMP signaling from the granulosa cells into the oocyte, which ultimately reduces cAMP hydrolysis and activity (8, 9).

In *C. elegans*, Prophase I release is a result of MSP and MAPK signaling (10). MSP is a signal that originates from the sperm, which are located in the spermatheca. MSP is secreted by vesicle budding, and acts as a ligand and binds to the ephrin receptor, VAB-1 on the oocytes, and receptors in the surrounding somatic sheath cells (11). MSP signals in a gradient-wise manner, where the most mature oocyte receives the strongest signal. MSP also plays a role in initiation of ovulation, fertilization, oocyte growth and cytoskeletal reorganization. MSP signaling to the sheath cells promotes contractions that contribute to ovulation. It does so through MSP activation of G α s (*gsa-1*), which then activates adenylate cyclase, resulting in elevated cAMP levels.

Mutations in *G α s* (*gsa-1*) inhibit oocyte maturation, while overexpression can induce meiotic progression in the absence of sperm. MAPK signaling occurs in the first six oocytes closest to the spermatheca via phosphorylated MAPK-1 (12). MSP and *G α s* signaling from the sheath cells must be activated in order for MAPK signaling to take place. NEBD requires POLO-like kinase 1 (PLK-1) or Cdk1 signaling. Depletion by RNAi results in NEBD defects prior to ovulation. Upstream of Cdk-1, OMA-1 and OMA-2 both function redundantly to promote oocyte maturation (11, 13, 14).

Metaphase II arrest & cell cycle re-entry

In vertebrates, a secondary arrest occurs in Metaphase II. In marine invertebrates such as the starfish, arrest occurs in G1 after Meiosis I and II are complete (3). *C. elegans* do not experience secondary arrest after MSP signals oocyte maturation. In *X. laevis*, and mammals, components of the cyostatic factor MOS/MEK1/MAPK/p90^{Rsk} and the early mitotic inhibitor2 (Emi2) are key to maintenance of Metaphase II arrest (15, 16). Both MOS and Emi2 signaling work together to inhibit the APC/C, and maintain MPF activity.

Activation

An activated egg is capable of transitioning from maternal control of development to zygotic control. After Metaphase II release, the egg is ready to be activated. Activation events include MII release, zona pellucida hardening, meiosis completion, post transcriptional modifications to maternal mRNAs and cytoskeletal rearrangements (17). Fertilization induces calcium signaling, and calcium oscillations that release the egg from Metaphase II. Calcium elevation activates calmodulin-dependent protein kinase I (CaMKII). Despite not having a

secondary arrest point, *C. elegans* also undergo calcium signaling (18, 19). CaMKII has been shown to be required for egg activation. CaMKII $\gamma^{-/-}$ mice are sterile because they are not able to decrease MAPK and MPF activity to allow meiotic resumption (20). *X. laevis* eggs are known to degrade Emi2 upon CaMKII activation. Once Emi2 is degraded, APC/C can target cyclin B and securing for degradation, thus inactivating MPF and releasing arrest.

Zinc is a Regulator of Oocyte Maturation in Metazoans

Oocyte maturation is a process by which the oocyte is released from Prophase I arrest in order to advance through meiosis. Once released from arrest, the oocyte is fertilized and will later become a viable embryo. Zinc ion regulation is a key factor that is involved in proper oocyte maturation. Zinc studies on maturing oocytes span multiple metazoan species, indicating that zinc involvement in germ cell production is an essential factor in promoting egg viability in multiple areas of the phylogenetic tree.

Maturing eggs in Metazoans undergo zinc fluxes

One of the earliest studies concerning zinc effects on embryonic development was conducted in the sea urchin, *Lytechinus pictus*. In this study by H. Timourian, *L. pictus* was utilized in order to study the general effects of zinc on normal embryo development and how it relates to zinc uptake. Utilizing ^{65}Zn , Timourian observed increased zinc uptake in the zygote from the time of fertilization up through the pluteus stage (CPM/ 10^4 eggs). Uptake corresponded to an approximately 600% increase (21). However, treating the developing eggs with excess zinc restricts endodermal and mesenchymal development, creating symmetry abnormalities as well as skeleton deficiencies. Furthermore, Timourian opined upon the concept that zinc was an

"animalizing substance", meaning zinc promotes differentiation of the animal half of the embryo, and restricts the development of structures in the vegetal half. This concept was originally proposed by R. Lallier in 1959, and in this study, was better defined. As an animalizing substance, zinc should exert its effect by interfering with naturally occurring morphogenic factors, transcription, translation and signal feedback mechanisms. Work in *L. pictus* provided early insights into large-scale zinc fluxes over the course of embryo development, and zinc is an element that is integral for proper structure formation.

Changes in total zinc content in developing oocytes were interrogated in later studies with the African frog, *X. laevis*. *X. laevis* oocytes are among the largest known, ranging in size from 50 to 1300 μm , and develop in six stages. During the early oocyte maturation (stages I-III), zinc content increases from 2 to 7 ng/oocyte. Interestingly, in stages IV through VI, the oocyte increases to 70 ng/oocyte, corresponding to a 35-fold increase (22, 23). Zinc was proposed to enter the oocytes via receptor-mediated endocytosis of vitellogenins. In the model proposed by *Falchuck et al.*, vitellogenin fuses with other vesicles and lysosomes, forming vesicular bodies. The oocyte processes this complex into lipovitellin and phosvitin, and phosvitin fuses into the yolk platelets. Egg fraction experiments with ^{65}Zn in stage II oocytes showed localized ^{65}Zn in the cytoplasm, whereas in the more mature stage IV oocyte, zinc movement follows the time course for processing of vitellogenin (23-26). While these studies were conducted before the identification of over 24 different zinc specific transporter proteins, these early experiments in *X. laevis* demonstrated that not only does the developing oocyte acquire large quantities of zinc throughout its development, but distribution of zinc changes over time and can be coupled with yolk protein components.

Another example of a dramatic zinc fluxes can be seen in the zebrafish, *Danio rerio*.

Riggio et al. examined three developmental stages of the oocyte for total zinc content via atomic absorption spectroscopy: stage 1, previtellogenic oocytes, stage 2 vitellogenic oocytes, and stage 3, late vitellogenic oocytes. Oocytes increase in size as they progress, ranging in size from 100 μm to 700 μm in diameter. Stage 1 oocytes contained approximately 30 ng/oocyte, stage 2 contained approximately 60 ng/oocyte, and stage 3 contained approximately 100 ng/oocyte. This corresponds to a 350% increase in zinc from stage 1 to 3. Studies further in embryogenesis determined total zinc quantities in the 2-cell stage (.45 h post-fertilization, appx. 100 ng/embryo), 512-cell stage (2.45 h post fertilization, appx 500 ng/embryo), blastula (3.5 h post fertilization, appx 400 ng/embryo), 30% epiboly (4.45 post- fertilization, 350 ng/embryo), and 50% epiboly (5.25 h post fertilization, appx 150 ng/embryo) (27). In *D. rerio*, we see a similar trend as with *X. laevis*, where total zinc levels increase dramatically in early stages of oocyte maturation.

Like *X. laevis* and *D. rerio*, *M. musculus* also undergoes large-scale changes in total zinc quantities. Initial breakthrough discoveries reported that the maturing oocyte acquires 20 billion total zinc ions (50% increase) during late (final 12-16 hours) oocyte maturation via conserved zinc importers and maternally derived factors, ZIP6 and ZIP10; in contrast to *X. laevis*, zinc has not been reported to complex with a yolk component (28). Following fertilization or parthenogenic activation at Metaphase II, the egg expels 10 billion total zinc ions from the cytoplasm; total zinc denotes the sum of all the zinc ions inside the cell, bound and unbound. Fluorescent probe staining revealed that the egg expels labile zinc pools (ions that are readily exchangeable) enclosed in cortical granules (29) rapidly, in a process known as the “zinc spark”. Zinc sparks have been reported for *M. musculus*, *M. mulatta*, *M. fascicularis* and *H. sapiens* (30,

31); labile zinc denotes ions that are readily exchangeable. In mouse, the “spark” event is exocytosis of zinc loaded vesicles, each of which contain one million zinc ions that fuse with the ooplasmic membrane. One role of the expelled zinc is fibril thickening, which reduces the number of sperm that can bind to the egg, suggesting the spark plays a role in polyspermy block (32).

Manipulating zinc levels in maturing oocytes disrupts normal meiotic progression

The dramatic fluxes observed in mammals during meiotic progression suggested that inhibiting the normal flux pattern may induce cell cycle abnormalities, thus preventing normal egg development. Prolonged exposure of the Germinal Vesicle to TPEN (N, N, N', N'-Tetrakis (2-pyridylmethyl) ethylenediamine) caused a premature Telophase I arrest phenotype, symmetrical cell divisions, and enlarged polar bodies, rendering the eggs inviable in *M. musculus* (33). These phenotypes were all indicators of an impaired transition from Meiosis I to Meiosis II.

Separate experiments demonstrated that when GV-stage oocytes were exposed to TPEN in a transient manner, an induced spontaneous release from Prophase I occurred. This spontaneous release also occurred when *Zip6* or *Zip10* function was knocked down by morpholinos (in 35% of oocytes) and following injection of function-blocking antibodies of ZIP6 or ZIP10 (in 90% of oocytes). Labile zinc visualization with ZincBy-1 revealed the absence of fluorescence in the GV cytoplasm, indicating that labile zinc was not transported into the cytoplasm by ZIP6 and ZIP10, and that knockdown was successful. Germinal vesicle breakdown (GVBD) was also observed 14-16 hours post-morpholino injection, which is also an indicator of meiotic resumption. Both TPEN, and *Zip6* and *Zip10* knockdown induced spontaneous meiotic resumption via the MOS-MAPK pathway (28, 34). Oocytes undergo GVBD, and MOS,

pMAP2K1/2, and pMAPK3/1 were activated in the presence of TPEN. Further support for MOS-MAPK pathway activation was seen when the MAPK inhibitor, U0126 rescued Prophase I arrest in oocytes with Zip6 and Zip10 knockdown.

Zinc availability impacts major transition stages during oocyte maturation

The Telophase I arrest phenotype and inhibition of the Metaphase to Anaphase transition in Meiosis I implicated the involvement of a candidate factor that is involved in mediating this transition. Early mitotic inhibitor 2 (Emi2) is a Cytostatic Factor (CSF) component that interacts with Cdc20 to induce Metaphase II arrest. Prior to Metaphase II arrest, Maturation Promoting Factor (MPF) levels are high, and are only lowered once Ca²⁺ signaling is initiated by sperm; the low levels of MPF then permit APC/C activation after fertilization. Emi2 is required for the transition from Meiosis I and Meiosis II in *X. laevis* and cell lines, and the C-terminal, zinc-binding region (ZBR) is required for APC arrest by Emi2 as this region impairs the association of Cdc20 with the APC/C and inhibits elongation of the ubiquitin chain (35-38).

Emi2 is required for the metaphase to anaphase transition during Meiosis II in mammals and functions independently of the MOS/MAPK pathway - a major difference from early maturation stages. Oocytes matured in the presence of TPEN contained reduced MOS levels, and phosphorylated MAPK1/2. However, the most downstream signaling component, MAPK 3/1 was not phosphorylated, indicating that this pathway was not fully activated in zinc insufficient oocytes. Furthermore, MOS rescue did not rescue disrupted cortical granule distribution. In cumulus denuded oocytes (COC's) 30% were arrested at Telophase I, and 51% had a single chromatin mass with incomplete retention of the midbody. The remaining oocyte contained multiple chromatin masses, or failed to complete cytokinesis. Knockdown of the ZBR in *M.*

musculus oocytes matured *in vitro* in 10 μ M TPEN were unable to properly maintain metaphase arrest and caused formation of an abnormal chromatin mass (no distinct chromosomes visible) instead of a normal MII spindle COC's (39, 40). Collectively, the findings in *X. laevis* and mammals demonstrate that transition stages of meiosis are zinc dependent.

Current Proposed Models for zinc regulation of oocyte maturation in M. musculus

In *M. musculus*, the GV oocyte is maintained in Prophase I arrest prior to oocyte maturation. The luteinizing hormone (LH) surge initiates GV release from Prophase I. After the LH surge, the rapid cAMP decrease promotes meiotic resumption. The decrease in cAMP levels permits increased MPF activity driving meiotic resumption. Zinc influx occurs once the maturing GV oocyte is released from Prophase I, and zinc is taken up into the maturing oocyte through the zinc importers ZIP6 and ZIP10. Active MPF promotes GVBD and progression to Metaphase II, where the egg arrests. During this period the maturing oocyte rapidly acquires 20 billion zinc atom and MPF levels are elevated. High zinc levels are required for Emi2 function, as binding to the zinc binding region (ZBR) permits Emi2 function. Zinc binding to the ZBR prevents activation of the APC/C by blocking Cdc20 activity, resulting in inhibition of elongation of the ubiquitin chain. Metaphase II release occurs upon fertilization, which initiates calcium signaling prior to zinc exocytosis. Calcium oscillations signal MPF degradation, which permits APC/C activation post-fertilization and cell cycle resumption. It is thought that zinc exocytosis leads the decrease in zinc levels, thus preventing binding to the Emi2 ZBR. Zinc is packaged in cortical granules that emanate outward toward the egg cortex.

Caenorhabditis elegans: A Robust Model System for understanding the role of Zinc fluxes in oocyte-to-embryo transitions

The published studies in *X. laevis* and mammals suggest multiple ways that zinc fluxes might control proper cell cycle advancement in maturing oocytes and progression of the fertilized egg into an embryo. My work on the invertebrate *Caenorhabditis elegans* permits new types of interrogation regarding zinc activity and regulation during oocyte maturation. *C. elegans* provide many advantages over other model systems. They produce a high yield of progeny, are translucent and thus ideal for live fluorescent microscopy imaging. They also exhibit a short reproductive lifespan. Harvesting of developing embryos is facile, and imaging can be performed *in vivo* on many well-characterized transgenic animals that express GFP fusion proteins, and mutant animals that restrict or permit specific features (41, 42). There is already a strong body of work established with zinc metabolism studies by which commercial zinc probes and analytical chemistry techniques were used in combination with standard genetics techniques to understand the role of zinc in gut homeostasis, and transcription mechanisms involved in response to high and low zinc levels in the worm (43-50). My germline studies demonstrate that a variety of techniques to interrogate zinc that were first used in other metazoans are completely applicable in *C. elegans*, including the usage of zinc probes, X-Ray Fluorescence Microscopy (XFM), and Inductively Coupled Plasma-Mass Spectrometry (ICP-MS). Because *C. elegans* exist in hermaphrodite and male forms, mating experiments were particularly useful to narrowing zinc depletion phenotypes to oocytes specifically. Unlike zinc studies with other metazoans, I was able to take advantage of working with an entire organism, instead of isolated single cells. This was particularly useful when placing oocyte maturation in context of the reproductive tract, and how the organism obtains its nutrients.

C. elegans hermaphrodite germline is organized within the spatio-temporal gonad

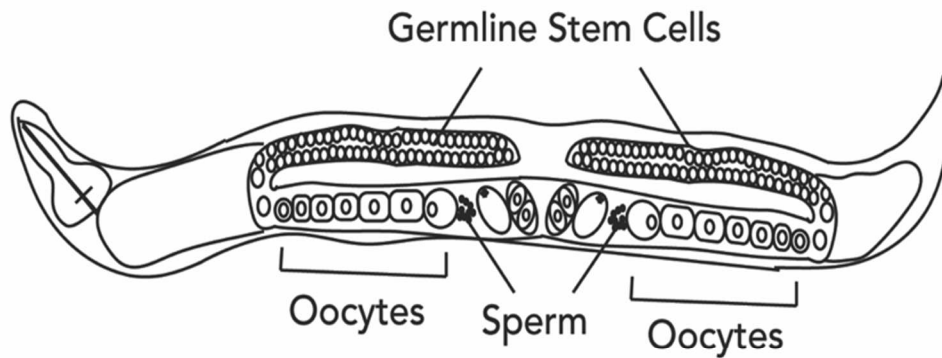
C. elegans are either hermaphrodites (self-fertilizing) or males (Figure 1.1). In hermaphrodites, the germline is contained within a u-shaped tube named the spatio-temporal gonad. The gonad contains three major regions, the distal, loop, and proximal regions, with the nuclei arranged in a syncytium (multiple nuclei within a single cytoplasm). Mitotically-dividing germline stem cells (GSC's) occupy the distal region of the gonad. Nuclei enter meiotic phase and then migrate from the distal region towards the loop region (51). Early in development, the gonad produces sperm that are packaged in a region called the spermatheca, but as the hermaphrodites become adults, they switch to oocyte production. Many of the nuclei undergo apoptosis in the loop region, and those that remain become oocytes in the proximal region where they arrest in Prophase I (Figure 1.2a) (42, 52). Oocytes are produced in an assembly line-like manner, single file. Oocytes increase in maturity as they move closer to the spermatheca and are numbered in descending order. Oocyte formation results from multiple cell signaling activities, including MAP kinase signaling (oocyte growth) (53), *lin-41* signaling in the loop region of the gonad (maintenance of oocyte Prophase I arrest) (6) and secreted Major Sperm Protein (MSP) signaling (nuclear envelope breakdown, rounding of the -1 oocyte, and signal for fertilization) (54). Developing oocytes acquire the maternal components they need to survive, including yolk, and maternal mRNAs (55).

Early Oocyte Maturation in C. elegans

By the time oocytes form, the chromosomes have already experienced DNA duplication and homologous recombination in the germline syncytium, and the fully formed oocytes (4n)

A.

Hermaphrodite



B.

Male

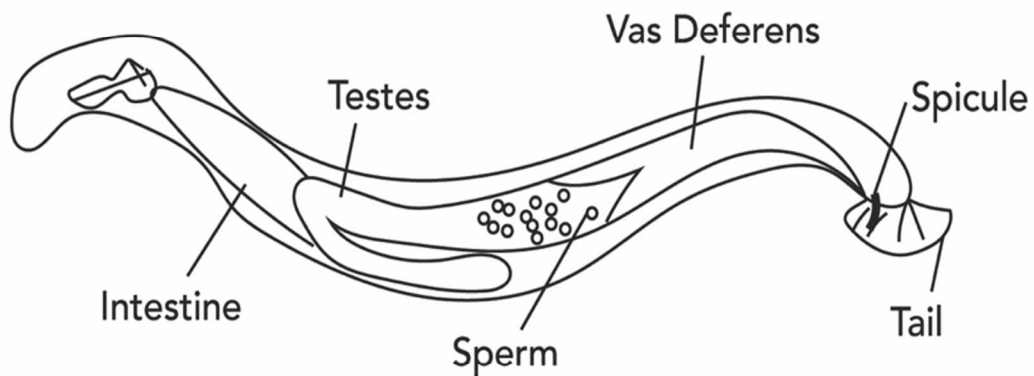


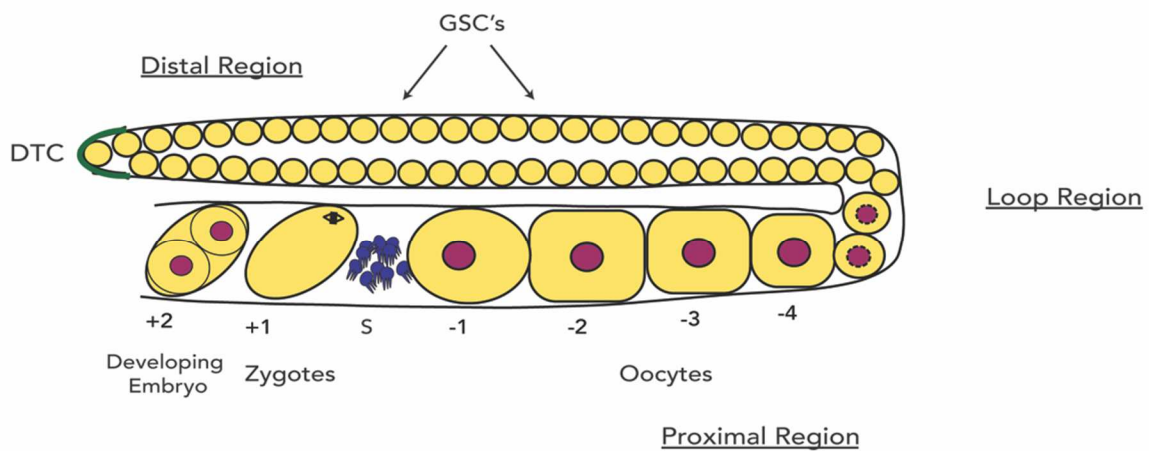
Figure 1.1- *Caenorhabditis elegans* are hermaphrodites or males. (A) Hermaphrodites contain germline stem cells that differentiate into sperm or oocytes in the final larval stage (L4). (B) Males contain only sperm which are also differentiated from germline stem cells.

contain 6 cruciform chromosome bivalents and are arrested in Prophase I. Prior to Prophase I release, the -1 oocyte first undergoes reproducible, hallmark activities, including nuclear envelope breakdown (NEBD, 6 minutes before fertilization), and cortical rearrangement (3 minutes before fertilization). The nucleus in the -1 oocyte migrates distally and away from the spermatheca entry site. A combination of sheath contractions and dilation pull the spermatheca over the -1 oocyte occur just prior to fertilization before ovulation (approximately every 20 minutes) (56).

Meiotic Divisions- Late Stage Prophase I through Meiosis II

During NEBD, microtubules form a cage-like structure around the bivalents, prior to the formation of a multipolar structure. This is followed by coalescence of multiple nascent poles until the bipolar meiotic spindle is formed (57). *C. elegans* meiotic chromosomes are enclosed within lateral microtubule bundles and chromosomes are segregated in a kinetochore independent manner (58, 59). Microtubule nucleation and motor proteins KLP-18/kinesin-12 and MESP-1 sort the minus ends of the microtubules away from the chromosomes in order to form the bipolar spindle and align along the metaphase plate (Metaphase I) prior to separation into Anaphase I. The Metaphase I spindle assembly is oriented parallel to the cortex of the cytoplasm. As the zygote progresses through Anaphase I, the spindle rotates to orient perpendicular to the cortex (60). Progression through Telophase I involves extensive separation of the chromosomes and half of the genome gets extruded in a polar body, signaling the end of Meiosis I, and the zygote is now $2n$ (complete approximately 17 minutes post-fertilization).

A.



B.

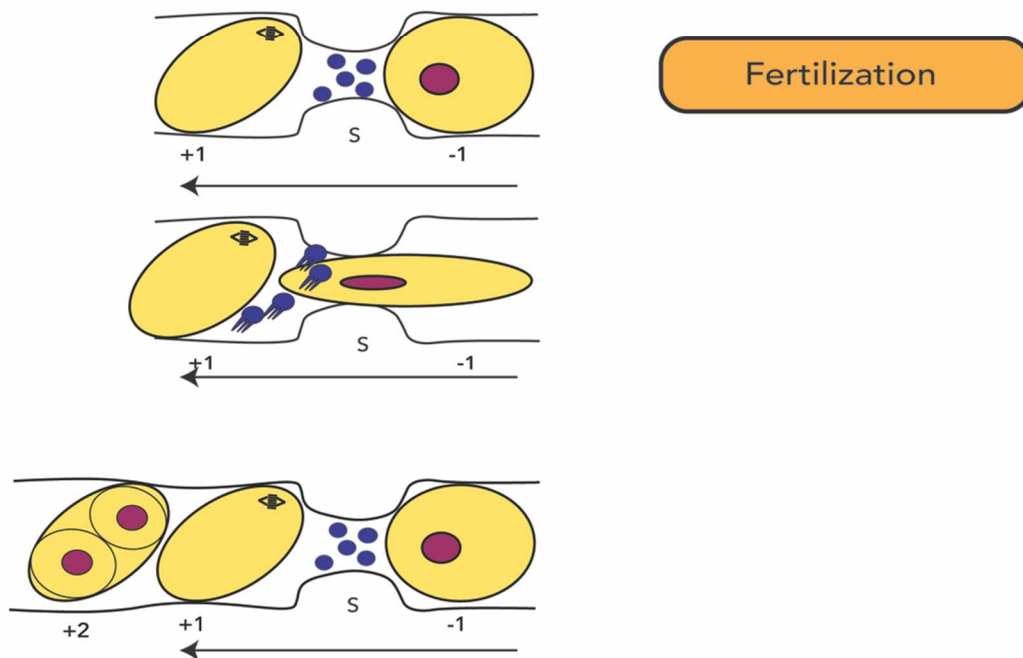


Figure 1.2 *C.elegan* reproduction (A) The spatio-temporal gonad in *Caenorhabditis elegans* is a u-shaped tube containing the Distal Tip Cell (DTC) which generates the germline stem cells (GSC's) in the distal region. The GSC's migrate toward the loop region, where many undergo apoptosis. The remaining GSC's are programmed to become sperm or oocytes in hermaphrodites. The oocytes increase in maturity as they are pushed toward the spermatheca (s). The -1 oocyte is most mature. (B) During fertilization the -1 oocyte undergoes maturation prior to ovulation and fertilization. It is pushed into the spermatheca by the surrounding ovary, and fertilized. The fertilized oocyte becomes the zygote and is now on the other side of the spermatheca and is denoted as +1.

A similar process is involved in Meiosis II, and upon completion the oocyte ploidy is reduced to 1n (complete approximately 26 minutes post-fertilization) (61).

Transition from Meiosis to Mitosis

The first mitotic prophase occurs after completion of Meiosis I and II. During the meiotic divisions, the sperm (1n) pronucleus and centrosome forms in the proximal end of the zygote. After meiosis is complete, the oocyte pronucleus first migrates toward the sperm pronucleus at the cortex, and then both migrate toward the center of the zygote together while their chromosomes condense in preparation for mitosis (10). When they join, the pronuclei membranes fuse (complete approximately 47 minutes post fertilization). Kinetochores assemble and create microtubule attachment sites. Microtubules interact with the chromosomes and the sperm-provided centrosomes and situate them on the metaphase plate (complete approximately 65 minutes post fertilization). Mitotic anaphase next occurs, and chromosomes segregate toward the spindle poles and the spindle poles separate themselves from each other. Cytokinesis occurs when an equatorial cortical contractile ring comprised of actin and myosin II assemble. Microtubules form at the midzone between separating anaphase chromosomes. A cleavage furrow constricts around the midbody to promote membrane fusion and complete cytokinesis and form the 2-cell stage (62).

*Eggshell establishment in *C. elegans**

In the developing zygote, oocyte maturation and eggshell establishment is synchronized. The eggshell is a multi-layer structure that functions as structural support and polyspermy block (chitin layer), regulation of permeability (chondroitin proteoglycan, CPG layer), protects the

embryo from the environment, and maintains embryo osmolarity (peri-embryonic space). Eggshell formation and permeability decreases beginning at Anaphase I and concludes at Anaphase II, with final modifications being made at the 2-cell stage (63, 64). Like mammals, it is formed in part from cortical granules, and is roughly the equivalent of the zona pellucida (65).

Scope of Thesis

Here, we test the hypothesis that zinc availability is a key factor for proper meiotic progression during late oocyte maturation in *C. elegans*. As a means for determining overall oocyte viability, we initially studied brood size as a general indicator of proper germline function under zinc insufficient (ZI) conditions. We determined that ZI reduces oocyte formation *in vivo*, resulting in reduced brood size. Isolated ZI zygotes exhibited polar body extrusion impairments during Meiosis II, including pronuclear migration abnormalities, polar body defects and hyperploidy during the meiosis to mitosis transition.

I also present novel findings for zinc regulation of germline formation and oocyte viability in *C. elegans*. In Chapter 2, I tested the hypothesis that mild zinc limitation by 10 μ M TPEN treatment of isolated zygotes impacts oocyte development. I will discuss how zinc insufficiency impacts oogenesis, brood size reduction, and how we determined these phenotypes arose specifically from zinc depletion. Hermaphrodites raised under zinc limiting conditions (from TPEN exposure) from the final larval stage into adulthood were considered zinc insufficient (ZI). ZI hermaphrodites produced fewer oocytes compared normal ones, and resulted in a reduced brood size in wild type animals. I determined that brood size reduction was specific to oocyte production impairments from mating experiments comparing control versus ZI conditions in hermaphrodites mated with males and with feminized worms mated with males.

The brood size reduction phenotype is corroborated in a publication from Hester et al, 2017, *Journal of Biochemistry and Physiology Part C Toxicology*, and was published in the same issue as my work. Finally, I will discuss improper polar body extrusion during Meiosis II, and how failure to extrude the second polar body results in abnormal spindle morphology, hyperploidy, and abnormal cytokinesis.

In Chapter 3, I tested the hypothesis that *C. elegans* undergo conserved zinc flux patterns during oocyte maturation. As a result of detecting such striking abnormalities from ZI, we next interrogated total zinc and labile zinc quotas in the gonad, and throughout oocyte maturation in order to determine not only if *C. elegans* zygotes displayed a large-scale zinc flux pattern, but also to see if the germline exhibited any dynamic changes as well. Late stage oocytes contained within the proximal gonad acquire increasing concentrations of labile zinc pools, and the most mature, -1 oocyte contains the highest concentration. This is in contrast to total zinc levels, which remain steady throughout the entire gonad. Zinc fluxes are specific to later stages of oocyte maturation, and are not found in other areas of the gonad. Utilizing X-Ray Fluorescence Microscopy (XFM), we uncovered large-scale zinc fluxes during late oocyte maturation. Between the Prophase I and pre-activated zygote stage, we detected a 471% increase in total zinc, and a 34% decrease from the pre-activated zygote stages to the activated egg stage. These dynamic changes were not observed during early oocyte maturation or in other loci in the gonad.

Late stage oocytes undergo dramatic zinc fluxes during meiotic maturation; they accrue large quantities of labile zinc after fertilization, and when the zygote reaches its quota near Metaphase II, it expels labile pools of zinc from the cytoplasm. Both total zinc and labile zinc profiles parallel each other during meiotic progression. I will also discuss labile zinc accumulation in the general eggshell region during zinc efflux. Zinc exocytosis from Metaphase

II onward indicates that zinc exit is not dependent on cell cycle arrest, nor is it initiated by fertilization. Furthermore, zinc accumulated in the general eggshell region during zinc exocytosis may function in a number of ways in the eggshell.

There are a number of evolutionarily conserved elements involved in promoting successful oocyte maturation in metazoans including zinc. Studies in maturing *C. elegans* oocytes revealed that they also engage in zinc fluxes. As with mammals, cell cycle arrest is disrupted with TPEN. These studies add to the current body of knowledge about how zinc regulates meiotic progression in invertebrates.

CHAPTER 2

ZINC AVAILABILITY DURING GERMLINE DEVELOPMENT IMPACTS OOCYTE DEVELOPMENT

The data presented here was published in *Comparative Biochemistry & Physiology Part C, Toxicology*

Abstract

Zinc is an essential metal that serves as a cofactor and structural regulator in a variety of cellular processes, including meiotic maturation. Cellular control of zinc uptake, availability and efflux are closely linked to meiotic progression in rodent and primate reproduction where large fluctuations in zinc levels are critical at several steps in the oocyte-to-embryo transition. Despite these well-documented roles of zinc fluxes during meiosis, only a few of the genes encoding key zinc receptors, membrane-spanning transporters, and downstream signaling pathway factors have been identified to date. Furthermore, little is known about analogous roles for zinc fluxes in the context of a whole organism. Here, we evaluate whether zinc availability regulates germline development and oocyte viability in the nematode *Caenorhabditis elegans*, an experimentally flexible model organism. We find that similar to mammals, mild zinc limitation in *C. elegans* profoundly impacts the reproductive axis: the brood size is significantly reduced under conditions of zinc limitation where other physiological functions are not perturbed. Zinc limitation in this organism has a more pronounced impact on oocytes than sperm and this leads to the decrease in viable embryo production. Moreover, acute zinc limitation of isolated zygotes prevents extrusion of the second polar body during meiosis and leads to aneuploid embryos. Thus, the zinc-dependent steps in *C. elegans* gametogenesis roughly parallel those described in meiotic-to-mitotic transitions in mammals.

Introduction

Zinc is a transition metal that serves as a cofactor and structural regulator in a variety of proteins that participate in numerous cellular processes (66-68). We have shown that fluctuations in total cellular zinc levels play central regulatory roles controlling meiosis in mouse, non-human primate, and human oocytes before and after fertilization (28, 29, 31, 34, 39, 69). In the mouse oocyte, total zinc levels increase by over 50% during meiotic maturation and this accumulation of zinc is required for the oocyte to progress properly to metaphase of meiosis II (33). Previous work has shown that fertilization and parthenogenesis initiate zinc exocytosis from zinc loaded cortical vesicles (29) (30) into the extracellular space through a series of coordinated events known as ‘zinc sparks’ (30). If zinc levels are not reduced, the egg cannot complete meiosis, and the zygote is unable to initiate the mitotic divisions. Therefore, zinc fluxes are fundamental events at several steps in the oocyte-egg-embryo transition, and are critical for mammalian reproduction. Despite these well-defined roles of zinc fluxes during meiosis (70, 71), only a few of the genes encoding zinc receptors have been identified as mediating these switching events in mammals or other model systems to date. Zinc receptors, i.e. macromolecules defined by their ability to move or bind zinc, with known roles in meiosis include the cation transporters ZIP6 and ZIP10 and downstream signaling pathway factors, such as Emi2 (72-75). The nematode *C. elegans* would be an ideal model system for identifying pathway members, especially if readily triggered meiotic phenotypes of zinc depletion can be established. Given that zinc availability has already been established to regulate proper meiotic progression in mammalian oocytes, we test here whether a similar type of inorganic regulation of egg biology might extend further into the phylogenetic tree using the invertebrate, *C. elegans*.

C. elegans exist as two sexes, hermaphrodites and males (73, 76, 77). These worms develop through four larval stages (L1-L4), entering adulthood in approximately 3 days (78). In self-fertilizing hermaphrodites, gonadogenesis completes and meiosis begins in the L4 stage. They first produce sperm and store these gametes in a compartment called the spermatheca, but upon becoming adults, there is a switch to oocyte production (79). At this stage, the remaining meiotic cells in the germline begin maturing into oocytes, which are then fertilized as they pass through the spermatheca, becoming embryos that are laid and hatch (10). Each hermaphrodite produces approximately 300 self-progeny before running out of sperm, but they can produce many more offspring if mated with a male and sperm availability is not limited.

Many features of this system make it ideal for evaluating the regulatory roles of zinc fluxes in reproduction. The hermaphrodite gonad has two arms and each is arranged as a production line, with a population of germline stem cells in the distal region differentiating to enter meiosis, and then forming oocytes in the proximal region, as they move towards the spermatheca (3, 61) (Figure 1.1). Therefore, this spatial-temporal gradient means that all stages of meiosis can be visualized simultaneously within the same worm. Moreover, *C. elegans* are transparent, allowing live imaging of the meiotic and mitotic divisions of the oocyte and embryo, and they are amenable to a wide variety of experimental manipulations. Based on these advantages, we assessed whether zinc availability impacts germline development or oocyte viability in a whole animal model.

Here, we test the hypothesis that growth of the worm under zinc deficient conditions will impair oocyte function and fertility. Zinc availability to both the worm and its food, *E. coli*, can be attenuated by addition of the metal chelator N,N,N',N'-Tetrakis(2-pyridylmethyl)ethylenediamine (TPEN) to the growth medium. TPEN has been employed in a

number of studies of meiosis in isolated mammalian oocytes (30, 39, 70, 71). In order to establish mild zinc limitation in which there is no observable impact on the general physiological status of *C. elegans*, progeny counts were evaluated as a function of TPEN concentration in the growth medium. We found that growth of adults under mild zinc depletion leads to a statistically significant drop in the number oocytes produced. Moreover, acute zinc limitation of isolated zygotes prevents the extrusion of the second polar body and causes chromosome segregation defects, resulting in aneuploid embryos. These results establish a zinc-dependent phenotype in the reproductive axis of *C. elegans* and support the idea that zinc-regulated pathways in meiosis are evolutionarily conserved.

Materials and Methods

Worm strains

EU1067: *unc-119(ed3) ruIs32[unc-119(+)* *pie-1^{promoter}::GFP::H2B*] III; *ruIs57[unc-119(+)* *pie-1^{promoter}::GFP::tubulin*] was used for fluorescence imaging of the meiotic spindle, gamete count, and for generating males (80). N2 (Bristol) wild type strain was used in all brood size experiments, food aversion, and pharyngeal contraction experiments (81). The mutant strain *fog-1(q253)* (82) was used in the mating experiment.

Growth media

Animals were grown on bacterial lawns plated on 6 cm agar plates following standard methods (83) with the following modifications. Plates containing growth media were prepared with a final concentration of 10 μ M TPEN (Sigma Aldrich, St. Louis, MO) to Nematode Growth Media (NGM) (83) (Sigma) prior to pouring the plates. After the plates solidified, 200 μ l of an

overnight growth of *E.coli* strain OP50 in Luria Broth (83) was added and allowed to dry at room temperature. Alternatively, a final concentration of 10 μ M of the copper-specific chelators Neocuproine (Sigma) or Ammonium tetrathiomolybdate (Sigma) were dissolved in ethanol or H₂O, respectively, and were added to the NGM as described above. For rescue experiments, plates were further supplemented with 20 μ M metal salts CuSO₄•5H₂O (Sigma), ZnSO₄•7H₂O (Sigma), FeSO₄•7H₂O (Sigma).

Brood Size Experiments

L4 stage hermaphrodites were picked onto control NGM or zinc insufficient NGM plates (1 worm/plate). Every 24 hours, the worm was transferred to a fresh plate. Progeny were counted 48 hours after the adult was removed from the plate. Progeny were scored from controls (day 1, n=50, day 2, n=43, day 3, n=40, day 4, n= 33, day 5, n=30 hermaphrodites) and zinc insufficient hermaphrodites (day 1, n=52, day 2, n=52, day 3, n=25, day 4, n=22, day 5, n=18). Similarly, brood size experiments were conducted on plates with bacteria killed by UV irradiation, heat exposure (75°C for 1 hour) and 250 μ g/ml Kanamycin (Sigma) (84). For DMSO vehicle: day 1, n=20, day 2, n=19, day 3, n=10, day 4, n=18, day 5, n=19. For TPEN in DMSO: day 1, n=25, day 2, n=20, day 3, n=10, day 4, n=16, day 5, n=15. For methanol vehicle: day 1, n=19, day 2, n=19, day 3, n=18, day 4, n=15, day 5, n=15. For TPEN in methanol: day 1, n=19, day 2, n=11, day 3, n=20, day 4, n=22, day 5, n=11. In the case of the TPEN in methanol group, some worms were stuck between the agar and the plate wall on day 1 and were liberated for later egg laying in the experiment, others were caught in water on the side wall and were also liberated.

Hatching Experiment

N2 animals were synchronized at the L4 stage and placed on either control plates (n=14 adults) or plates with 10 μ M TPEN (n=12 adults). Each group was incubated at 20°C for 24 hours to allow for egg laying. After incubating, the adults were removed and allowed an additional 24 hours for the embryos to hatch. After this time, the number of embryos that hatched were quantified.

Eating Behavior Experiments

Young adult eating behavior was quantified by counting the number of pharyngeal contractions per 30 seconds in control (n= 31) and zinc insufficient groups (n= 29). Food avoidance was quantified as the percent of worms eating (worms on the plate eating/ total worms on plate x100) for control (n=35) and zinc insufficient groups (n=37).

Metal Rescue Experiments

L4 stage hermaphrodites were picked onto control or TPEN plates and incubated at 20°C for 6 hours. From the TPEN group, some were selected to remain on the TPEN plates, while single adults were placed onto the rescue plates, supplemented as described above, and transferred to a fresh plate every 24 hours. Progeny were counted 48 hours after the adult was removed from the plate. For controls: n= 30, 18 hours post rescue, and n= 21, 42 hours post-rescue. For the 10 μ M TPEN group: n= 32, 18 hours post rescue, and n= 25, 42 hours post-rescue. For the Cu rescue group: n=30, 18 hours post rescue, and n= 17, 42 hours post-rescue. For the Zn rescue group: n=25, 18 hours post rescue, and n= 18, 42 hours post-rescue. Finally, for the Fe rescue group: n=27, 18 hours post rescue, and n= 20, 42 hours post-rescue.

Copper chelation

L4 hermaphrodites were picked onto plates supplemented with 10 μ M Neocuproine or 10 μ M ammonium tetrathiomolybdate (AT) and compared to control worms picked onto standard NGM. For Neocuproine we scored progeny for controls on day 1, n=10, day 2 n=10, day 3, n=10, day 4, n= 8, day 5, n=8, and for the chelated group day 1, n=20, day 2, n=19, for day 3, n=18, day 4, n=17, day 5, n=15. For ammonium tetrathiomolybdate, we scored progeny for controls on day 1, n=20, day 2, n=19, day 3, n=18, and for the chelated group day 1, n=23, day 2, n=27, day 3, n=27. Every 24 hours a single worm was transferred to a fresh plate to deposit their offspring. After 2 days the offspring were counted. The ammonium tetrathiomolybdate experiment on day 2 and 3 had more worms because four worms on day 1 were stuck crawling between the plate and the agar and did not lay eggs on day 1. We liberated these worms and allowed them to keep laying eggs for the rest of the experiment.

Gamete counts

L4 stage EU1067 hermaphrodites and adult males were picked onto control and TPEN plates and incubated for 24 hours at 20°C. They were then ethanol fixed and mounted using Vectashield containing 10 μ g/ml Hoechst. Fluorescence images were captured by the Leica DM5500 epifluorescence microscope. Oocytes were scored based on the presence of 6 chromosome bivalents within a distinct nuclear envelope and cellular membrane (10, 85). For the control, we scored n=71 and for hermaphrodites grown on TPEN plates we scored n=78 at L4, and n=32 at L3. Sperm inside the spermatheca were identified with Hoechst (76, 86). We scored n=40 for the control group, and for the hermaphrodites grown on TPEN plates we scored n=35 at L4, and

n=32 at L3. For the male sperm counts, we scored n=19 control males, and n=22 males grown on TPEN.

Production of Males

Males were generated by heat shock in EU1067 animals. Approximately 5 late L4 stage hermaphrodites per plate were incubated at 30°C for 3 hours. After this incubation, worms were returned to 20°C and allowed to produce F1 progeny. Some males were developed from this F1 generation, which were then used to set up matings to produce additional males.

Mating Experiment

Hermaphrodites versus males: Early L4 stage hermaphrodites and males were picked onto either control or zinc insufficient plates to incubate for 24 hours at 20°C. After incubating, the following mating pairs were allowed to mate on control plates for 24 hours:

Control hermaphrodites x control males (n=56 matings)

Control hermaphrodites x zinc insufficient males (n=51 matings)

Zinc insufficient hermaphrodites x control males (n=61 matings)

Zinc insufficient hermaphrodites x zinc insufficient males (n=46 matings)

After mating, adults were removed from the plates and the progeny were counted 24 hours later.

Feminized versus male worms: Early L4 stage *fog-1(q253)* worms were picked onto either control or zinc insufficient plates to incubate 24 hours at 25°C to produce the feminized phenotype. At this restrictive temperature, *fog-1(q253)* mutants do not produce sperm (82), so we refer to them as “females” for simplicity. At the same time, males were also picked onto separate

control or zinc insufficient plates to incubate for 24 hours at 20°C. After incubating, the following mating pairs were allowed to mate for 24 hours:

Control females x control males (n=26 matings)

Control females x zinc insufficient males (n=18 matings)

Zinc insufficient females x control males (n=16 matings)

Zinc insufficient females x zinc insufficient males (n=20 matings)

After mating, adults were removed from the plates and the progeny were counted 24 hours later.

Meiotic Progression time-lapse imaging

Sample preparation: Adult EU1067 hermaphrodites were picked into an 8 μ L drop of egg buffer (87) supplemented with 10 μ M TPEN within a 35mm culture dish with a 10 mm well (World Precision Instruments, Sarasota FL). Zygotes were cut out of the hermaphrodites with a 20-gauge needle (BD). The dish was placed on the microscope stage and embryos in Meiosis II were selected for imaging.

Imaging: Zygotes were imaged on a SP5 II Laser Scanning Confocal Microscope located in the Biological Imaging Facility at Northwestern University. We used the 63x objective with the 488 laser to detect GFP and the HyD detector. Single plane images were captured at 45 second intervals until the zygotes reached the 2-cell stage. We imaged 5 control, and 6 zinc insufficient maturing oocytes. Movies were allowed to progress until cellular features moved out of focus. We then stopped the movies, refocused and resumed filming immediately, thus splitting the movies into separate files. Listed video time frames were based on the start of filming of each segment.

Metal Content of NGM Plates

Inductively Couple Plasma Mass Spectrometry (ICP MS) was performed at Quantitative Biological Instrument Core (QBIC) at Northwestern University. The full content of an NGM plate (10 ml) was dissolved in 5 ml of 3% Nitric acid (Sigma Aldrich, St. Louis, MO) diluted with ultra-pure H₂O (18.2 MΩ·cm) for one hour in triplicate. A multi-element internal standard (CLISS-1, Spex Certiprep, Metuchen, NJ, USA) was then added to produce a final solution of 3.0% nitric acid (v/v) with 5.0 ng/ml internal standard in a total sample volume of 10 ml.

ICP-MS was performed on a computer-controlled (Plasmalab software) Thermo XSeries II ICP-MS (Thermo Fisher Scientific, Waltham, MA, USA) operating in standard mode and equipped with a CETAC 260 autosampler (Omaha, NE, USA). Each sample was acquired using one survey run (10 sweeps) and three main (peak jumping) runs (100 sweeps). The isotopes selected for internal standard analysis were ⁵⁹Co, ^{101,102}Ru, ⁸⁹Y, ¹¹⁵In, and ¹⁶⁵Ho. Total iron, copper and zinc was determined using average values for the respective isotopes (⁵⁷Fe, ^{63,65}Cu, and ^{64,66,68}Zn). Instrument performance was optimized daily through autotuning followed by verification via a performance report (passing manufacturer specifications).

Statistical analysis

The results were depicted as mean and standard error of mean (SEM). The students t- test, and 2-way analysis of variance (ANOVA) were used to evaluate significant differences between control and treatment groups. All statistical analysis was conducted using Graph Pad software from Prism. Values considered statistically significant were below p<0.05.

Results

Zinc insufficiency impacts C. elegans reproduction

To determine if zinc insufficiency impacts *C. elegans* fertility, we picked L4 stage hermaphrodites onto plates containing 10 μM of TPEN, in excess of the chelating agent relative to the total zinc, copper and iron content of the plate (Figures 2.1A, Table1). Hermaphrodites grown on these plates produced smaller broods from days 1 through 3 (Figure 2.1B) compared to those grown on control plates. The dose dependence of TPEN exposure was determined by titrating TPEN in the growth media at 2.5 μM , 5 μM and 10 μM concentrations. As the TPEN concentration incrementally increased, the brood size decreased correspondingly (Figure 2.1C). At TPEN concentrations above 20 μM , adult worms crawled off of the plates. We tested the viability of the eggs that were laid on the TPEN plates by quantifying the number that hatched. Within 24 hours of egg laying by a young adult hermaphrodite, all of the embryos hatched in both control and TPEN groups (Figure A.1). Since *C. elegans* are typically grown on plates with live bacteria as a food source, we next sought to determine if the observed brood size reduction following exposure to 10 μM TPEN might be the result of general effects on the adult worm or the bacteria. First, we scored the pharyngeal pumping rate of TPEN treated worms and also tested for food avoidance behaviors; in these assays, we found no significant differences with control worms (Figures A.2, A.3). Moreover, we observed similar effects on brood size when we triple-killed the bacteria prior to providing them as a food source to the worms (Figure A.4), demonstrating that it is unlikely that the effects on worm viability resulted from effects of TPEN treatment on the bacterial food source. We conclude that these experimental conditions, i.e., bacterial and worm growth on medium containing 10 μM TPEN, constitutes a mild zinc

limitation condition that has little impact on the general health of the worm. This condition is nonetheless sufficient to induce a reduction in brood size by primarily impairing the reproductive axis of the worm. Given that TPEN can bind copper, zinc and iron ions with high affinity(88), we next tested which of these essential transition metal ions gave rise to the limitation phenotype using rescue experiments as described previously (33). After incubating L4 stage hermaphrodites for 6 hours on TPEN-containing plates, we moved the worms to TPEN plates supplemented with either copper, zinc, or iron salts, and scored the resulting brood size. While copper or zinc supplementation returned the brood size to near normal levels 48 hours after rescue, iron supplementation did not restore the brood size to control levels at any point, indicating that the TPEN phenotype at this concentration does not result from iron-limitation (Figure 2.2A). While the observed rescue upon copper addition could indicate that the effects of TPEN are due to copper limitation, since TPEN has a higher affinity for Cu (II) (89) (10^{-19} M compared to 10^{-16} M for Zn), an alternative possibility is that added copper is preferentially sequestering TPEN in the media and thus blocking its ability to reduce zinc availability in the rescue experiment. To distinguish between these possibilities, the effect of copper limitation on brood size was directly evaluated using two copper-specific chelators (10 μ M ammonium tetrathiomolbydate or 10 μ M Neocuproine (89)). Neither treatment led to reduced brood size relative to controls (Figure 2.2B, C), consistent with the hypothesis that the effects we observed following TPEN treatment were due to zinc limitation.

Oocytes are more vulnerable to zinc insufficiency than sperm

To establish whether the brood size defect under this zinc insufficiency condition is the result of impaired development of sperm, oocytes, or both, hermaphrodites were subjected to

zinc insufficient conditions prior to oocyte formation (61). Hermaphrodites exposed to zinc insufficient conditions in either L3 or L4 and then scored as young adults exhibit a significant reduction in the number of oocytes compared to the controls (Figure 2.3A, B), consistent with the interpretation that reduced zinc availability impacts oocyte production. In contrast, under the same conditions sperm production showed smaller differences that vary with stage (Figure A.5). While hermaphrodites exposed to zinc insufficient conditions in L3 show a small reduction in the

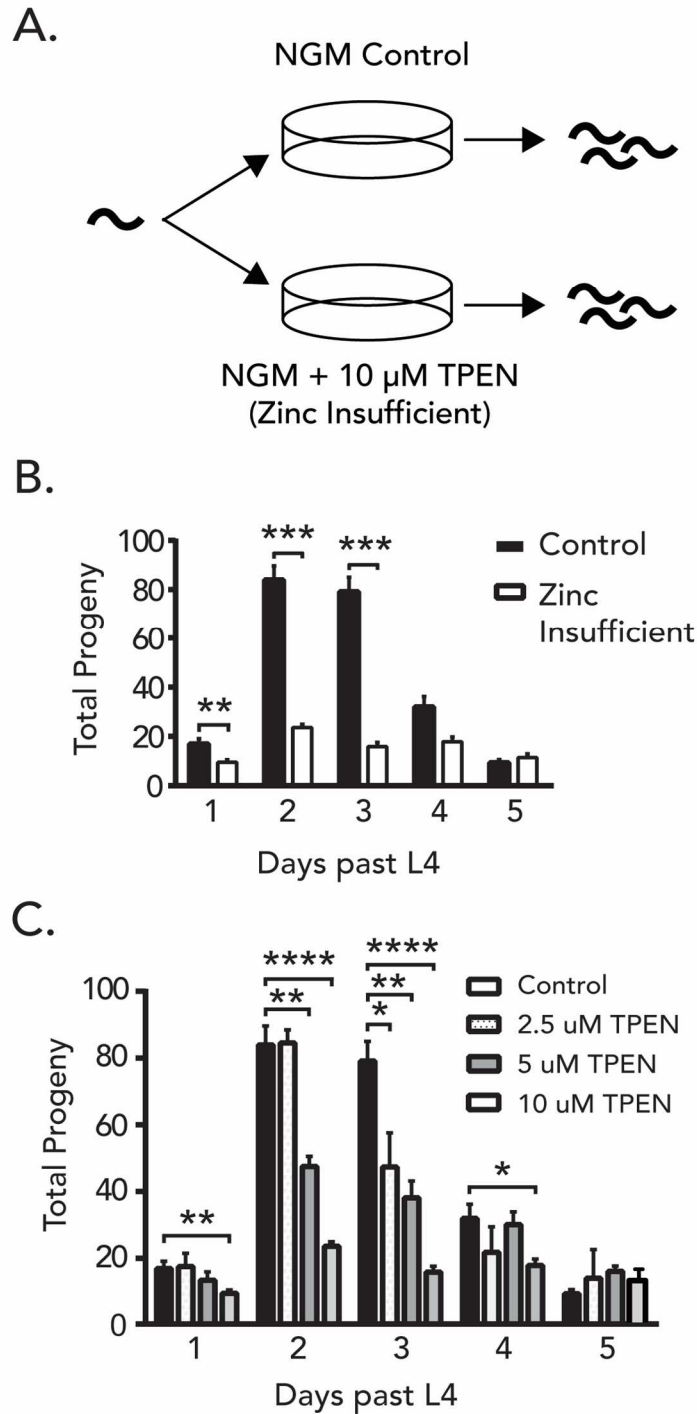


Figure 2.1 TPEN impacts brood size development. (A) 10 μ M TPEN is infused into the worm growth medium (NGM). Zinc insufficient (ZI) worms were grown on these plates compared to controls which were grown normally. (B) ZI worms that were grown on TPEN plates produce smaller broods compared to controls. (C) Brood size reduction is from TPEN exposure and is dose dependent.

While hermaphrodites exposed to zinc insufficient conditions in L3 show a small reduction in the number of sperm per gonad arm, exposure to 10 μ M TPEN in late L4 did not cause a reduction in sperm number (Figure 2.3A). These results show that the large decrease in brood size of animals grown on 10 μ M TPEN is the result of effects on oocyte rather than sperm production. To more directly test this idea, control and TPEN treated worms were mated in pairs in which each gamete (either oocyte or sperm) was exposed to zinc insufficient conditions prior to mating (Figure 2.4A). For these experiments, males were mated with either WT L4 hermaphrodites (prior to the time when they would begin to generate self-progeny) or with feminized *fog-1(q253)* mutant animals which do not produce sperm. A significant brood size reduction was measured each time the oocyte-bearing animals were exposed to zinc insufficiency (Figure 2.4B). To determine whether zinc insufficiency has any effects on sperm production in males, male sperm was counted in control and zinc insufficient groups; no significant difference was observed (Figure 2.5A, B).

Zinc insufficient oocytes experience spindle defects and hyperploidy during the meiosis to mitosis transition

To assess whether zinc insufficiency has effects on the meiotic and mitotic divisions, independent of effects on events earlier in the germline, zygotes from untreated worms were dissected into media containing 10 μ M TPEN. This treatment profoundly altered several steps in the transition from meiosis to mitosis after fertilization. Time lapse images of embryos expressing GFP::tubulin and GFP::histone (to label microtubules and chromosomes, respectively) revealed that zygotes treated with 10 μ M TPEN did not extrude a second polar body at the end of Meiosis II but instead formed an extra female pronucleus (Figure

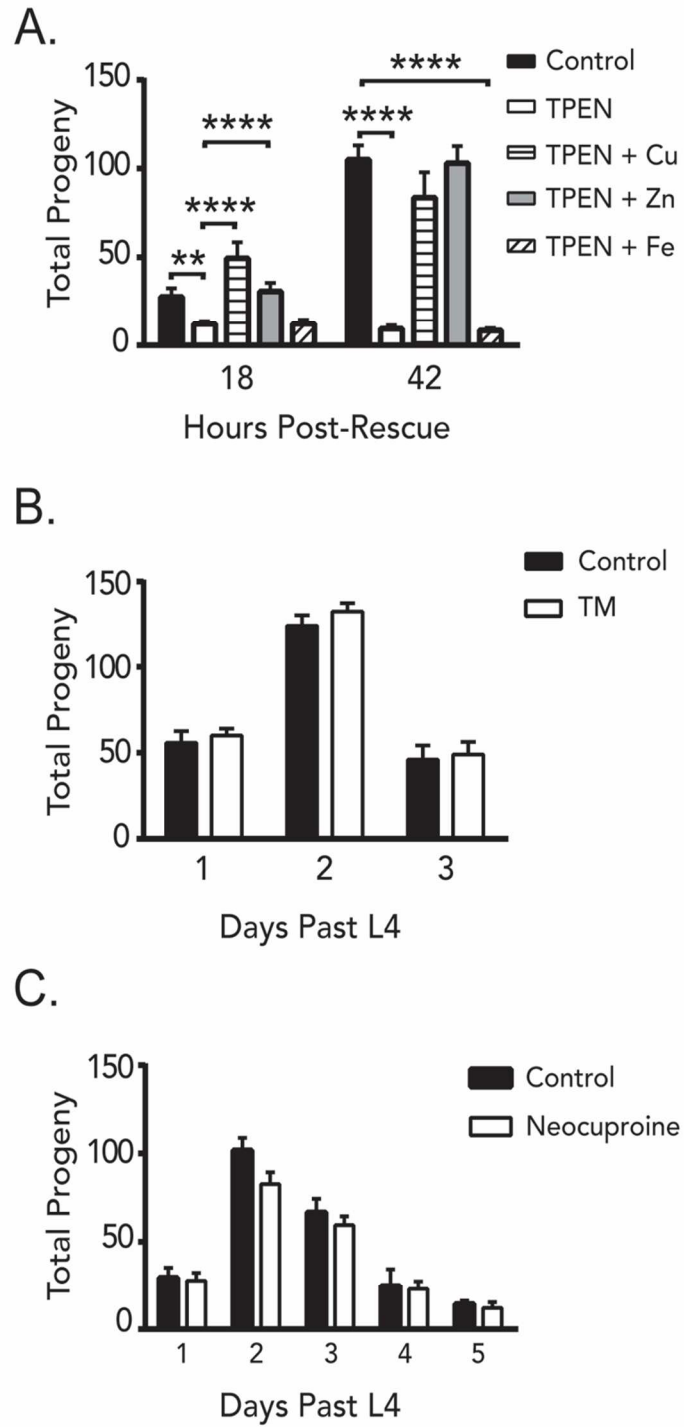


Figure 2.2 Brood size reduction is zinc specific. (A) Both Cu and Zn rescue brood size 18 hrs and 42 hrs post rescue. (B,C) Cu chelators Tetrathiomolybdate and Neocuproine did not the reduce brood sizes in adult hermaphrodites.

2.6A and movies A.6); these two female pronuclei then migrated toward the male pronucleus and upon nuclear envelope breakdown, a spindle formed. However, these spindles exhibited defects. In control embryos (Figure 2.6a), spindles orient along the long axis of the embryo and then initiate anaphase (62, 90). However, in the TPEN treated GFP::tubulin and GFP::histone (to label microtubules and chromosomes, respectively) revealed that zygotes treated with 10 μ M TPEN often did not extrude a second embryos, we observed spindles that initiated anaphase but exhibited lagging expressing chromosomes, demonstrating that TPEN affects the fidelity of chromosome segregation (Figure 2.6B). TPEN treatment of three additional zygotes revealed similar effects. In one occasion, a zygote did not extrude the second polar body with normal timing during Telophase II. Instead, the zygote later pinched off the second large polar body within the extra embryonic space, between the cytoplasm and the eggshell (approximately 8 minutes after the beginning of pronuclear migration; Figure A.6A, B and Movies A.8A-C), suggesting that it is sometimes possible for the cell to overcome polar body retention. In an extreme case, another zygote successfully extruded both polar bodies, but they were later pulled back into the cytoplasm, and the zygote arrested during Pseudocleavage (Figure A.7B, Movie A.11G-L). The zygote formed a “popcorn” shape, the pronuclei never migrated properly, and the two polar bodies remained near the edge of the cytoplasm (Figures A.7c). In contrast, the control zygote was able to undergo Pseudocleavage during a similar time frame and the pronuclei were

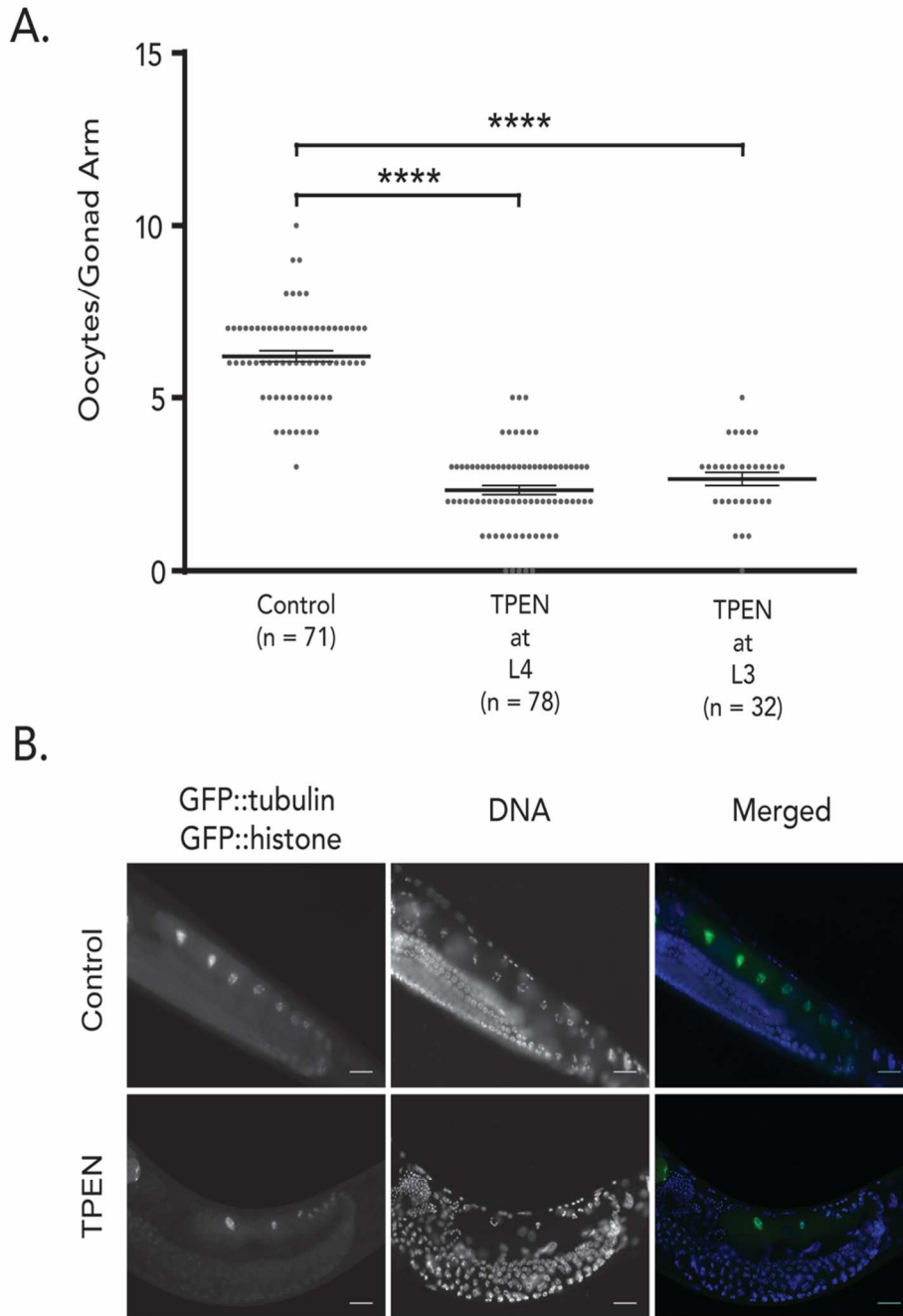


Figure 2.3 Zinc insufficiency impacts oocyte production. (A) Growing L3 and L4 stage hermaphrodites under ZI conditions reduces the number of oocytes produced. (B) Adult hermaphrodites labeled with GFP:: tubulin and GFP:: histone and stained with DAPI show fewer oocytes.

able to migrate normally (Figure A.7a). Therefore, TPEN treatment has severe effects on completion of the meiotic divisions and results in mitotic defects.

Discussion

Zinc fluxes are known to both regulate oocyte maturation and the egg-to-embryo transition in mammals (30, 33), however little is known about whether zinc availability plays any role in invertebrate germ cell function. Guided by results showing that TPEN-induced zinc insufficiency controls meiotic progression in oocytes as well as the egg-to-embryo transition in mouse (30, 34), we show that *C. elegans* reproductive function is similarly sensitive to zinc limitation. We found that this reproductive phenotype was robust and showed that it most likely arises from the ability of TPEN to restrict zinc, as opposed to copper and iron availability. We studied the effects on chromosome segregation, and potentially affects cell cycle progression. The observed defects lead to severe aneuploidy in the embryos, pointing to a crucial role for zinc in meiotic and mitotic fidelity. Specifically, the late meiotic and early mitotic divisions in the *C. elegans* embryo are highly sensitive to physiological or pharmacological-induced changes in zinc availability, consistent with zinc limitation experiments in mouse oocyte development and fertilization. Aneuploidy in mammals is already linked to impairment of gamete development (91, 92), and we demonstrate here that aneuploidy occurring in *C. elegans* impairs gamete development as well. The fact that eggs laid by zinc-deficient animals are able to hatch, whereas isolated embryos dissected into TPEN-media have severe defects, highlights an interesting also find that acute treatment of isolated zygotes with TPEN disrupts polar body extrusion, difference between these two conditions. In the case of an intact worm, the fact that they are still able to produce viable progeny (albeit fewer than wildtype) suggests that the adult worms are still able to utilize zinc either from the food or from zinc stores within the body. Isolated embryos cannot

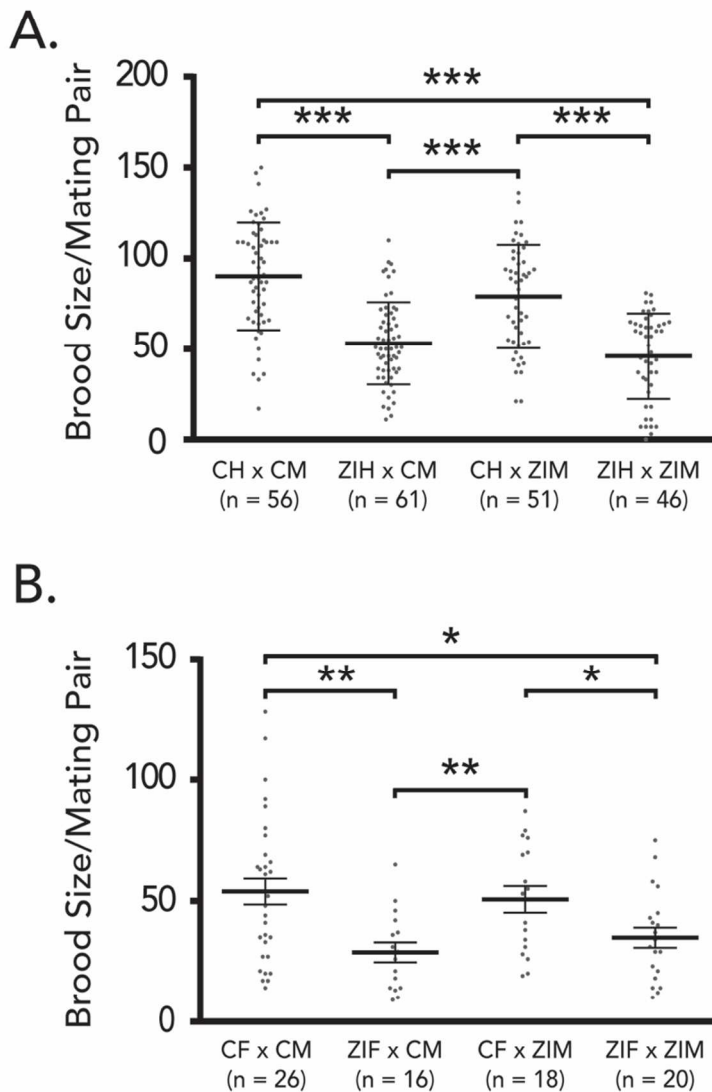


Figure 2.4 Brood size is reduced when oocytes are exposed to ZI. (A) Mating between hermaphrodites and males show reduced brood size when the hermaphrodites are exposed to ZI conditions. (B). A similar trend is exhibited when feminized worms are exposed to ZI conditions.

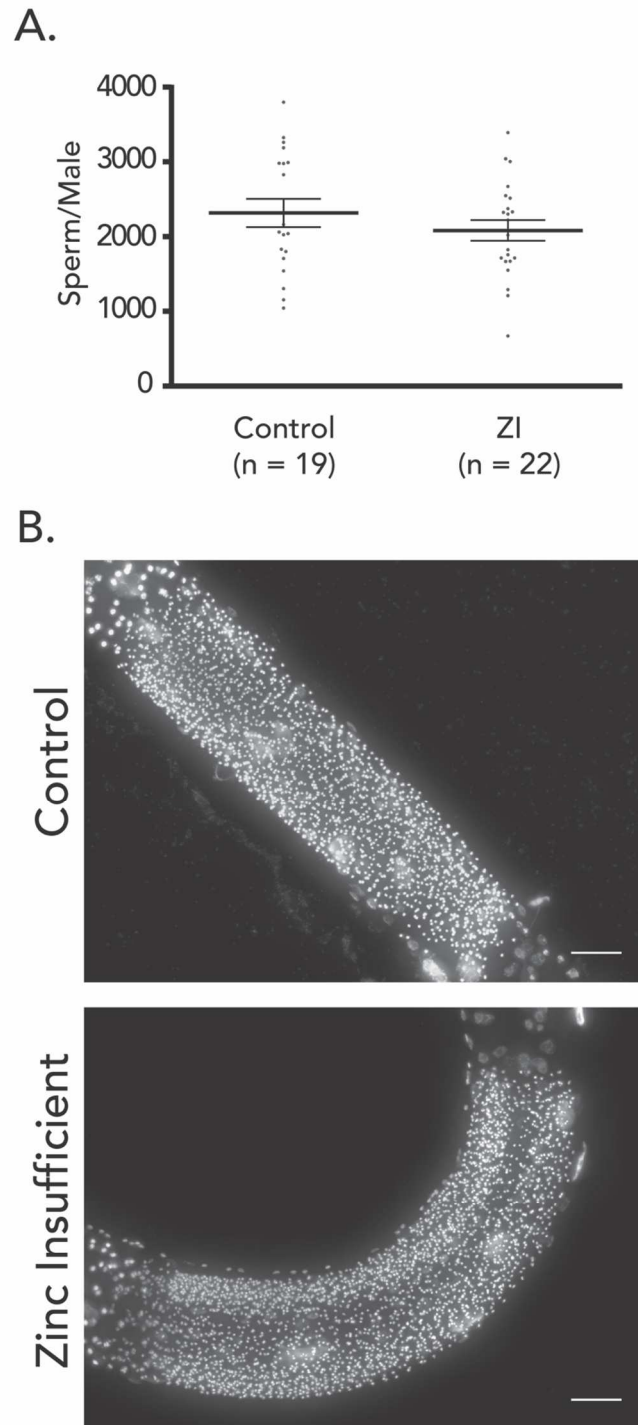


Figure 2.5 ZI does not impact sperm production in WT males.(A) ZI males produce a normal sperm number compared to the controls. (B). Males stained with DAPI shows a similar number of sperm in controls and ZI groups.

do this, so we suspect that the defects in polar body extrusion and mitosis arises from the inability of the isolated egg to acquire zinc from another source. Finally, we demonstrate how this approach to zinc limitation can be exploited in mating experiments, a critical feature for future experiments that will exploit the powerful genetic opportunities in this model organism to identify pathway members that mediate zinc signaling events.

Perhaps most significant, these studies expand our understanding of inorganic regulatory pathways across evolution. Our prior work provides insights into mouse, monkey and human meiotic progression where egg development occurs during embryonic development and terminal meiosis is triggered in the adult. These early studies of zinc limitation in the worm (45, 47-49) enable the design of more mechanistic studies that can resolve how putative zinc signaling events operate in an organism that depends on stem cell generation of oocytes. Our results confirm that zinc uptake is necessary for the generation of quality oocytes in this context as well.

Canonical zinc trafficking and zinc-responsive transcription mechanisms are known in single cell organisms (93-101) but are just beginning to be mapped in multicellular organisms. Many signs point to specialized zinc-responsive pathways in the early stages of development in mammals such as those involving Emi2 control of APC/C activity in meiosis (39, 71). Given our new results showing zinc-dependence at related stages in invertebrate meiotic and mitotic cell cycles, we plan to test the speculative idea that zinc was coopted very early in evolution as a meiotic transition signal. The ease of scoring these zinc-dependent phenotypes in the worm are important for future genetic screens that probe the mechanistic basis of this regulation. An inorganic signal, such as zinc fluxes across membranes or changes in availability inside the cell during a time of reductive division and in the absence of appreciable transcription, is an elegant

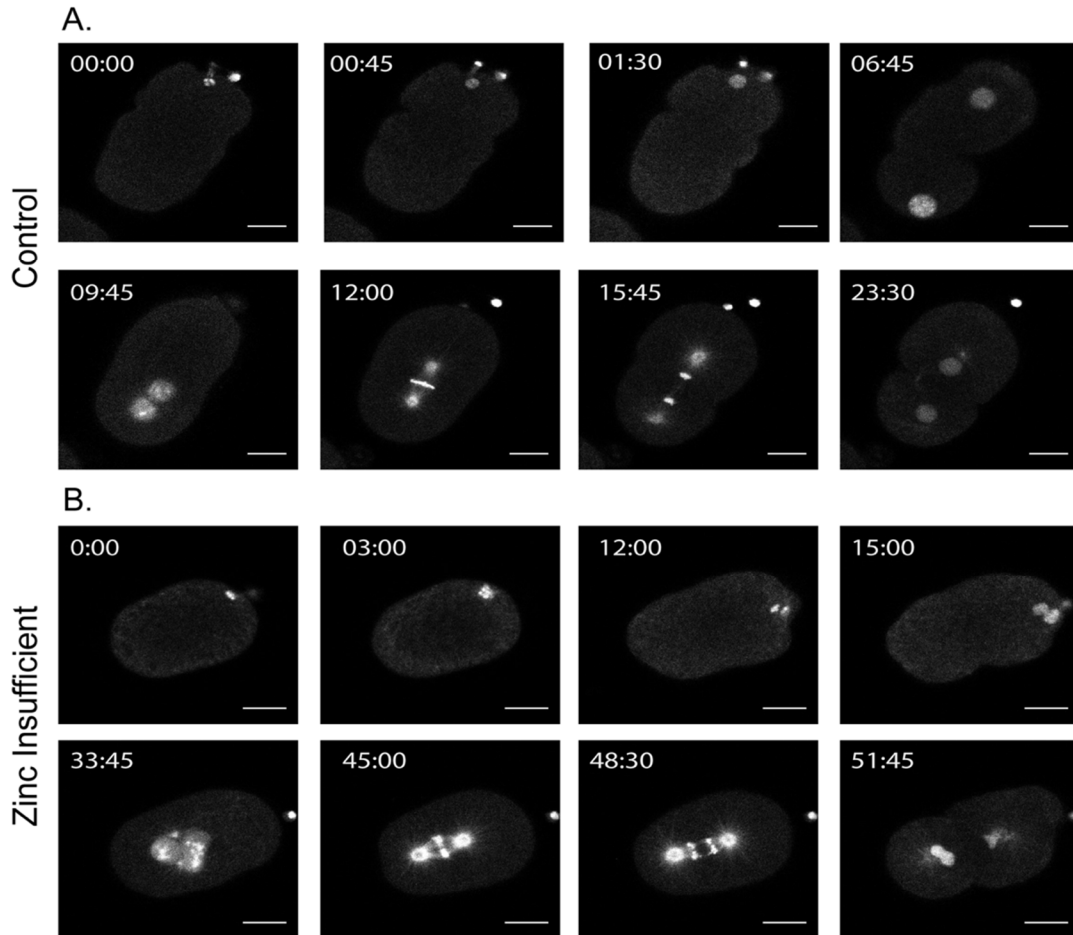


Figure 2.6 Acute zinc insufficiency causes defects in the meiotic and mitotic divisions. Example time lapse movies of embryos dissected from untreated worms into media containing 10 μ M TPEN; worms are expressing GFP::tubulin and GFP::histone to visualize spindle dynamics. Acute exposure to TPEN causes dramatic defect in meiosis and mitosis. In (A), the second polar body is properly extruded at 45s. One maternal and one paternal pronucleus are apparent (06:45). They properly migrate, fuse, and the metaphase spindle forms (12:00). The cell then successfully divides to the 2-cell stage. In (B), the second polar body fails to extrude (15:00). This is followed by the appearance of two maternal pronuclei, which join the male pronucleus (33:45). The mitotic spindle forms (45:00) and chromosomes segregate (48:30), but exhibit lagging chromosomes. Scale bar=10 μ m, n=5 in the control group, and n=6 in the TPEN treated group.

solution to advancement of the meiotic cell cycle. Additional studies will illuminate the specific receptors, transporters and mechanisms by which zinc is mobilized and deployed in a stage specific manner.

CHAPTER 3**ZINC FLUXES REGULATE MEIOTIC PROGRESSION IN MATURING *C. ELEGANS*
OOCYTES**

The data in this chapter is being prepared for publication. I conducted all studies except data in Figure 3.2E & 3.2F, which were conducted by Aaron Sue

Abstract

Zinc fluxes are critical for successful meiotic progression in mammalian oocytes and have been characterized in detail in mouse; however, it is unknown if fluctuations in zinc regulate meiotic progression in the invertebrate *Caenorhabditis elegans*. A zinc flux is the combined accrual (zinc influx) and expulsion (zinc efflux) of zinc during oocyte maturation and occurs for both total and labile zinc. Total zinc is the sum of all the zinc ions inside the cell, bound and unbound. Labile zinc ions are weakly bound to a range of biological molecules and are readily accessible to fluorescent probes. We demonstrate here that significant fluctuations in zinc occur in *C. elegans* during meiotic progression. Total zinc uptake occurs through from Prophase I through the zygote stage, followed by efflux through the pronuclear fusion. Live cell imaging revealed that labile zinc influx occurs through Metaphase II and efflux from Anaphase II through pronuclear fusion. During the drop of total and labile zinc content, we found that labile zinc accumulation in the eggshell region increased. Zinc fluxes were not observed in the distal, loop or proximal region of the gonad or during mitotic divisions in the embryo. Increasing labile zinc concentrations were observed in oocytes as they were positioned closer to the spermatheca. These results also demonstrate that dynamic zinc fluxes are conserved between *C. elegans* and mammals, demonstrating that zinc is an integral component of meiotic progression.

Introduction

Large-scale fluctuations of calcium are well-known to mediate oocyte maturation(102-104). In mammals and recent studies show the same is true for zinc. Early studies quantified total zinc levels throughout various stages of oogenesis and oocyte maturation, and span many metazoan species, demonstrating that zinc is an integral component of the oocyte in vertebrates and invertebrates alike (21, 25, 27, 33). Cellular zinc content is tightly regulated can be broken down to two categories: total zinc and labile zinc. Total zinc is the sum of all the zinc ions inside the cell, bound and unbound, whereas labile zinc ions are weakly bound to a range of biological molecules and are readily accessible to fluorescent probes which typically have an affinity in the nanomolar range (105, 106).

Oocyte maturation in mammals is the period between the release from Prophase I arrest through Metaphase II arrest (107), and we have previously defined the final 12-16 hrs. as late oocyte maturation. In *C. elegans*, oocyte maturation is the period between Prophase I release and Metaphase I. Events that occur around the time of Prophase I, including nuclear envelope breakdown and cytoskeletal rearrangement are early oocyte maturation events (10). Since oocyte maturation refers to different time frames in mammals and *C. elegans*, we define early oocyte maturation as events that occur just before fertilization, and late oocyte maturation as the continuous meiotic divisions after fertilization.

The role of fluctuating zinc during oocyte maturation is best characterized in mouse. Mouse (*M. musculus*) oocytes accrue (defined as zinc influx) approximately 20 billion total zinc ions during the final 12-16 hours of maturation up until Metaphase II (MII) arrest. Then, upon fertilization, the mouse MII egg expels approximately 10 billion total zinc ions (defined as zinc efflux) before continuing cell division (28, 33). The combined accrual (zinc influx) and expulsion (zinc efflux) of zinc during oocyte maturation are collectively known as a zinc flux.

The rise and fall of total zinc levels during specific stages of meiotic progression in mouse lead to further interrogation of changes in labile zinc using zinc fluorescent probes, and the discovery that after fertilization, the egg rapidly expels labile zinc in bursts known as the “zinc spark”. These exocytosis events have been shown to occur in mouse (*M. musculus*), rhesus macaque (*M. mulatta*), crab-eating macaque (*M. fascicularis*) and humans (*H. sapiens*) (30, 31).

An important question emerging from these discoveries is how zinc regulates meiotic progression. Maturation in the presence of the chelator TPEN, oocytes are considered zinc insufficient. Zinc insufficient oocytes arrest in Telophase I and extrude enlarged polar bodies (33). These findings provided extensive evidence that zinc fluxes regulate the meiotic cell cycle that controls embryo viability in mammals. Further investigation into how zinc fluxes regulate cell cycle transitions lead to mouse studies revealed the roles of Early Mitotic Inhibitor 2 (Emi2) regulation of the metaphase to anaphase transition in Meiosis II. Emi2 is a zinc-binding protein and inhibitor of the Anaphase Promoting Complex Cyclosome (APC/C)(35, 38, 40, 108). Oocytes in vitro matured with impaired zinc binding domain (ZBR) function could not form proper MII spindles. Instead the 73% of oocytes with an impaired ZBR formed abnormal chromatin masses. Inhibition of the ZBR also disrupted asymmetrical cell division, creating polar bodies that are larger than 50% of normal oocyte diameter- phenotypes reminiscent of TPEN exposure (34). Next, to test the effect TPEN had on EMI2 function, control GV oocytes were injected with *Emi2* cRNA to allow for overexpression at MI before in vitro maturation. All control GV oocytes arrested at MI. However, when GV oocytes were matured along with TPEN, only 44% arrested at MI, demonstrating that zinc insufficiency in GV oocytes inhibited the ability of Emi2 to induce MI arrest. Next, MII eggs were treated with the ionophore zinc pyrithione (ZnPT) to increase intracellular zinc during a period where zinc is normally expelled (34). Control

activated MII eggs were able to progress through the cell cycle. However, activated MII eggs treated with ZnPT were unable to achieve activation and did not seem to progress in the cell cycle.

From these findings, it was proposed that fluctuating intracellular zinc levels acts as a switch; once zinc levels increase above the required threshold, Emi2 is activated, contributing to Metaphase II arrest. Once intracellular zinc is expelled, Emi2 no longer participates in APC/C inhibition, thus promoting progression to Anaphase II.

Despite the growing evidence that links zinc availability with successful oocyte maturation in mammals, the first evidence that zinc availability was also key to successful germline development in invertebrates emerged recently through initial studies with the soil nematode, *Caenorhabditis elegans* (109, 110). Zinc insufficient adult hermaphrodites produce fewer oocytes that result in a smaller brood size compared to controls (109, 110). Additionally, zinc insufficient zygotes cannot extrude the second polar body in Meiosis II, resulting in hyperploidy and cell cycle arrest (110). While these studies provided the foundation for zinc studies of the germline in *C. elegans*, it is not yet known if zinc fluxes are conserved in *C. elegans* or if zinc fluxes drive meiotic progression. It is also not known if zinc fluxes occur specifically during meiotic progression, or if they are required during earlier stages of germline development.

Here we show that *C. elegans* exhibits a dramatic flux in zinc levels, with influx occurring between Prophase I and the zygote stage. Efflux occurred from the zygote stage through the 1-Cell mitotic stage. Labile zinc influx began from Metaphase I up through Metaphase II, which was followed by an immediate efflux from Anaphase II through pronuclear fusion. This general pattern of zinc accrual and release is similar to mammals. While studies of

the zinc flux pattern have not been extensively studied in other metazoans, a number of species do exhibit large scale zinc accrual during oogenesis or oocyte maturation. This suggests that dynamic changes in zinc levels in the oocyte is integral for a number of organisms. While labile zinc was released from the cytoplasm, zinc accumulated in the general eggshell region. The fluxes were restricted to the meiotic progression phase of oocyte maturation, as drastic changes were not observed during early oocyte maturation or in other regions of the gonad. Our new findings suggest that impaired polar body extrusion during Meiosis II may result from the inability of the zygote to meet the zinc quota between Prophase I and Metaphase II. However, unlike mammals, efflux is not followed by cell cycle arrest suggesting that arrest is not required for zinc efflux during the transition from Metaphase II to Anaphase II. Our studies in *C. elegans* have broadened our window into the role zinc plays in different phases of germline development, including oogenesis, oocyte maturation, and meiotic progression. They also place zinc ion regulation of the germline within a new context, and show zinc is involved in germline regulation in metazoans.

Materials and Methods

Worm strains

EU1067: *unc-119(ed3)ruIs32[unc-119(+)*pie-1*^{promoter}::GFP::H2BIII;ruIs57[unc-119(+)*pie-1*^{promoter}::GFP::tubulin]* was used to visualize the meiotic spindle in the labile zinc fluorescence experiments (58). N2 (Bristol) wild type strain was used in oocyte maturation XFM experiments. AV335 *emb-27(g48)II; unc-119(ed3) ruIs32[unc-119(+)*pie-1*^{promoter}::*gfp*-H2B]III; ruIs57[[unc-119(+)*pie-1*^{promoter}::*gfp*-tubulin]* was used in Metaphase I arrested zygotes for XFM(58). *fog-*

1(q253) I was used in TPEN challenge experiments (111). GH378 *pgp-2(kx48)* I was used in in vivo labile zinc fluorescence experiments (48).

Growth media

All control animals were grown on Nematode Growth Media (indicated as NGM-C) (112) and fed from the OP-50 bacterial lawn. Worms were also cultured on NGM plates infused with TPEN (indicated as NGM-TPEN) at a final concentration of 10 μ M (Sigma Aldrich, St. Louis, MO) for X-Ray Fluorescence Microscopy experiments.

Egg Buffer

The egg buffer for meiotic progression experiments was supplemented with 100 nM ZincBY-1, and TPEN challenge experiments in isolated gonads and oocytes. Components for the egg buffer include 25 mM HEPES, pH 7.3, 118 mM NaCl, 48 mM KCl, 2 mM CaCl₂, and 2 mM MgCl₂ (113).

Meiosis Media

The meiosis media for meiotic progression experiments were supplemented with 50 and 100 nM ZincBY-1. The components included (for 10 ml) 1 ml of 500 mg/100 ml Inulin in culture safe water, 1 ml of 0.25 M HEPES pH 7.4, 6 ml Leibowitz L-15 media, and 2 ml of Heat Inactivated Fetal Bovine Serum (Fisher).

Zinc Probes

For all labile zinc experiments of isolated zygotes and gonads, and live animals oocyte staining

we utilized ZincBY-1 ($\lambda_{\text{ex}}=520$ nm, $\lambda_{\text{em}} = 543$ nm) (29). For supporting live animal oocyte staining experiments we utilized FluoZin-3 AM ($\lambda_{\text{ex}}=520$ nm, $\lambda_{\text{em}} = 543$ nm) (Invitrogen).

X-Ray Fluorescence Microscopy Sample Preparation

Whole Gonad and Prophase I Arrested Oocyte Isolation: We cultured L4 stage N2 worms at 20°C in Nematode Growth Media (NGM) to allow growth to day-1 adults before dissecting the gonads into 0.1 M ammonium acetate buffer with a 20-gauge needle onto a microscope slide with the aid of a stereomicroscope. Worms that were raised under control conditions are indicated as NGM-C, and worms that were raised on plates infused with 10 μM TPEN are indicated as NGM-TPEN. Next, we isolated gonads by dissecting below the pharynx to allow the gonad to release from the worm. A row of oocytes was contained within the gonad. Then, we mouth pipetted and whole mounted the isolated gonads onto a 1.5 mm Silicon Nitride window (Silson) to air dry (n=15 oocytes, n=10 NGM-C and n=8 NGM-TPEN).

X-Ray Fluorescence Microscopy Meiotic Progression Experiment

We bisected the animals near the vulva to obtain wild type zygotes (N2) in meiotic (n=7), 1-cell (n=10) and 2-cell stages (n=9) by stereomicroscopy, and selected cell stages based on presence of polar bodies and visualization of pronuclei and nuclei. We cultured L4 stage AV335 worms overnight at 20°C. The following morning, we cultured them at 25°C on NGM plates for 7 hours to arrest the spindles in Metaphase I before dissecting into 0.1 M ammonium acetate buffer. We mounted them similarly to isolated gonads (n=15). We dissected and mounted zygotes similarly as isolated gonads.

X-Ray Fluorescence Microscopy Scanning Parameters and Analysis

Samples for XFM were mouth pipetted onto silicon nitride windows after dissecting in ammonium acetate buffer. Isolated zygotes 1-Cell and 2-Cell stage zygotes were raster scanned at a 50 ms dwell time at a 2 μm step size, and isolated MI stage zygotes were raster scanned at 100 ms dwell time at a 5 μm step size. Larger, isolated gonads were raster scanned at a 15 ms dwell time at a 5 μm step size, and the fluorescence data were analyzed using the MAPS software (114). All XFM experiments were performed at the 2-ID-E beamline at the Advanced Photon Source (Argonne National Laboratory in Argonne, IL). A beam splitting Si (220) monochromator focused the X-ray beam using Fresnel zone plates at an energy of 10 keV, and provided a focused beam size of 0.5 μm x 0.4 μm . Total metal quantities are represented as $\mu\text{g}/\text{cm}^2$ on the XFM maps. Total metal atoms were measured as atoms/ROI, where total atoms within a specific area of the gonad was measured as atoms/area. Statistical significance was determined by performing 1-way ANOVA analysis and student t-tests. p values below 0.05 were considered statistically significant. For meiotic progression experiments, we performed a 2-way ANOVA analysis and students t-tests. p values below 0.05 were also considered statistically significant.

Confocal Fluorescence Microscopy

Isolated Zygotes for meiotic progression experiments: All meiotic progression experiments in isolated zygotes conducted on a SP5 II Laser Scanning Confocal Microscope located at the Biological Imaging Facility (BIF) at Northwestern University. Control zygotes were dissected from young adult hermaphrodites (EU1067) directly into 7 μl of either 50 or 100 nM ZincBY-1 as indicated (29) in a 35-mm glass bottom FluoroDish (World Precision Instruments). Time-

Lapse videos were acquired at room temperature using the 63x objective were captured with the HyD detector, the 488 laser to detect GFP and the 514 laser to detect ZincBY-1. Videos were captured at 60s intervals with a 0.8 μm step size, in short segments of meiosis (appx 10-20 minutes, (n=11)). Imaging at 50 nM ZincBY-1 (n=7) eliminated probe chelation effects, and allowed for complete imaging of meiosis.

Tests for Zinc Specific Fluorescence

In order to test whether the observed fluorescence signal arose from zinc and not from auto-fluorescence, we imaged isolated gonads on the same SP5 II laser Scanning Confocal Microscope as the isolated zygotes, and also carried out controls where excess TPEN was added. Since TPEN binds zinc around five to six orders of magnitude more tightly than ZincBY-1, addition of excess TPEN removed zinc from the probe and allowed measurement of background fluorescence. We prepared wild type (N2) samples by dissecting them into Egg buffer alone, 10 μl of 75 nM ZincBY-1 (n=5), 10 μl of 75 nM ZincBY-1 + 50 μM TPEN (n=5), 10 μl of 75 nM ZincBY-1 + 10 μM Zn Pyrithione (n=5), and 50 μM TPEN alone (n=5). All samples incubated for 15 minutes before being covered with a coverslip that was slightly elevated with high vacuum grease beads (Dow Corning) and sealed with nail polish. Gonads were imaged with a 20x objective with the HyD detector, and the 514 laser to detect ZincBY-1. Laser power was set to 54% with 238% gain. Gonads were imaged 0.29-0.38 μM step size. To ensure that changes in ZincBY-1 fluorescence intensity were due to biological changes within the zygotes, we conducted photo bleaching controls using a drop 8 μl of 50 nM ZincBY-1 under mineral oil for 15 minutes with the 514 laser and scanned a depth of 30 μm at 0.8 μm step size.

Tests for Zinc Specific Fluorescence in Isolated Oocytes

Oocytes from *fog-1(q253)* I mutants were cultured at 25°C at L3 stage until young adulthood to prevent sperm production. We utilized this strain to prevent cell cycle advancement while incubating in the test conditions. Unfertilized oocytes were dissected out onto a 35-mm glass bottom FluoroDish (World Precision Instruments). We prepared the oocytes by dissecting them into Egg buffer alone (n=5), 10 µl of 75 nM ZincBY-1 (n=5), 10 µl of 75 nM ZincBY-1 + 50 µM TPEN (n=5), 10 µl of 75 nM ZincBY-1 + 10 µM Zn Pyrithione (n=5), and 50 µM TPEN alone (n=5). All samples were incubated for 15 minutes before being covered with a coverslip that was slightly elevated with high vacuum grease beads (Dow Corning) and sealed with nail polish. All oocytes were imaged on the same SP5 II laser Scanning Confocal Microscope as the isolated zygotes. Oocytes were imaged with a 63x objective with the HyD detector, and the 514 laser to detect ZincBY-1. Laser power was set to 54% with 238% gain.

Live Imaging

Preparation of live worms: For *in vivo* experiments, we adapted the worm preparation protocol (47) by reconstituting 5 mM ZincBY-1 or FluoZin-3 AM (Invitrogen) stock solution in dimethylsulfoxide (DMSO) (Sigma) and diluted in M9 buffer to a final concentration of 50 µM. For experiments using serotonin in the dye solution, we dissolved serotonin creatinine sulfate (Sigma) in M9 buffer using sonicating and mildly heating (65°C) to a final concentration of 50 µM and used this solution to dilute the dye. Next, we picked young adult animals in 100 µL of 50 µM ZincBY-1 (n=11) or FluoZin-3 (n=4) solution and incubated in the dark at 20°C for 3-4 hours. The 50µM dye solution containing the soaking live worms was dispensed onto an NGM plate with OP50 and allowed the worms to recover for up to 150 minutes.

Imaging and analysis of live worms: We adapted the live worm imaging protocol (115) and immobilized dye-soaked worms on a 3% agarose pad using a few droplets of a mixture of equal parts 0.1 μm polystyrene beads (Polysciences) and 50 mM serotonin creatinine sulfate. Next, we imaged animals on a Leica DMI6000 Spinning Disk Inverted Confocal Microscope with a Yokogawa CSU-X1 spinning disk module with Microlens-enhanced Nipkow disk and Photometrics Evolve Delta512 camera. Animals were captured at 20X air objective using 488 and 561 nm solid state lasers, and processed and analyzed all images using Fiji software (116, 117).

Fluorescence Microscopy Data Analysis on Oocytes from Live Animals

In ImageJ, 3 squares of equal area were drawn within each distinguishable oocyte and 3 squares in the background. Next, the mean fluorescence intensity of each box was measured from a single slice, then averaged the values for these boxes to generate an average fluorescence intensity value of that oocyte or background. To get the true fluorescence intensity, the average intensity of the background was subtracted from each oocyte average. To account for variation, we normalized the fluorescence intensities by setting the background corrected "-1" oocyte value to 100%.

Fluorescence Microscopy Data Analysis on Isolated Zygotes

Cytoplasmic Volume Estimation in isolated zygotes: The EU1067 strain was advantageous because we could define the cytoplasm from GFP::tubulin fluorescence. The Volumest plugin (118) in ImageJ was used to estimate the cytoplasmic volume (reported as μm^3).

Fluorescence Intensity Measurements in Isolated Zygotes

Fluorescence intensity was determined for each channel by using the sum slice max projection in Image J. From this projection, we performed background subtraction by rolling ball radius based on the number of pixels/embryo. We measured the fluorescence intensity by selecting an ROI of the cytoplasm as defined by GFP::tubulin (EU1067) and used that same ROI to define the cytoplasm by ZincBY-1 in the sum slice analysis (116, 117).

Results

*Labile zinc fluxes occur during late oocyte maturation in *C. elegans**

In order to determine if fluctuations in labile zinc occur during late oocyte maturation in *C. elegans*, we dissected zygotes directly into egg buffer containing 100 nM of the zinc responsive fluorescent probe, ZincBY-1 (29) in order to evaluate fluorescence intensity while surveying select stages of late oocyte maturation. ZincBY-1 has been used at nanomolar concentrations and, unlike AM-ester containing zinc probes, it does not require an enzyme cleavage mechanism to function (119). Worms expressing GFP::tubulin and GFP::histone combined with ZincBY-1 (emission at 540 nm) allows us to follow changes in both zinc the meiotic spindle in different channels, thus facilitating the identification of specific cell cycle stages. Initially we surveyed comparable stages previously documented in mammals: Metaphase I, Metaphase II and the 2-Cell mitotic stage. ZincBY-1-specific cytoplasmic fluorescence was observed at Metaphase I and II, but was absent in the 2-Cell mitotic stage, thus we found significant changes in cytoplasmic labile zinc concentrations between Metaphase I and the 2-Cell mitotic stage (Figure 3.1A).

Several control experiments were conducted to test whether fluorescence in this channel arose from labile zinc detection. A series of controls were also performed on isolated oocytes from *fog-1(q253)* mutants; since this strain does not produce sperm at the restrictive temperature (25°C), the oocytes remain unfertilized and don't advance through the cell cycle, enabling us to compare different experimental treatments without concern for cell cycle advancement and potential permeability changes. First, oocytes that were not exposed to ZincBY-1 did not display fluorescence. Second, adding 50 µM of the chelator TPEN after 75 nM ZincBY-1 exposure eliminated ZincBY-1 fluorescence. Third, adding 10 µM of the zinc ionophore, zinc pyrithione after 75 nM ZincBY-1 exposure increased ZincBY-1 fluorescence as expected. Finally, fluorescence was not observed in oocytes exposed to TPEN alone (Figure B.1). Therefore, we concluded that ZincBY-1 fluorescence resulted from formation of zinc/probe complexes and represents labile zinc pools.

Total zinc fluxes occur during late oocyte maturation in *C. elegans*

Once we confirmed that changes in ZincBY-1 fluorescence resulted from fluctuating labile zinc pools, we expanded our analysis of oocyte maturation to compare labile zinc with total zinc distribution.

Total zinc content was obtained by X-Ray Fluorescence Microscopy (XFM) on Prophase I arrested oocytes within the intact gonad, since unfertilized worm oocytes are difficult to isolate (wild type, atoms counts are averaged between all oocytes and (corresponding to the germinal vesicle stage in *M. musculus*)), Metaphase I arrested zygotes (AV335, a mutant with temperature-sensitive mutation in the Anaphase Promoting Complex (APC/C)), as well as

zygotes undergoing the meiotic divisions (wild type), and mitotic 1-cell and 2-cell stage embryos (wild type). XFM maps revealed distributed total zinc across all Prophase I oocytes and provide quantitative insights into copper and iron as well. The oocytes exhibited a significant enrichment of zinc within each nucleus. However, iron and copper did not exhibit this feature (Figure 3.1B). Zygotes undergoing the meiotic divisions have significantly ($p < 0.0001$) more zinc atoms/ROI ($2.2 \times 10^{10} \pm 3.8 \times 10^9$) than Prophase I arrested oocytes ($2.7 \times 10^9 \pm 2.7 \times 10^8$). The same trend occurs for iron and copper (Table 1). While these results demonstrate that a significant influx occurs in all three metals after fertilization, changes in total zinc are significantly larger. The total number of zinc atoms were at least an order of magnitude higher than iron and copper throughout late oocyte maturation. Given that excess iron and copper does not rescue brood size (110), treatment with copper-specific chelation does not reduce brood size, and that zinc quota changes occur at specific transition stages, we focused on how zinc regulates meiotic progression.

To more precisely define the stage at which zinc increases occur, we used a strain with a temperature-sensitive mutation in the anaphase-promoting complex to arrest oocytes at Metaphase I (AV335) for XFM analysis. Although the average number of zinc atoms/ROI of these MI zygotes ($4.6 \times 10^9 \pm 1.1 \times 10^8$) was larger than in Prophase I ($2.7 \times 10^9 \pm 2.7 \times 10^8$), these values were an order of magnitude lower than those at the zygote stage ($2.2 \times 10^{10} \pm 3.8 \times 10^9$), suggesting that accumulation we observed most likely begins before Metaphase I and continues as the meiotic divisions progress. Mirroring our observations of labile zinc (Figure 3.1C), we

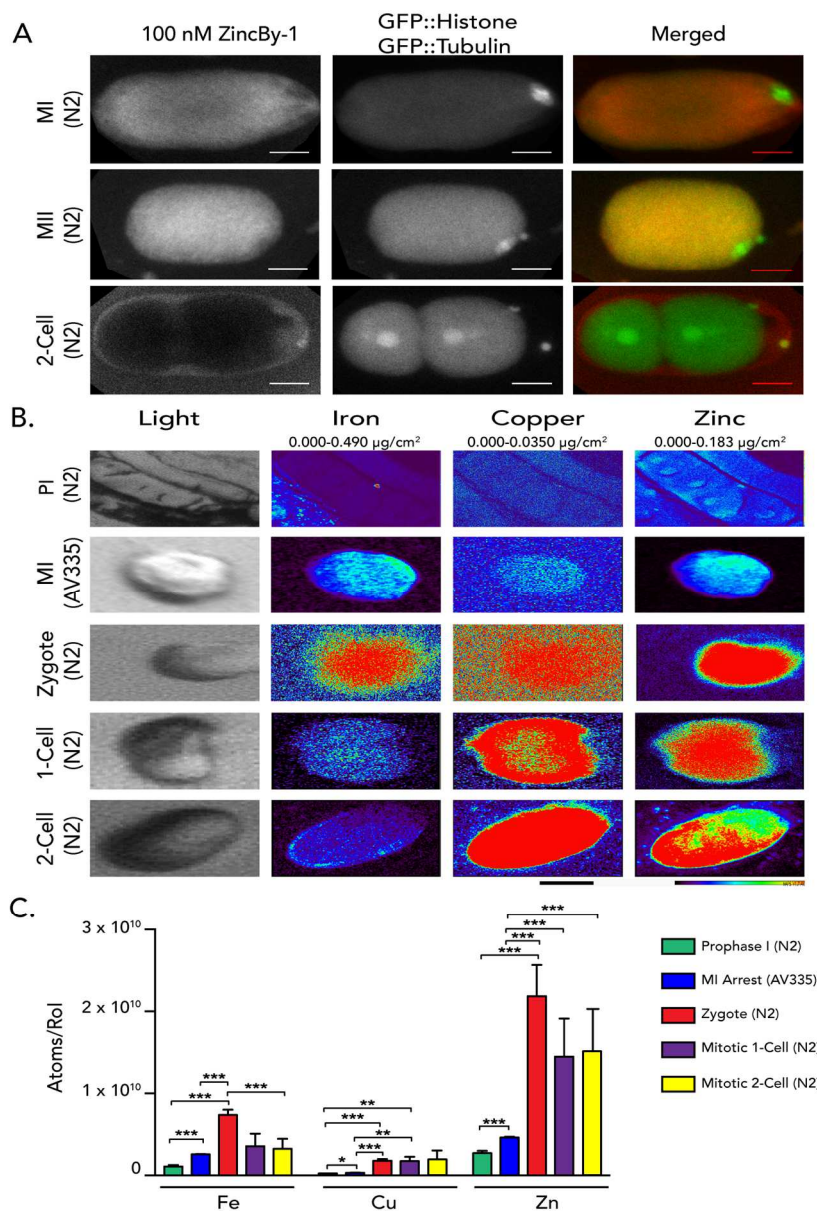


Figure 3.1 Zinc fluxes are generally conserved in *Caenorhabditis elegans*. (A) Isolated zygotes labeled with GFP::tubulin and GFP::histone show that in MI, ZincBy-1 fluorescence is detected throughout the cytoplasm. In MII, ZincBy-1 fluorescence increases in the cytoplasm. Finally, in 2-Cell stage zygote displays dim ZincBy-1 fluorescence in the cytoplasm, and detectable ZincBy-1 fluorescence in the eggshell. (B). XFM maps for Fe, Cu and Zn in PI, MI, Zygote, 1-Cell, and 2-Cell stages. (C) Corresponding atom counts/ROI for Fe, Cu, and Zn. Fe and Zn generally display a similar flux pattern of influx and efflux, while Cu displays a general increase and then levels remain generally steady.

also found that total zinc levels were lower in 1-Cell ($1.5 \times 10^{10} \pm 4.7 \times 10^9$) and 2-Cell ($1.5 \times 10^{10} \pm 5.3 \times 10^9$) mitotically dividing embryos. Similar to zinc fluctuations, we also found that total iron levels decreased in mitotically dividing embryos while copper levels remained elevated (Table 1).

Metal atoms/ROI is based on calculations in area, which introduces some degree of uncertainty when considering cellular concentration. To account for this, we utilize metal: phosphorus and metal: sulfur ratios to serve as a proxy for a more accurate volume estimation. Phosphorus and sulfur scale to volume, and calculating changes in their cellular ratios we can better predict the accuracy of total iron, copper and zinc concentrations. By using metal ratio with phosphorus or sulfur, we find that, zinc concentrations were significantly higher compared to iron and copper, a result in concordance with total atom counts (B. 2 and B. 3).

Zinc fluxes are not detected in the distal or proximal gonad

Given the 470 % increase up through the zygote stage and the subsequent 34 % decrease in total zinc content upon progression through the 2-Cell mitotic stage, we next set out to determine whether there were similar fluxes earlier stages of oogenesis by mapping metal content across the intact gonad. The *C. elegans* germline has a spatio-temporal organization, which allows visualization of all stages of meiotic progression in each gonad. Germline stem cells occupy the distal region of the gonad, and then migrate towards the loop and proximal regions as they enter and then progress through meiosis (51). In adult hermaphrodites, oocytes in the proximal region of the gonad progress towards the spermatheca, encounter sperm, and undergo meiotic divisions upon fertilization. Each major region of the gonad is stereotypically

organized in a visibly discrete manner, so XFM analysis of each region is facile. Taking advantage of this stereotyped gonad organization, we utilized XFM to interrogate the total changes in zinc content across the entire ex vivo gonad in order to see if fluctuations corresponded to any particular region. The gonad contained $3.0 \times 10^6 \pm 3.8 \times 10^5$ total zinc atoms/area (total iron and copper atoms/gonad were both lower (Figure 3.2A, B, Table 2). Atom/area analysis demonstrated a similar result (Figure B.4). Separately analyzing each major region of the germline (distal, proximal, loop) demonstrated that the total zinc atoms/area is comparable in each region (1.3×10^6 to 1.6×10^6 atoms/area) and we therefore, did not uncover any obvious gradient or fluxes correlating with specific regions. Similarly, we did not observe significant differences between iron and copper counts in each region (Figure B.5)

We also isolated gonads from animals that were cultured TPEN infused media prior to oocyte formation in order to determine if TPEN exposure induced gonad abnormalities and if zinc insufficiency perturbed any particular region more severely than another. These experiments were designed to elucidate if upstream impairments of zinc availability affected downstream development. First, we found that TPEN exposure did not alter gonad size compared to controls (Figure B.6), despite a significant reduction in total zinc in all regions ($p=0.0125$ in distal, 0.0112 in loop, and 0.0029 in proximal). Furthermore, TPEN did not significantly reduce total iron or copper counts in the gonad (Figure 3.2B, Figure B.5). This result suggests that the effects of TPEN exposure on the reduction in oogenesis and brood size (110) are unlikely to result from gross germline defects and but could result from the effect of zinc insufficiency in the distal region exerting downstream effects on the oogenesis in the proximal region (Figure B 6 and B.7). These results combined with the fact that we do not observe large-scale zinc changes between regions in the germline supports the idea that zinc fluxes are specific to meiotic

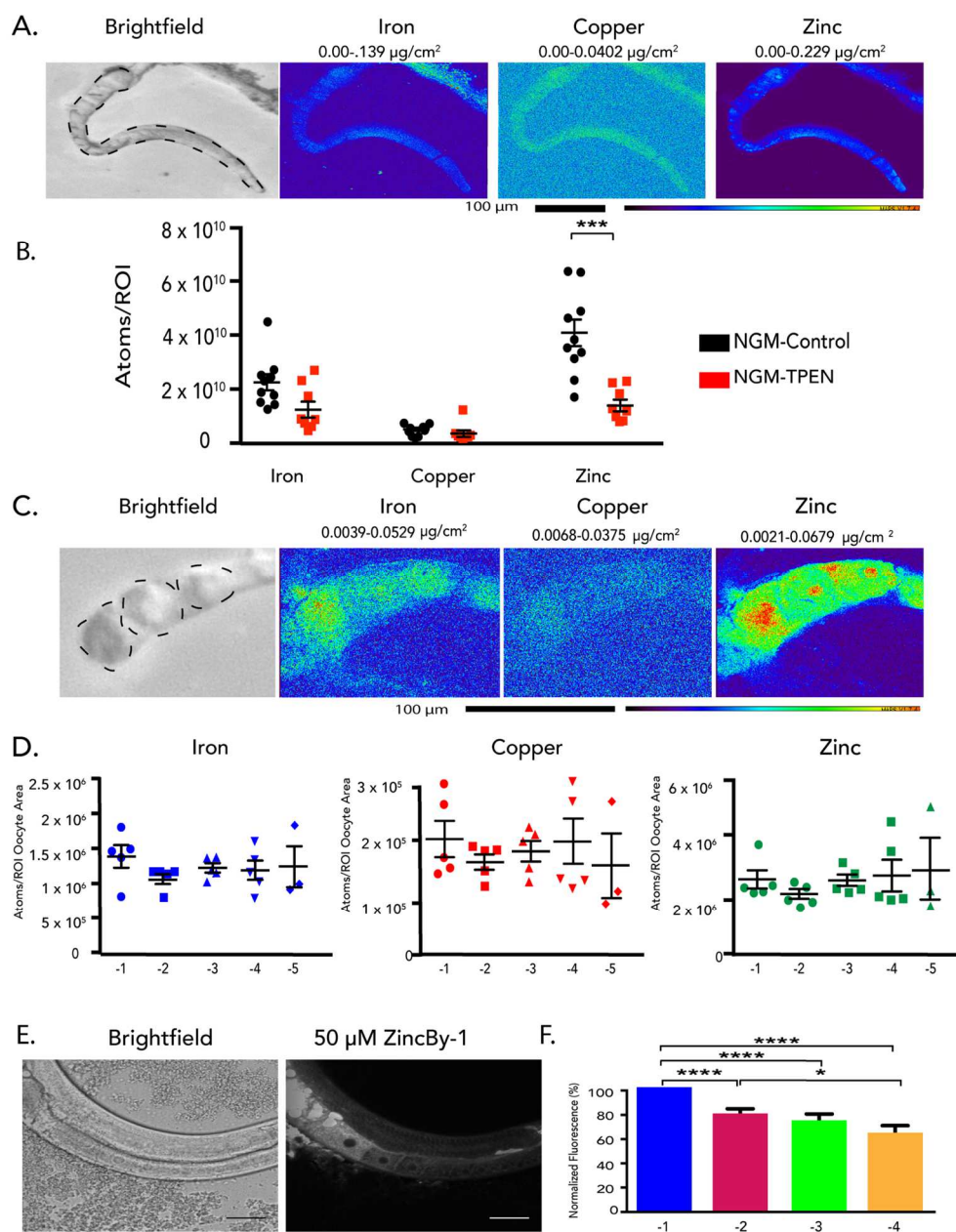


Figure 3.2 Zinc fluxes are unique to meiotic progression. (A) XFM maps of Fe, Cu, and Zn show distribution throughout the entire gonad. The ROI is outlined in the BF image (in $\mu\text{g}/\text{cm}^2$). (B) Corresponding atom counts/ROI in NGM-Control and NGM-TPEN gonads. (C) XFM maps of Fe, Cu, and Zn in oocytes (in $\mu\text{g}/\text{cm}^2$) from isolated gonads. The ROI outlines the oocytes in the BF image. (D). Corresponding atom counts/ROI in oocytes for Fe, Cu, and Zn. For each metal there is a decrease in total counts as each oocyte decreases in maturity. (E) BF and ZincBy-1 fluorescence images of oocytes in live WT animals. (F) Normalized fluorescence intensity in oocytes -1 through -4 in live, WT animals shows a decrease in fluorescence as the oocytes decrease in maturity.

progression and not prior. Furthermore, these results in combination with previous copper rescue and copper chelation experiments (110) demonstrate that copper is not likely involved in proper gonad formation or oocyte maturation. Likewise, variation in iron levels do not seem to be involved in gonad formation since TPEN exposure did not reduce total iron content and adding back excess iron does not rescue brood size from TPEN chelation (110).

Increases in total zinc coincide with increased oocyte size

Next, we examined whether total zinc content in oocytes changes prior to fertilization. The -1 oocyte is located adjacent to the spermatheca, and is the only one that can be fertilized. Other oocytes further away from the spermatheca are numbered in descending order (61). The XFM map revealed total zinc distribution across all oocytes (-4 through -1(Figure 3.2C)), and also an increase in total zinc atoms/oocyte ROI ranging from 2.9×10^9 to 3.8×10^9 as each oocyte was situated closer to the spermatheca. The same trend was observed for iron and copper (Figure B.8 and B.9). When we accounted for the number of atoms per unit area, we found that total iron, copper and zinc atoms/oocyte area were consistent and statistically insignificant in each oocyte regardless of its position in the gonad (Figure 3.2D). We concluded that total iron, copper and zinc increased in because the size of the oocytes increased and we see no significant fluctuation in total zinc in the first four oocytes.

Labile zinc pools amass before fertilization

We next utilized ZincBY-1 to monitor labile zinc distribution in live animals. In live animals soaked in 50 μ M ZincBY-1, we detected clear fluorescence in the cytoplasm of each oocyte, but not within the nucleus, which is the opposite profile we observed with total zinc. We

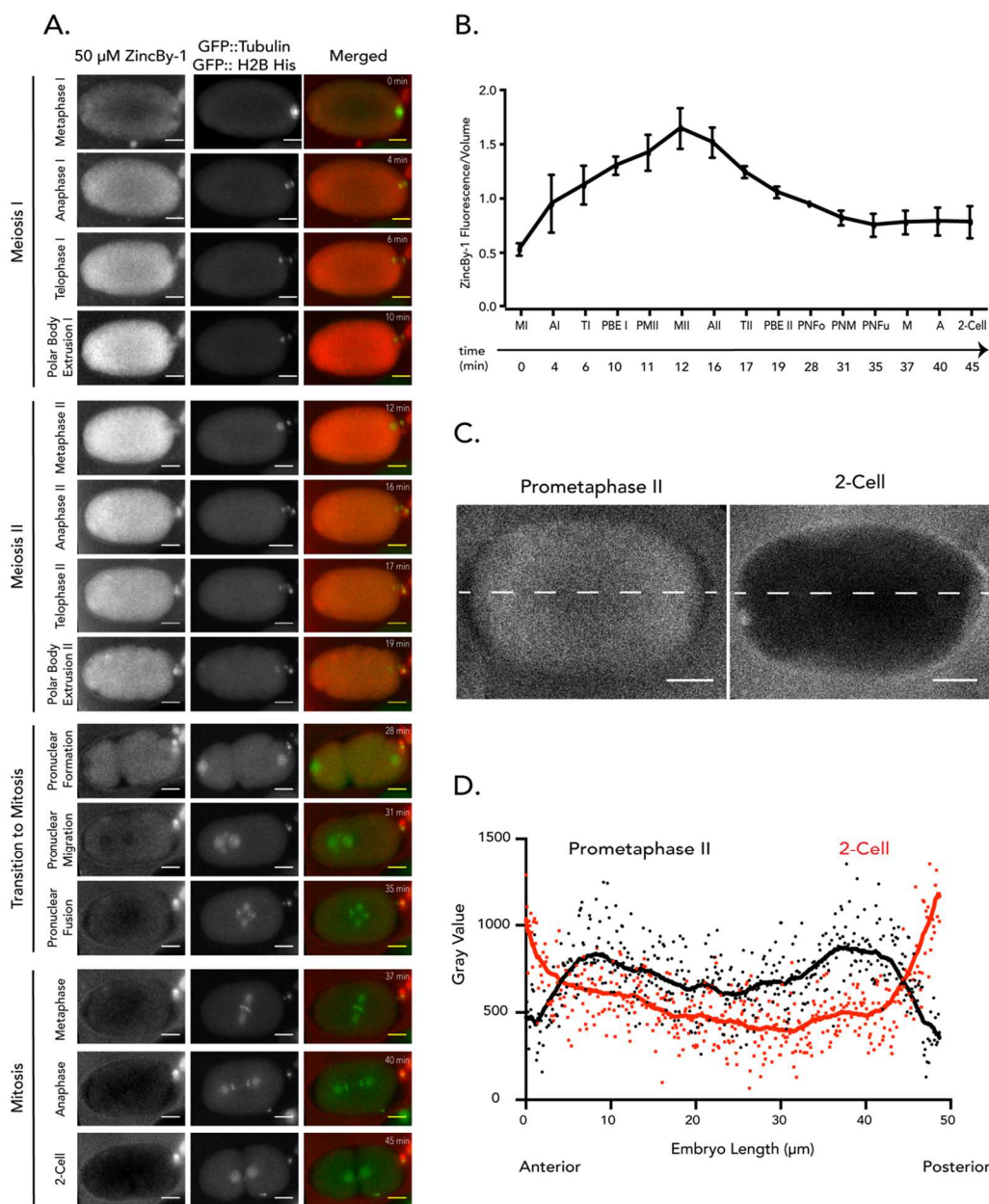


Figure 3.3 ZincBy-1 detects labile zinc fluxes during meiotic progression (A) Labile zinc detection by ZincBy-1 displays a fluorescence increase from MI to MII, followed by a decrease at AII. The decrease continues through Pronuclear Fusion and fluorescence levels remain low through the 2-Cell stage. (B) Corresponding fluorescence/volume shows the fluorescence changes throughout meiotic maturation and time. (C) Fluorescence image comparing the cytoplasmic ZincBy-1 fluorescence decrease from Prometaphase II and the 2-Cell stage. Scale bar is 10 μ m. (D) A fluorescence comparison by gray value of Prometaphase II compared to 2-Cell showing that labile zinc is present in the cytoplasm prior to eflux, and after eflux it is in the eggshell space.

also detected enhanced labile zinc in the oocytes that were positioned closer to the spermatheca. The -1 oocyte was most intensely fluorescent of all of the oocytes (Figure 3.2E, F, Table 2). To test whether this the ZincBY-1 fluorescence arose from the zinc/probe complex, we subjected gonads to TPEN treatment in a similar experiment as isolated oocytes, and confirmed that these signals arise from labile zinc pools detected by ZincBY-1 (Figure B.10). Experiments utilizing an alternative zinc probe, 50 μ M FluoZin-3 AM revealed the same profile type as observed with ZincBY-1 (Figure B.11). Taken together, our findings suggest that total zinc levels are consistent in *C. elegans* and are present in all regions of the gonad. However, labile zinc increases significantly as oocytes undergo late stages of oocyte maturation. This suggests that labile cytoplasmic pools may be required when the -1 oocyte begins early maturation activities.

The *C. elegans* zygote acquires cytoplasmic zinc up to Metaphase II, followed by cytoplasmic zinc loss through the 2-Cell stage

To understand the precise temporal and spatial pathway of labile zinc changes in the cytoplasm across in Metaphase I and II, and 2-Cell mitotic stages (Figure 1), we performed live cell imaging of zinc dynamics, something that has not been possible in oocytes from other metazoans. Since zygotes rapidly progress through these stages, we used ZincBY-1 staining in zygotes labeled with GFP::*histone* and GFP::*tubulin* (spindle markers) in order to delineate cell cycle stage. We found that after fertilization, the oocyte continuously acquired labile zinc in the cytoplasm through Metaphase II, where peak ZincBY-1 fluorescence was observed, as measured by fluorescence intensity/volume. Then, beginning in Anaphase II, we found a continuous decrease in cytoplasmic ZincBY-1 fluorescence until pronuclear fusion. At pronuclear fusion, cytoplasmic ZincBY-1 fluorescence levels remained extremely low in the cytoplasm through the

2-Cell mitotic embryo stage (Figure 3.4A, B, Movie 1). The drop in ZincBY-1 fluorescence occurred over two major phases of embryogenesis – the metaphase to anaphase transition in MII and the transition into mitosis. Because efflux of labile zinc has been observed during meiotic cell divisions in mammals, and now *C. elegans*, we tested to see if zinc fluxes are specific to meiosis. Time-lapse experiments tracking ZincBY-1 fluorescence from the 2-cell through the 8-cell stage demonstrated that once cytoplasmic zinc levels drop, they remain that way (Movie 2). Therefore, fluxes in labile zinc are limited to the window between fertilization and pronuclear fusion.

Zinc accumulates in the eggshell region during efflux

Next, we assessed where labile zinc localized once leaving the cytoplasm. Specifically, we sought to determine if labile zinc was retained by the eggshell region or was released from the embryo. *C. elegans* embryos contain a multi-layer eggshell that functions as a polyspermy block, protects the embryo from the environment, and maintains embryo osmolarity (64, 120-122). Eggshell formation begins at Anaphase I, concurrent with a decrease in embryo permeability (63, 65, 120). To answer this question, we tracked ZincBY-1 fluorescence in zygotes just prior to ZincBY-1 fluorescence decrease, (Figure 3A) beginning at Prometaphase/Metaphase II and ending at the 2- Cell mitotic stage. During the beginning of this period, eggshell formation has already begun and the zygote displayed low ZincBY-1 fluorescence in the area between the cytoplasm and a faintly staining layer corresponding to the forming eggshell (Figure 3.3C). At Prometaphase II/Metaphase II, ZincBY-1 fluorescence was visible in the cytoplasm, but not in the general eggshell region. From Anaphase II on, we observed a concomitant decrease in cytoplasmic fluorescence and a steady increase in

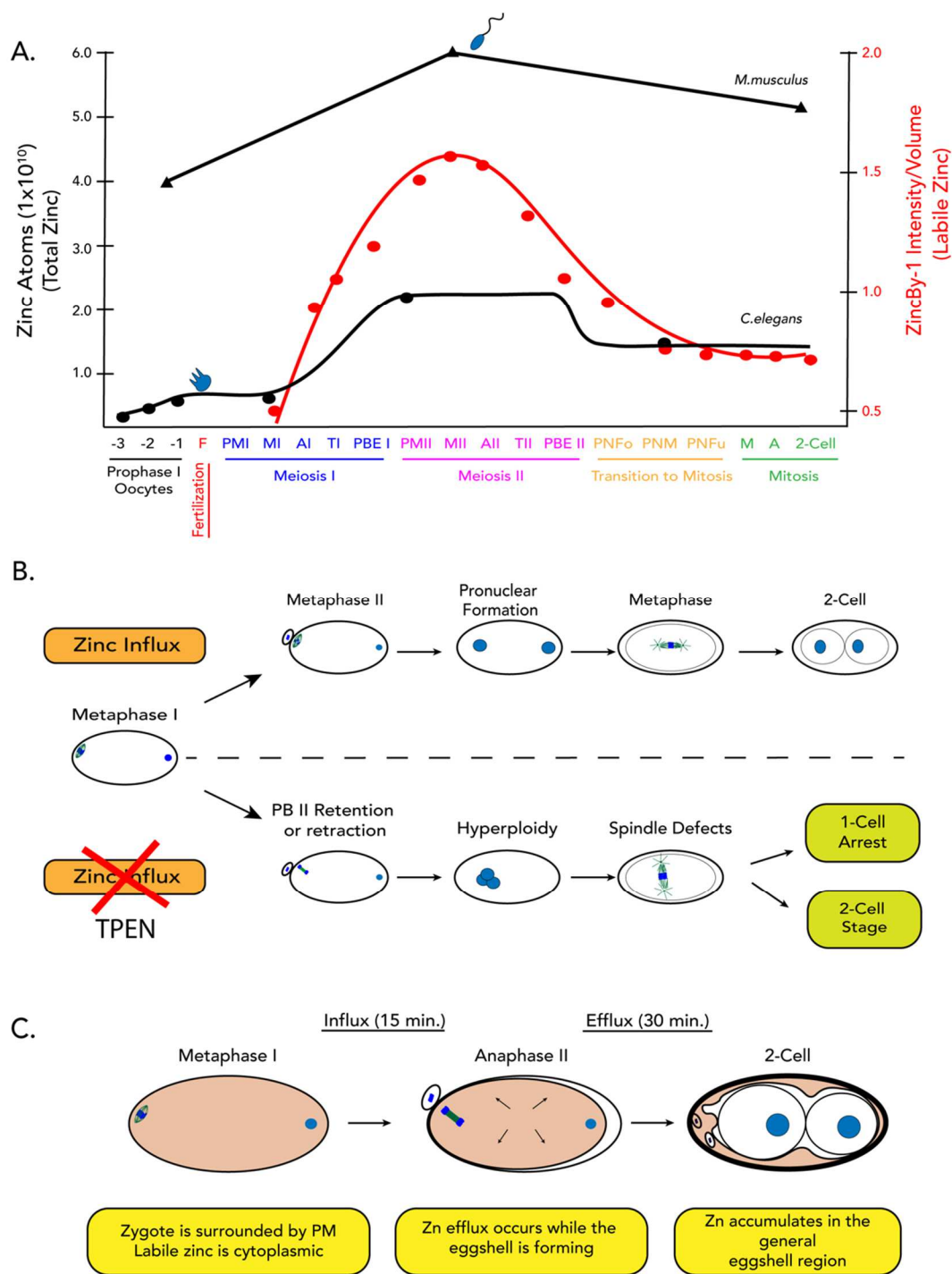


Figure 3.4. (A) A comparison of fluctuations of zinc between *C. elegans* and mouse. Both organisms accrue large quantities of total and labile zinc during early stages of meiotic progression, and acquire the maximum concentration at Metaphase II. (B) TPEN induced zinc insufficiency in isolated, developing zygotes experience polar body retention or retraction during Meiosis II, resulting in hyperploidy, spindle defects and cell cycle arrest. (C.) Labile zinc is acquired during early stages of Meiosis I, during which time the zygote is surrounded by a plasma membrane and is permeable. Influx continuously occurs until Anaphase II, where zinc is expelled from the cytoplasm over 30 minutes. Finally, labile zinc accumulates in the general eggshell region.

fluorescence in the eggshell region. At the 2-Cell mitotic stage, ZincBY-1 fluorescence was detected in the entire space between the cytoplasm and an outer eggshell layer (Figure 3C, Movie 3). Line-scans across zygotes at Prometaphase II/Metaphase II showed elevated ZincBY-1 fluorescence (measured in gray area) in the inner 30 μm of the zygote, corresponding to the cytoplasm, compared to the outer 10 μm of each side of the cytoplasm, corresponding to the Anterior and Posterior poles. The 2-Cell stage embryo showed the inverse concentration of labile zinc in, was lower in the cytoplasm compared to the eggshell region (Figure 3C, D). In order to determine if there was an artifact of prolonged ZincBY-1 exposure labile zinc exocytosis, we limited dye exposure time (by incubating with buffer for 1 min), while the zygote was permeable, and then rinsed with buffer. Just as with prolonged ZincBY-1 exposure, fluorescence accumulated in the entire eggshell region (Movie 4). This indicated that the probe doesn't alter labile zinc distribution in the eggshell region over time. These results demonstrate that zinc efflux and zinc accumulation in the eggshell region occurs simultaneously.

Discussion

Zinc regulation of oocyte maturation has emerged as a major factor in egg development across metazoans. Through studies in *C. elegans*, we have provided the first comprehensive characterization of zinc fluxes in the regulation of germline development. Our initial studies demonstrated that zinc limitation with TPEN results in reduction of *C. elegans* brood size, and shown that the phenotype results from reduced oogenesis in live animals (110). Independent studies from Hester et al. corroborate the brood size reduction phenotype, and also reports that zinc insufficient animals contain gonads with an extended number of pachytene chromosome into the loop region, and improper oocyte stacking (109). Prolonged growth under zinc limitation

disrupts polar body extrusion at the end of Meiosis II, and leads to spindle size and positioning abnormalities, and hyperploidy (110). These early studies in *C. elegans* provided the first evidence that zinc is required for aspects of oogenesis, oocyte maturation, and normal brood size production in *C. elegans*. Here we have shown that both total and labile zinc fluxes occur in parallel during oocyte maturation in *C. elegans*. A large influx of total and labile zinc occurs post-fertilization. Total zinc accrues by 470% in the cytoplasm through the zygote stage (encompassing multiple meiotic stages) while the labile zinc concentration peaks at Metaphase II. Next, efflux reduces total zinc concentration by 35%, while labile zinc concentration drops dramatically in the cytoplasm and is greatly reduced. While these findings demonstrate that zinc fluxes are present during meiotic progression in *C. elegans*, the function is open for speculation.

Zinc fluxes are generally conserved between C. elegans and mammals and promote meiotic progression

Meiotic progression is known to be regulated by zinc fluxes in mammals, and it was previously unknown if the same occurred in invertebrates until we demonstrated that zinc fluxes are conserved in *C. elegans*. We now demonstrate that the total zinc content of the egg significantly increases in *C. elegans* and mammals alike: beginning after Prophase I arrest, (the 1 oocyte in *C. elegans*, and the germinal vesicle in mammals) peaking during meiosis in the zygote stage in *C. elegans* and Metaphase II in *M. musculus*. In *mouse*, total zinc is increased by 50%, while total zinc in *C. elegans* increased by 470% (Figure 4). During zinc exocytosis, the mouse egg loses 20% of total zinc ions via cortical vesicle exocytosis, while the *C. elegans* zygote loses 31% of total zinc. Furthermore, fluxes in labile zinc in *C. elegans* generally

mirrored the flux in total zinc. Labile zinc influx in *C. elegans* also mimicked the mouse labile zinc profile. The absence of cell cycle arrest points after fertilization in *C. elegans*, provided the opportunity to document fluxes in each meiotic stage, and the transition to mitosis, demonstrating a continuous labile zinc accrual until Metaphase II at which point an immediate efflux begins through early 2-Cell. It is quite interesting that this general flux pattern persisted throughout evolution, despite differences in meiotic regulation between *C. elegans* and mammals. Combined studies in these organisms brings forth compelling evidence that zinc was co-opted early in evolution to promote egg viability.

Zinc fluxes are pronounced during meiotic progression

C. elegans is an ideal model system that provides an unprecedented opportunity to examine zinc fluxes not only in the context of the live worm, but also as it relates to the germline as it changes across the gonad. Using XFM analysis, we conclude that total zinc concentrations are constant in all regions of the gonad upstream of the uterus, including the distal, the loop, and proximal regions. Furthermore, by changes in the concentration established through fluorescence, and the zinc/probe complex created with ZincBY-1 exposure in the worm, we determined that labile zinc pools increasingly accumulate as the oocyte mature in the germline. Collectively, the XFM and ZincBY-1 studies show that extensive changes in total and labile zinc content occur exclusively post-fertilization, and that labile zinc pools are present in a distinct gradient, as oocytes increasing in fluorescence are positioned closer to the spermatheca. Oocyte formation is a period where the gonad acquires consistent, low zinc levels at the same time it acquires other necessary maternal factors. It is possible that zinc may be considered a maternal factor, since both maternal factors and zinc both are considered nutrients, and regulates both

meiotic progression, and transitions between meiotic and mitotic cell cycles (123). Furthermore, we demonstrated that oocytes maturing *in vivo* are somehow acquiring zinc from the parent worm in ways that isolated zygotes cannot. The gradient in labile pools represent a “priming” event that prepares the -1 oocyte for ovulation. for early oocyte maturation activities (cortical rearrangement, and nuclear envelop breakdown), since that specific oocyte contains the highest labile zinc concentration. Because we only observed the gradient with labile zinc, and not total zinc it, may be attributed to labile pools being rapidly mobilized to participate in cell cycle progression. It also serves as the first step in a more extensive zinc acquisition phase that is important for subsequent spindle assembly, chromosome translocation and polar body extrusion.

Large-scale zinc accrual during oocyte maturation has persisted throughout evolution

The XFM results reveal that *C. elegans* undergo massive zinc accrual after fertilization (470%). However, zinc accrual is not unique to *C. elegans*. Zinc influx has been detected in multiple metazoan species by different zinc detection methods. Radioactive ^{65}Zn tracking on *X. laevis* (African clawed frog) oocytes representing stages I through IV demonstrated a 34% increase (25). XFM analysis revealed that *M. musculus* eggs undergo a 50% zinc accrual between GV (germinal vesicle) and Metaphase II arrest (33). Atomic absorption spectroscopy experiments demonstrated that zinc levels in *D. rerio* (zebra fish) oocytes increased by 350% between Stage I and Stage II (27). Finally, *L. pictus* (sea urchin) zinc levels increase by 600% post-fertilization until the pluteus stage and zinc tracked by radioactive ^{65}Zn (21) (Table 3). These combined studies in different species emphasize that zinc accrual is a persistent characteristic of late oocyte maturation and early zygote formation across metazoans despite regulatory, lifespan, and habitat differences. *C. elegans* is an example of a model organism that

utilizes zinc to maintain embryo viability. Taken within the context of the reproductive tract, we have gained insight into not only how zinc is involved in the production of a successful germline, but how dynamic zinc quota changes are crucial to advance late oocyte maturation. This evidence demonstrates that since fluxes are not involved mitotic divisions in embryo development, that zinc is key for specification of the germline throughout evolution.

Zinc exocytosis occurs independently of cell cycle arrest

These lines of evidence support the conclusion that zinc exocytosis after Metaphase II is a persistent evolutionary characteristic of meiosis between *C. elegans* and mammals. Despite this similarity, zinc exocytosis is independent of cell cycle arrest in *C. elegans*- a clear difference from mammals. Mammalian germinal vesicles arrest at Prophase I, and later the egg arrests at Metaphase II. Metaphase II in mouse arrest is maintained in part from Emi2 inhibition of the APC/C as a component of the Cytostatic Factor. By contrast, *C. elegans* zygotes only arrest at Prophase I until release by fertilization. Once the oocyte is fertilized, meiotic progression is continuous. Interestingly, *C. elegans* zygotes do not possess an obvious Emi2 ortholog, which means alternative mechanisms mediate the switch from zinc influx to efflux at the metaphase to anaphase transition during Meiosis II. Since we observed that polar body extrusion impairments occur during this period, it is reasonable to speculate that the underlying mechanisms mediating the transition from metaphase to anaphase is and is affected by zinc insufficiency. Exploring regulators of the Metaphase II to Anaphase II transition would likely provide a viable starting point for understanding the mechanistic differences between *C. elegans* and mammals.

Zinc export in Metaphase II and the 2-cell mitotic embryo is moderate and progressive compared to the mammalian zinc spark

Zinc exocytosis events *C. elegans* and mammals differ in two ways. First, duration of zinc exocytosis is shorter in mammals than *C. elegans*. During post-fertilization stages, *C. elegans* zygotes expel zinc for approximately 23 minutes beginning at the Metaphase II/Anaphase II transition in a continuous and moderate release. In contrast, mammalian zinc exocytosis occurs as a rapid ejection (on average 25 seconds). Second, the number of exocytosis events differs between mammals and *C. elegans*. Zinc efflux occurs only once in *C. elegans* zygotes, while mammalian eggs may eject labile zinc multiple times (30, 69). Such stark contrasts may reflect different reproductive strategies. *C. elegans* produce a high number of progeny within a very short reproductive window, and after Prophase I release there are no cell cycle arrest points. The best reproductive strategy may be to allocate time for a single, moderately paced zinc ejection for producing up to 300 viable progeny. By contrast, mammals produce far fewer progeny over time. Allocation of resources for multiple, rapid zinc ejections may be the best strategy for such a small number of offspring.

Labile zinc may play a role in eggshell function

Labile zinc accumulates in the eggshell region during zinc exocytosis. From where the accumulated zinc in the eggshell originates is an open question. The eggshell itself has many functions, including osmolarity maintenance, polyspermy block and protection from the environment. The ability of the egg to perform these functions lies in the fact that it possesses multiple layers. Our observations demonstrate that labile zinc was distributed within the entire

eggshell region (space between the cytoplasmic membrane and the outermost eggshell layer), but it's unknown which layer(s) zinc specifically associates.

Our knowledge of the fate of zinc exported from the Metaphase II egg can be compared with the results from recent *M. musculus* studies. The zona pellucida is a glycoprotein matrix that surrounds maturing oocytes and undergoes various structural changes during oocyte maturation. After the sperm fuses with the egg the ZP “hardens”. ZP hardening prevents polyspermy (32). It was recently discovered in post-fertilization studies that the *M. musculus* egg packages cortical granules with an average zinc concentration of 0.5 M. Post-egg activation, the ZP accumulates zinc and the fibril structure thickens, suggesting that zinc exocytosis plays a role in polyspermy block (29, 32).

The *C. elegans* eggshell is similar to the ZP in mammals in that it performs a similar function (122). Cortical granule exocytosis occurs during Anaphase I in *C. elegans* (65). Additionally, zygote permeability decreases between Anaphase I and II (23,25). Given the timing of cortical granule exocytosis beginning at Anaphase I and zinc exocytosis at beginning at Anaphase II, it is unlikely that zinc is packaged within cortical granules as it is in mammals. Anaphase II occurs approximately 10 minutes after Anaphase I. More likely, zinc exocytosis may serve as one of the final modifications made to the eggshell. To fully understand why zinc accumulates there, further study is warranted to determine the precise area of localization. Timing of eggshell layer formation may provide the first clues to how zinc movement into the eggshell fits within the developmental timeline.

Zinc fluxes are key for proper transition between phases of oocyte maturation

Our *C. elegans* studies have revealed that zinc availability may be key for three particular transition phases of oocyte maturation. First is the release from Prophase I arrest/meiosis re-entry. Initiation of early oocyte maturation and release from Prophase I arrest in *C. elegans* is mediated by a number of factors, including Major Sperm Protein (MSP) and MAPK signaling (10). Since we observed a labile zinc gradient in oocytes prior to fertilization, and then labile zinc influx after fertilization, it is reasonable to speculate that there is some intracellular zinc-responsive mechanism driving rapid zinc influx. Second is the metaphase to anaphase transition in Meiosis II: this transition occurs when the zygote switches from the zinc influx phase to the zinc efflux phase. In mammals, this transition is mediated by Emi2 regulation of the APC/C. Given that there is no known Emi2 homolog in *C. elegans*, we speculate that another zinc-dependent regulator of the APC/C may be at play that does not involve a protracted arrest as is seen in mammals. Third, is the meiosis to mitosis transition. We previously demonstrated that zinc insufficient *C. elegans* zygotes fail to extrude the second polar body during Meiosis II, resulting in hyperploidy, and abnormal spindle positioning beginning as early as mitotic interphase in the 1-Cell stage. Despite retaining the second polar body, the zygote does not arrest in 50% of the time, and instead continues in the cell cycle to the 2-cell stage even though it contains extra chromosomes. This is in contrast to mammals in multiple ways: 32% of those eggs divided symmetrically and retained a Telophase I spindle and arrest at a previously unknown checkpoint (33). Furthermore, cumulus oocyte complexes cultured in 10 μ M TPEN exhibited a single chromatin mass with an incomplete midbody at Telophase I, multiple chromatin masses or cytokinesis failure. All of these phenotypes specifically occur at the transition from Meiosis I to

Meiosis II, and with complete arrest, suggesting that some checkpoints have been activated to prevent further error. The fact that these hyperploid *C. elegans* zygotes progress to mitosis, may indicate that key, known checkpoints did not detect errors under zinc insufficient conditions, and the reason is yet to be investigated.

Our studies with the simple model system *C. elegans*, allowed us to expand and diversify our questions related to zinc function. By conducting both *in vitro* and *in vivo* studies, we were able to place zinc fluxes during meiotic progression within the context of the gonad and the whole organism. This opportunity has allowed us to understand that zinc fluxes are related to meiotic divisions and not mitotic ones. It also shows that zinc fluxes are not critical to maintenance of most of the gonad, but that zinc levels are still important for its function. From our combined studies, we have demonstrated the diverse number of ways zinc regulates germline development. Further speculation on the mechanisms behind zinc fluxes will likely explain its unique function in germline development

CHAPTER 4

GENERAL DISCUSSION

Zinc ion regulation of maturing oocytes is emerging as a major factor in egg development across metazoans. Developing zygotes regulates meiotic progression through two types of zinc fluxes: total and labile. Through previous studies with mammals, we learned that the successful maturation of mammalian oocytes requires a dynamic zinc flux: influx of zinc is required to reach the appropriate quota of an average of 60 billion zinc ions and influx of 10-15 billion zinc ions is required for the completion of the meiotic cell cycle. Studies in *C. elegans* reveal several of these characteristics as well as several important variations in the timing and nature of the zinc flux. The fact that I observed the zinc flux at similar stages of meiotic progression as mammals, speaks to the idea that zinc has been an integral element in sexually reproducing metazoans since early evolution. Furthermore, by utilizing *C. elegans* as a model system, we can move beyond zinc studies in single cells, and also examine more of their reproductive features and compare *in vitro* conditions with *in vivo* ones. Access to the whole reproductive tract will provide the context of how unique zinc fluxes are, and will help in understanding how an organism utilizes zinc signaling from the time before oocytes are formed to the formation of a viable embryo.

Zinc plays a regulatory role in C. elegans germline formation

Zinc insufficiency impairs oogenesis and reduces fecundity in C. elegans

The earliest clues we found in worms is that hermaphrodites cultured under zinc limited conditions produce fewer oocytes, resulting in reduced brood sizes. Brood size reduction was specifically related to oocyte impairments due to zinc insufficiency, since sperm count and function was not adversely affected at 10 μ M TPEN. This early finding provided initial evidence that zinc limitation impacted the reproductive tract, oogenesis, and fecundity (110). Furthermore,

by confirming that mildly limiting zinc levels specifically affects the germline and does not globally impairing other major organs in the worm, suggests that the germline is particularly sensitive to mild zinc limitation relative to somatic cells and organs. My germline studies in *C. elegans* have been complemented by work from Hester et al (109). This group independently confirmed that oogenesis and fecundity is impacted by zinc insufficiency.

By following the chain of events in development within the reproductive cycle, we can even look to the germline stem cells produced in the distal gonad to understand the underlying mechanisms behind oogenesis. One possible explanation raised by Hester et al. is that zinc insufficient hermaphrodites produce more germline stem cells that do not differentiate. They found an extended pachytene region that invaded the proximal region of the gonad. This suggests that the differentiation of GSC's into oocytes may be abnormal (109): too many GSC's persist into the proximal region and a reduced number of oocytes are produced.

Zinc fluxes are generally conserved between C. elegans and mammals

Our work shows that late oocyte maturation and the egg- to-embryo transition is regulated by zinc fluxes in mammals, but it was unknown if the same occurred in invertebrates until we demonstrated that zinc fluxes are conserved in *C. elegans*. Total zinc dramatically increases in *C. elegans*, *X. laevis*, *L. pictus*, and mammals alike, as influx begins after Prophase I arrest. In *M. musculus*, total zinc is increased by 50% from GV to Metaphase II, while the *C. elegans* oocyte rapidly accrues zinc, increasing by 471% from the -1 oocyte to the activated zygote stage (Figure 2.4). After fertilization, the mouse egg expels 20% of total zinc ions from zinc loaded cortical vesicles, while the *C. elegans* zygote expels 31% from the cytoplasm. This general flux pattern persisted throughout evolution, despite regulatory and lifespan differences

and different habitats. Given that we see similar trends across all the above-mentioned metazoans, it brings forth compelling evidence that zinc was co-opted early in evolution to promote egg viability.

Zinc exocytosis is not dependent on Metaphase II arrest

Zinc exocytosis after Metaphase II is a persistent evolutionary characteristic of the meiotic cell cycle in both *C. elegans* and mammals. Mammals arrest in Prophase I and in Metaphase II, while *C. elegans* only arrest at Prophase I. Zinc exocytosis in mammals is dependent on Metaphase II release, but in *C. elegans* zinc exocytosis occurs in the absence of Metaphase II arrest. In mammals, zinc release into the zona pellucida (ZP) occurs post-Metaphase II release either by fertilization or chemical activation (30, 69). Additionally, Emi2 inhibition of the APC/C may operate by zinc-responsive signaling to contribute to Metaphase II arrest in mammals (40). Interestingly, *C. elegans* zygotes do not possess an obvious Emi2 ortholog, and do not undergo Metaphase II arrest, suggesting that an alternative mechanism regulates the metaphase to anaphase transition during the Meiosis II to Mitosis transition.

Zinc fluxes are specific to late oocyte maturation

Utilizing *C. elegans* as a model system provided us the unprecedented opportunity to examine zinc fluxes not only in the context of the live worm, but also as it relates to the gonad. By XFM analysis, we conclude that total zinc levels are constant in all regions of the gonad upstream of the uterus, including the distal, loop, and proximal regions. Furthermore, by observing the zinc/probe complex created with ZincBy-1 exposure in the worm, we determined that labile zinc pools increasingly accumulate as the oocyte mature in the germline. Collectively,

the XFM and ZincBy-1 studies show that drastic changes in total and labile zinc content occur exclusively post-fertilization, and that labile zinc pools are present in a distinct gradient (increasing fluorescence) as oocytes mature, *in vivo*. This gradient in labile zinc over the course of oocyte development may represent labile pools that are rapidly mobilizing to participate in early oocyte maturation processes, such as cortical rearrangement, nuclear re-localization, and nuclear envelope breakdown. These activities normally occur in the -1 oocyte prior to fertilization, so it is logical to hypothesize that the -1 oocyte may have a specialized use for the higher zinc quota in order to be competent for fertilization. Interestingly, I did not detect labile zinc in the nucleus with ZincBy-1, but XFM maps show total zinc is elevated in the nucleus relative to the cytosol. This difference may be due to the inability of ZincBy-1 to compete with nuclear zinc-binding proteins for zinc within the nucleus. Alternatively, ZincBy-1 may be detecting labile pools of zinc that are readily exchangeable during processes that rapidly occur during early stages of oocyte maturation in preparation for fertilization. One can speculate that the difference between opposing labile and total zinc distribution in the nucleus comes from zinc binding to proteins within the nucleus more tightly. Meaning zinc binding proteins in the nucleus have a higher affinity for zinc than ZincBy-1. ZincBy-1 detection of labile zinc in the cytoplasm may reflect the need for rapid zinc mobilization for early oocyte maturation. Zinc would transiently occupy zinc binding regions of zinc finger proteins in order to actively participate in early oocyte maturation.

Zinc export between MII and the 2-Cell stage is slow and progressive compared to the mammalian zinc spark

The zinc exocytosis events in *C. elegans* and mammals differ in two ways. First, the duration of zinc exocytosis is shorter in mammals than *C. elegans*. During post-fertilization stages, *C. elegans* zygotes expel zinc for approximately 23 minutes beginning at the Metaphase II/Anaphase II transition in a continuous and moderate release. In contrast, mammalian zinc exocytosis occurs as a rapid ejection (on average 25 seconds). Second, the number of exocytosis events differs between mammals and *C. elegans*. Zinc efflux occurs only once in *C. elegans* zygotes, while mammalian eggs may eject labile zinc multiple times (30, 69). These stark contrasts may reflect different reproductive strategies and reproductive anatomies.

C. elegans reaches peak fecundity approximately two days after exit from their final larval stage (L4). They self-fertilize, and cell divisions are rapid with no arrest points after fertilization. Furthermore, *C. elegans* produce a high number of progeny within a very short reproductive window. The best reproductive strategy may be to allocate time for a single, moderately paced zinc ejection which may be the best evolved mechanism for producing up to 300 viable progeny. By contrast, mammals produce far fewer progeny over time. Allocation of resources for multiple, rapid zinc sparks, and zinc exocytosis coupled with cortical granule release may be the best reproductive strategy to ensure mammalian reproductive success.

Another factor which may explain the differences in zinc exocytosis, is the location of the germ cell relative to the cell cycle arrest points. In the *C. elegans* reproductive tract, the distance from the ovary to the uterus spans approximately 200 μm , or approximately 20% of the length of the animal. A simple body plan means that the oocyte travels through a short tube in a single direction in the space of approximately 20 minutes after release from Prophase I arrest. In mammals, the oocyte is formed and arrested at Prophase I in the ovary during fetal development and remains there for months or years until Luteinizing Hormone (LH) signals the resumption of

meiosis. Only then does the oocyte progress from Prophase I to Metaphase II arrest. In order for the Metaphase II egg to be available for fertilization it must travel to the fallopian tube. The cell cycle arrest points may reflect on the need to pause the cell cycle, so that the egg is at the right stage by the time it encounters sperm.

Labile zinc may play a role in eggshell function

Labile zinc exits the cytoplasm during exocytosis, and accumulates in the general eggshell region

Our observations show that labile zinc was distributed within the general eggshell region, with no localization with one specific layer, however we have not proven that it originates from the cytoplasm. The eggshell itself has many functions, including osmolarity maintenance, polyspermy block and protection from the environment. The ability of the egg to perform these functions lies in the fact that it possesses multiple layers. To fully understand why zinc accumulates there, further study is warranted to determine the precise area of localization. Probes or mutant strains, which delineate specific layers of the eggshell, would be useful to narrow specific regions of zinc binding.

Timing of zinc exocytosis suggests zinc may not function in the polyspermy block

Labile zinc accumulates in the eggshell throughout zinc exocytosis, however we do not know if zinc accumulated in the eggshell originates from the cytoplasm, or if the zygote absorbs zinc from surrounding somatic cells in the uterus. Since we do not observe accumulation until the Metaphase II to Anaphase II transition, it is likely that labile zinc originates from the cytoplasm. The zygote is fully permeable during the earliest stages of meiosis, and decreases

beginning at Anaphase I. At Anaphase II the zygote is considered impermeable, so zinc acquisition is likely from the cytoplasm, and not the uterus.

Studies in *M. musculus* demonstrated that zinc is released from the cortical granules and binds to the Zona Pellucida (ZP) upon activation, thus altering ZP fibril thickness. Other evidence demonstrates Zn-ZP interaction partially blocks sperm binding (32). In *C. elegans* the chondroitin proteoglycan layer contains cortical granules, but at present, it is unknown if a relationship between zinc exocytosis, permeability changes or eggshell structure that parallels mammals(29). Permeability changes and cortical granule release into the eggshell are mostly complete before zinc exocytosis occurs. Eggshell permeability decreases between Anaphase I and II (63), and cortical granule release begins at Anaphase I (63, 65). Since zinc exocytosis beginning at Anaphase II occurs after these events have initiated, it unlikely that zinc is co-localized with cortical granules or takes part of permeability changes, and therefore may not a polyspermy block factor. Identifying where zinc deposition in the eggshell layers may clarify its function in eggshell formation.

Zinc fluxes are key for the proper transition from meiosis to mitosis

Zinc insufficient zygotes exhibit spindle defects between the meiosis to mitosis transition in in vitro conditions

Treatment of live, isolated *C. elegans* zygotes with TPEN impairs polar body extrusion during Meiosis II. As a result, extra DNA is retained within the cytoplasm, two oocyte pronuclei form along with the sperm pronucleus, leading to a triploid egg (29%). Often, the resulting mitotic spindle is large and abnormally positioned within the cytoplasm. As a result of the defects, only 50% of the zygotes progress to the 2-cell stage. Similar treatment in *M. musculus*

oocytes also display cell cycle defects near the Meiosis I to Meiosis II transition. TPEN treatment resulted in symmetrical divisions (32%), and the cells arrest with retention of the Telophase I spindle intact (33). These abnormalities resulted in cell cycle arrest. In a later experiment, cumulus oocyte complexes cultured in 10 μ M TPEN exhibited a single chromatin mass with an incomplete midbody at Telophase I, multiple chromatin masses or cytokinesis failure. Cell cycle arrest does suggest that the ZI mouse egg may have activated checkpoints to prevent further error. Despite *C. elegans* zygotes ability to progress to mitosis even with extra DNA, suggests that checkpoint mechanisms failed to detect errors under zinc insufficient conditions.

These results, when compared with brood size and hatching experiments that TPEN treatment of isolated, live zygotes is more severe than the effects of growing worms on TPEN containing media. In intact animals, even though TPEN-induced zinc limitation reduced brood size, all of the progeny hatched. Those maturing oocytes have access to zinc stores from the parent worm, which may be particularly crucial in the very early meiotic stages. During early meiosis the zygote is permeable and acquires high levels of zinc. In isolated conditions, the zygotes exhibited several defects when isolated in TPEN. In this scenario, exposure to TPEN during the permeability window produced defects presumably because the zygote wouldn't be able to acquire sufficient zinc from any other source. TPEN presumably, strongly affects zinc availability to perturb zinc function. This leads me to conclude that during zinc acquisition in late oocyte maturation, the worm provides zinc with appropriate concentration and timing to ensure success, and it is likely that permeability window is when the zygote loads zinc acquired from a source within the parent worm.

Checkpoint machinery in the zygote does not consistently detect errors during the meiosis to mitosis transition

Despite clear abnormalities with polar body extrusion, the zygote does not arrest at the metaphase to anaphase transition. There are currently three canonical checkpoints mechanisms in *C. elegans* (DNA damage, apoptosis and spindle assembly(124)), but the zinc insufficient zygote cannot trigger any of these mechanisms. Even with multiple checkpoint mechanisms in place, the zygote exposed to prolonged (exposed to TPEN since permeable stages) zinc insufficiency (TPEN exposure beginning at permeability stages, prior to Meiosis II) can still progress to the 2-cell embryo stage 50% of the time. This population does not activate checkpoint machinery even with extra chromatin and enlarged spindles. How the zygote is able to progress to the 2-cell embryo stage is unknown, but perhaps there are checkpoint mechanisms that will activate at that stage. It is also unclear if the zygote that makes it to the 2-cell stage is able to continue further in the cell cycle or not, or if checkpoint mechanisms during the meiosis to mitosis transition exist, and are zinc-dependent.

Future Directions

Zinc regulation of oogenesis and early maturation

The discovery by Aaron Sue (described in Chapter 3) that labile pools of zinc are present in a gradient as oocytes are positioned closer to the spermatheca, is a very unique observation. The function of this gradient is unknown, but given that the -1 oocyte contains the highest labile zinc concentration and is the only oocyte to participate in early maturation events (nuclear envelope break-down (NEBD), cortical rearrangement, and re-localization of the nucleus toward

the distal side of the oocyte) may suggest that a particular zinc threshold is required in order to execute them. To test the hypothesis that available zinc pools impact signaling of the zinc finger proteins in the oocytes initially requires identifying abnormal phenotypes within the oocytes under zinc limited conditions, and identifying candidate zinc finger proteins that operate within oocytes that promote proper oocyte formation and early maturation events. Zinc finger proteins participate in cell signaling within the gonad to form oocytes in the proper location, and undergo oocyte maturation properly.

There are two candidate zinc finger proteins that are expressed in the proximal gonad in a similar gradient pattern as zinc, with the -1 oocyte containing the highest expression (13). OMA-1 (oocyte maturation defective) and OMA-2 are both TIS11 zinc finger proteins consisting of the C – X₈₋₁₀ – C – X₅-C-X₃-H motifs and share 64% identity with each other. OMA-1 is a ribonucleoprotein particle (RNP) component in oocytes that represses translation of OMA-1/2 in the oocyte (125). Translational control and transcriptional quiescence in oocytes in most animals contributes to genetic regulation of developing oocytes until meiotic resumption or hormonal stimulation, including MSP signaling in *C. elegans* (126). Repression by OMA-1/2 is an example of a zinc finger protein that functions in this way. OMA1/2 also prevents transcription of *nos-2*, *mom-2*, *zif-1*, and *glp-1* mRNAs by binding their 3'UTRs and suppressing their translation. Translation of these genes directs cells to adopt a somatic fate, so suppression promotes oocyte formation (127, 128). Both OMA-1/2 act redundantly to initiate oocyte maturation, and OMA-1/2 are expressed in fully cellularized worm oocytes with peak expression in the -1 oocyte (13). It is thought that *oma-1* and *oma-2* play a role in early oocyte maturation since OMA-1/2 expressing oocytes are spherical, a characteristic resulting from cytoskeletal rearrangement. They also show a wrinkled nuclear envelope appearance by lamin staining, indicating that NEBD has

occurred. OMA-1/2::GFP fluorescence is irregular and punctate in most oocytes. This suggests that OMA-1/2 containing oocytes can complete nuclear envelope breakdown and cytoskeletal rearrangements. However, OMA-1/2 mutants experience re-replicated DNA and cannot Prophase I (13).

It is interesting that the ZincBy-1 fluorescence intensity pattern mirrors that of OMA-1/2 expression, and may mean there is some type of relationship between zinc availability and OMA-1/2 function. Tests to determine if manipulating zinc levels with TPEN impact Oma expression, and timing of early oocyte maturation events could be important to determine if zinc is involved in preparing the oocytes for fertilization. Conversely, tests to determine if depleting OMA proteins alters the labile zinc gradient, and early oocyte maturation events such as cortical rearrangement, and NEBD timing may reveal if there is a strong OMA/zinc gradient relationship. Those experiments may be the first steps to determining if zinc signaling mediates these activities.

Metaphase II to Anaphase II transition studies

Zinc exocytosis after Metaphase II is a conserved characteristic that *C. elegans* share with mammals, despite the absence of an arrest point in the worm. This suggests that an unknown zinc-dependent mechanism may regulate the metaphase to anaphase transition. A potential candidate for zinc-dependent regulation of the metaphase to anaphase transition in Meiosis II is the Cullin-RING family of ubiquitin ligases. Members of the Cullin family participate in cell cycle regulation, signal transduction, and transcription (129). They are also highly conserved across metazoans. In *C. elegans*, CUL-2 functions along with Elongin-C (adaptor protein) and RBX-1/Roc1 (zinc finger RING box subunit) to properly regulate the metaphase to anaphase

transition in Meiosis II. Other notable functions include cyclin B degradation, and proper mitotic progression. ZIF-1 is a SOCS-box substrate recruitment factor that binds to Elongin-C and targets CCCH-finger polarity proteins for degradation (130). The variable substrate recognition subunit (SRS) includes ZYG-11 (*zygote defective: embryonic lethal*). *Zyg-1* plays similar roles as *cul-2*, and also plays a role in proper Metaphase II timing, PAR-2 (a C3HC4-type RING finger required for embryo polarity) localization, Cyclin B1 and B3 degradation, and cytoplasmic partitioning (130-132).

Mutations in *cul-2* result in Metaphase II delay, failure to degrade cyclin B1 and B3, ectopic localization of PAR-2, aberrant cytoplasmic extensions, non-granular zones in the cytoplasm of the zygote, lack of chromosome condensation, failure to degrade CCCH polarity proteins and cell cycle arrest (131-135). Mutations in *zyg-11* result in similar phenotypes, but polarity protein degradation and cell cycle progression in G1 is normal. Mutations in *zif-1* result in failure to degrade CCCH polarity proteins. A number of these phenotypes are reminiscent of phenotypic aberrations induced by prolonged TPEN exposure including aberrant cytoplasmic partitioning, ectopic localization of PAR-2 and cell cycle arrest.

A potential way to begin to understand how zinc insufficiency could be affecting this pathway is to first monitor the timing between the metaphase to anaphase transition in Meiosis II. Since RNAi depletion and mutants of *zyg-11* and *cul-2* both show lengthy transitions, we can easily verify if that is happening under zinc insufficient conditions with time-lapse microscopy and a worm strain with a GFP labeled spindle. Next, by determining if depleting *cul-2*, *zif-1* or *zyg-11* has any effect on zinc exocytosis, we may be able to uncover the relationship between cell cycle timing and zinc exocytosis. Furthermore, immunofluorescence microscopy would determine the location of some of the members of this pathway within the zygote. Abnormal

staining may indicate specifically when and where defects begin and help to pinpoint the specific players that are impaired by zinc insufficiency.

Embryo polarity studies

There are a number of players involved in establishing egg polarity in *C elegans*, and some of those markers are zinc finger proteins. PIE-1 (Pharynx and Intestine in Excess) is a C-x8-x5C-C3H type zinc finger protein (136). PIE-1 is a maternal factor and represses RNA polymerase II dependent gene expression in the germline. PAR-2 is a C3HC4 type RING-finger protein. PAR-2 functions to establish the anterior-posterior polarity in the zygote and is localized to the Posterior blast at the cortex of the one and 2-cell embryo. As mentioned in the previous section, mutations in CUL-2, and SOCS-box substrate recruitment factor, ZIF-1 results in ectopic localization of PAR-2 and failure to degrade CCCH polarity proteins. For this reason, studying the effects of zinc insufficiency on embryo polarity would be an appropriate step. To understand how zinc insufficiency impacts embryo polarity, zygote could be isolated in TPEN and observed for alterations of PAR-2 and PIE-1 distribution. Moreover, the distribution of all zinc finger polarity markers should be further evaluated for symmetrical distribution, and changes in protein expression under zinc insufficient conditions. This will be an important observation, since CUL-2 and ZIF-1 degrade CCCH zinc finger proteins. If all zinc finger polarity proteins show symmetrical distribution, it is possible that zinc insufficiency has a sweeping effect on polarity. If symmetry is specific to CCCH containing zinc finger proteins, then it is possible CCCH zinc-finger proteins are not degraded in the appropriate blast cells, and it may suggest that zinc efflux may impact the CUL-2 complex in a similar manner as Emi2 in mammals. An allelic series of mutations within the zinc finger domain of ZIF-1 may demonstrate

if 2-cell stage asymmetry is mediated by ZIF-1 in a zinc-dependent manner. Should this be the case, it would be the first time that zinc-induced asymmetry would be described in Metazoans.

Cytokinesis and polar body extrusion defect studies

The second polar body fails to extrude during Meiosis II under zinc insufficient conditions. As a result, the spindle midbody does not break down with appropriate timing, and extra DNA is retained creating a hyperploid condition, the entire spindle apparatus retracts into the cytoplasm after briefly breaching the cortex, or the entire spindle apparatus never breaches the cortex. Another phenotype that I observed under zinc insufficient conditions is a cytokinesis defect. Improper segregation of the cytoplasm occurred during pronuclear migration and 2-cell stage establishment. These were both obvious and interesting phenotypes resulting from zinc insufficiency, but the mechanism behind these phenotypes needs to be further investigated. A potential option for pursuing the mechanism behind these phenotypes is to study the role that the conserved protein Anillin may play in the inappropriate polar body extrusion.

Anillins are involved in cytoskeletal dynamics during cytokinesis and cellularization. In general, they form a bridge, that crosslink the cytoskeletal components filamentous actin (F-actin), myosin II (137) and RhoA (138). In *C. elegans*, Anillins are active in the early embryo, and participate in cortical contractility activities including polar body extrusion, cortical ruffling, pseudocleavage and cytokinesis. There are three homologs in *C. elegans*: ANI-1, ANI-2, and ANI-3 (139). Depletion of *ani-1* by RNAi leads to polar body extrusion failure, and hyperploidy in developing embryos (140), phenotypes that are reminiscent of zinc insufficiency. Polar body extrusion failure in *ani-1* depleted zygotes show that the DNA meant for extrusion never penetrates the cytoplasmic cortex because ANI-1 is not present to provide structural support for

myosin and F-actin to bundle and contract to separate the DNA from the spindle apparatus.

Furthermore, there is evidence that Anillins contribute to proper polarity establishment in the early embryo. Embryos that were *ani-1* depleted by RNAi revealed symmetrical distribution of two major polarity markers, PAR-2 (in 69% of embryos) and PIE-1 (in 56% of embryos) (138). This symmetry phenotype is reminiscent of what I have seen in my preliminary work with PIE-1 and PAR-2 (unpublished results), which may suggest that zinc plays a role in successful polar body extrusion, cytokinesis and maintenance of embryo asymmetry.

When Anillin is depleted in the late embryo, the membranes of *Drosophila melanogaster* embryo experience blebbing and spindle midbody abscission impairments (141). This particular phenotype occurs similarly when citron kinase (CIT-K) is also depleted (142). *Cit-k* encodes a serine/threonine-protein kinase, and CIT-K complexes with Anillin and localizes to cleavage furrows via RhoA, and localizes to the spindle midbody in later stages of cytokinesis in mammalian zygotes and in HeLa cells (143). CIT-K contains a C-6-H-2 zinc finger domain, but its function has not been studied. I performed a preliminary test to see which *C. elegans* genes are homologous to *cit-k*. BLAST analysis of the human CIT-K protein sequence against *C. elegans* revealed *mrck-1* as the gene with the closest homology. *Mrck-1* is expressed during embryogenesis and affects embryonic elongation via MLC-4/myosin regulatory light chain (144). Utilizing the zinc finger predictability software ZincExplorer as a quick, first-pass tool, I inputted the *C. elegans mrck-1* sequence to determine if any sites within the gene were highly predicted to be zinc finger domains (145). Indeed, ZincExplorer found predicted C-7-H-2 (Figure C.3) with a high prediction scores above 0.4 (predictability threshold) in multiple locations of the protein sequence. MRCK-1 could be the first zinc finger candidate to study within the context of polar body extrusion and cytokinesis impairments.

If *mrck-1* is the correct candidate gene, it is possible that zinc insufficiency impairs MRCK-1 function, preventing MRCK-1 from complexing with Anillin, RhoA, and myosin, thus preventing timely spindle midbody abscission in Meiosis II and perturbing cytokinesis activities. Follow up studies could entail depleting *mrck-1* by RNAi and delete sections of the zinc finger domain via CRISPR to see how that affects Anillin, RhoA and myosin localization to the spindle at polar body extrusion in meiosis II. Zinc rescue of mislocalized abscission components could show zinc-dependency. Worm strains are available that are mCherry or GFP labeled for Anillin, RhoA and myosin, so visualization via microscopy is possible.

Eggshell studies

We previously described that labile zinc accumulates in the general eggshell region during zinc efflux. We currently do not know the origin of labile zinc that ends in the eggshell space (if it is translocating from the cytoplasm). It is also unknown where labile pools of zinc are localized within the eggshell layers. To answer these questions, we may be able to follow zinc accumulation during meiotic progression by using the radiotracer ^{65}Zn . The developing zygote loses permeability over time, and when the eggshell is fully formed it is less likely to absorb elements from the outside. Radioactive zinc labeling experiments would enable us to test the hypothesis that zinc is not coming from the outside of the zygote after permeability loss. Next, it would be important to determine if zinc is localized to a specific eggshell layer under zinc sufficient and insufficient conditions. TPEN treatment of developing zygotes may lead to eggshell impairments such as misshapen embryos from osmolarity changes, thin-looking eggshells and embryos that do not hatch.

Additionally, time-lapse imaging utilizing worm strains labeled for different eggshell components would be useful to determine if there is co-localization with ZincBy-1. For example, CAV-1::GFP, UGTP::GFP both mark components that are contained within cortical granules that can be used to compare timing of zinc exocytosis with cortical granule incorporation into the eggshell in live-imaging experiments. Another option could be to remove the eggshell and submit controls and zinc insufficient groups for XFM, to determine if total zinc content is altered in these conditions, which could inform us if zinc quotas are met.

Significance of the thesis

My work introduces zinc as a major regulator of germline development in *C. elegans*. Through my zinc studies of the germline, I have added *C. elegans* to the growing list of metazoans that utilize zinc to contribute to the production of healthy oocytes. All of the previous studies in other metazoans have provided substantial insight into the characterization and mechanisms zinc is known to play in oocyte viability. Here, I have utilized *C. elegans* to not only understand how change in zinc quotas and fluctuations in of labile zinc change throughout oocyte maturation, but I have also described for the first time, the zinc quotas in the three major regions of the gonad, and determined that zinc fluxes are specific to late stages of oocyte maturation and nowhere else within the gonad. This was an unprecedented opportunity since such experiments cannot be conducted in other model systems. *C. elegans* is a desirable model system to study zinc dynamics in the germline at multiple points of development. Zinc studies in *C. elegans* has helped us to further understand the factors involved in egg quality. Because the germline has distinct spatio-temporal features that are not available in the other model systems mentioned in this thesis, we can exploit *C. elegans* as a simple model system in a number of

ways experimentally, therefore diversifying the types of zinc-related questions one can ask. Moreover, by conducting both *in vitro* and *in vivo* studies, I was able to place zinc fluxes during oocyte maturation within the context of the gonad and the whole organism. This is very meaningful, because these studies demonstrate the diverse number of ways zinc regulates germline development, and we can further speculate on why zinc has been co-opted throughout evolution to function in the germline. Furthermore, my work has scratched the surface for how zinc is regulated within the germline, and now there are several additional opportunities to study zinc mechanism of action during the earliest stages of development.

REFERENCES

1. Zhang K, Smith GW. Maternal control of early embryogenesis in mammals. *Reprod Fertil Dev.* 2015;27(6):880-96. Epub 2015/02/20. doi: 10.1071/RD14441. PubMed PMID: 25695370; PMCID: PMC4545470.
2. Whitaker M. Control of meiotic arrest. *Rev Reprod.* 1996;1(2):127-35. Epub 1996/05/01. PubMed PMID: 9414449.
3. Von Stetina JR, Orr-Weaver TL. Developmental control of oocyte maturation and egg activation in metazoan models. *Cold Spring Harb Perspect Biol.* 2011;3(10):a005553. doi: 10.1101/cshperspect.a005553. PubMed PMID: 21709181; PMCID: PMC3179337.
4. Han SJ, Chen R, Paronetto MP, Conti M. Wee1B is an oocyte-specific kinase involved in the control of meiotic arrest in the mouse. *Curr Biol.* 2005;15(18):1670-6. Epub 2005/09/20. doi: 10.1016/j.cub.2005.07.056. PubMed PMID: 16169490.
5. Nader N, Courjaret R, Dib M, Kulkarni RP, Machaca K. Release from *Xenopus* oocyte prophase I meiotic arrest is independent of a decrease in cAMP levels or PKA activity. *Development.* 2016;143(11):1926-36. Epub 2016/04/29. doi: 10.1242/dev.136168. PubMed PMID: 27122173.
6. Spike CA, Coetzee D, Eichten C, Wang X, Hansen D, Greenstein D. The TRIM-NHL protein LIN-41 and the OMA RNA-binding proteins antagonistically control the prophase-to-metaphase transition and growth of *Caenorhabditis elegans* oocytes. *Genetics.* 2014;198(4):1535-58. Epub 2014/09/28. doi: 10.1534/genetics.114.168831. PubMed PMID: 25261698; PMCID: PMC4256770.
7. Peng XR, Hsueh AJ, LaPolt PS, Bjersing L, Ny T. Localization of luteinizing hormone receptor messenger ribonucleic acid expression in ovarian cell types during follicle development and ovulation. *Endocrinology.* 1991;129(6):3200-7. Epub 1991/12/01. doi: 10.1210/endo-129-6-3200. PubMed PMID: 1954899.
8. Norris RP, Freudzon M, Mehlmann LM, Cowan AE, Simon AM, Paul DL, Lampe PD, Jaffe LA. Luteinizing hormone causes MAP kinase-dependent phosphorylation and closure of connexin 43 gap junctions in mouse ovarian follicles: one of two paths to meiotic resumption. *Development.* 2008;135(19):3229-38. Epub 2008/09/09. doi: 10.1242/dev.025494. PubMed PMID: 18776144; PMCID: PMC2572224.
9. Norris RP, Ratzan WJ, Freudzon M, Mehlmann LM, Krall J, Movsesian MA, Wang H, Ke H, Nikolaev VO, Jaffe LA. Cyclic GMP from the surrounding somatic cells regulates cyclic AMP and meiosis in the mouse oocyte. *Development.* 2009;136(11):1869-78. Epub 2009/05/12. doi: 10.1242/dev.035238. PubMed PMID: 19429786; PMCID: PMC2680110.
10. Greenstein D. Control of oocyte meiotic maturation and fertilization. *WormBook.* 2005:1-12. doi: 10.1895/wormbook.1.53.1. PubMed PMID: 18050412; PMCID: PMC4781623.
11. Miller MA, Ruest PJ, Kosinski M, Hanks SK, Greenstein D. An Eph receptor sperm-sensing control mechanism for oocyte meiotic maturation in *Caenorhabditis elegans*. *Genes Dev.*

- 2003;17(2):187-200. Epub 2003/01/21. doi: 10.1101/gad.1028303. PubMed PMID: 12533508; PMCID: PMC195972.
12. Lee MH, Ohmachi M, Arur S, Nayak S, Francis R, Church D, Lambie E, Schedl T. Multiple functions and dynamic activation of MPK-1 extracellular signal-regulated kinase signaling in *Caenorhabditis elegans* germline development. *Genetics*. 2007;177(4):2039-62. Epub 2007/12/13. doi: 10.1534/genetics.107.081356. PubMed PMID: 18073423; PMCID: PMC2219468.
 13. Detwiler MR, Reuben M, Li X, Rogers E, Lin R. Two zinc finger proteins, OMA-1 and OMA-2, are redundantly required for oocyte maturation in *C. elegans*. *Dev Cell*. 2001;1(2):187-99. Epub 2001/11/13. PubMed PMID: 11702779.
 14. Hall DH, Winfrey, V.P., Blaeuer, G., Hoffman, L.H., Furuta, T., Rose, K.L., Hobert, O., Greenstein D. Ultrastructural features of the adult hermaphrodite gonad of *Caenorhabditis elegans*: relations between the germ line and soma. *Developmental Biology*. 1999(212):101-23.
 15. Tunquist BJ, Maller JL. Under arrest: cytostatic factor (CSF)-mediated metaphase arrest in vertebrate eggs. *Genes Dev*. 2003;17(6):683-710. Epub 2003/03/26. doi: 10.1101/gad.1071303. PubMed PMID: 12651887.
 16. Madgwick S, Jones KT. How eggs arrest at metaphase II: MPF stabilization plus APC/C inhibition equals cytostatic factor. *Cell Division*. 2007;2:4.
 17. Horner VL, Wolfner MF. Transitioning from egg to embryo: triggers and mechanisms of egg activation. *Dev Dyn*. 2008;237(3):527-44. Epub 2008/02/12. doi: 10.1002/dvdy.21454. PubMed PMID: 18265018.
 18. KT J. Mammalian egg activation: From Ca²⁺ spiking to cell cycle progression. *Reproduction*. 2004;130:813-23.
 19. Ducibella TFR. The roles of Ca²⁺, downstream protein kinases, and oscillatory signaling in regulating fertilization and the activation of development. *Developmental Biology*. 2008;315:257-79.
 20. Backs J, Stein P., Backs, T., Duncan, FE, Grueter, CE., McAnally J., Qi, X., Schultz, RM, Olson EN. The γ isoform of CaM kinase II controls mouse egg activation by regulating cell cycle resumption. *Proceedings of the National Academy of Sciences*. 2010;107:81-6.
 21. Timourian H. The effect of zinc on sea urchin morphogenesis. *J Exp Zool*. 1968;169(1):121-32. Epub 1968/09/01. doi: 10.1002/jez.1401690114. PubMed PMID: 5696639.
 22. Falchuk KH, Montorzi M. Zinc physiology and biochemistry in oocytes and embryos. *Biometals*. 2001;14(3-4):385-95. Epub 2002/02/08. PubMed PMID: 11831467.
 23. Nomizu T, Falchuk KH, Vallee BL. Zinc, iron, and copper contents of *Xenopus laevis* oocytes and embryos. *Mol Reprod Dev*. 1993;36(4):419-23. Epub 1993/12/01. doi: 10.1002/mrd.1080360403. PubMed PMID: 8305203.
 24. Montorzi M, Falchuk KH, Vallee BL. *Xenopus laevis* vitellogenin is a zinc protein. *Biochem Biophys Res Commun*. 1994;200(3):1407-13. Epub 1994/05/16. doi: 10.1006/bbrc.1994.1607. PubMed PMID: 8185593.
 25. Falchuk KH, Montorzi M, Vallee BL. Zinc uptake and distribution in *Xenopus laevis* oocytes and embryos. *Biochemistry*. 1995;34(50):16524-31. Epub 1995/12/19. PubMed PMID: 8845382.
 26. Montorzi M, Falchuk KH, Vallee BL. Vitellogenin and lipovitellin: zinc proteins of *Xenopus laevis* oocytes. *Biochemistry*. 1995;34(34):10851-8. Epub 1995/08/29. PubMed PMID: 7662665.

27. Riggio M, Filosa S, Parisi E, Scudiero R. Changes in zinc, copper and metallothionein contents during oocyte growth and early development of the teleost *Danio rerio* (zebrafish). *Comp Biochem Physiol C Toxicol Pharmacol*. 2003;135(2):191-6. Epub 2003/07/16. PubMed PMID: 12860058.
28. Kong BY, Duncan FE, Que EL, Kim AM, O'Halloran TV, Woodruff TK. Maternally-derived zinc transporters ZIP6 and ZIP10 drive the mammalian oocyte-to-egg transition. *Mol Hum Reprod*. 2014;20(11):1077-89. doi: 10.1093/molehr/gau066. PubMed PMID: 25143461; PMCID: PMC4209882.
29. Que EL, Bleher R, Duncan FE, Kong BY, Gleber SC, Vogt S, Chen S, Garwin SA, Bayer AR, Dravid VP, Woodruff TK, O'Halloran TV. Quantitative mapping of zinc fluxes in the mammalian egg reveals the origin of fertilization-induced zinc sparks. *Nat Chem*. 2015;7(2):130-9. doi: 10.1038/nchem.2133. PubMed PMID: 25615666; PMCID: PMC4315321.
30. Kim AM, Bernhardt ML, Kong BY, Ahn RW, Vogt S, Woodruff TK, O'Halloran TV. Zinc sparks are triggered by fertilization and facilitate cell cycle resumption in mammalian eggs. *ACS Chem Biol*. 2011;6(7):716-23. doi: 10.1021/cb200084y. PubMed PMID: 21526836; PMCID: PMC3171139.
31. Duncan FE, Que EL, Zhang N, Feinberg EC, O'Halloran TV, Woodruff TK. The zinc spark is an inorganic signature of human egg activation. *Sci Rep*. 2016;6:24737. doi: 10.1038/srep24737. PubMed PMID: 27113677; PMCID: PMC4845039.
32. Que EL, Duncan FE, Bayer AR, Philips SJ, Roth EW, Bleher R, Gleber SC, Vogt S, Woodruff TK, O'Halloran TV. Zinc sparks induce physiochemical changes in the egg zona pellucida that prevent polyspermy. *Integr Biol (Camb)*. 2017;9(2):135-44. Epub 2017/01/20. doi: 10.1039/c6ib00212a. PubMed PMID: 28102396; PMCID: PMC5439353.
33. Kim AM, Vogt S, O'Halloran TV, Woodruff TK. Zinc availability regulates exit from meiosis in maturing mammalian oocytes. *Nat Chem Biol*. 2010;6(9):674-81. doi: 10.1038/nchembio.419. PubMed PMID: 20693991; PMCID: PMC2924620.
34. Kong BY, Bernhardt ML, Kim AM, O'Halloran TV, Woodruff TK. Zinc maintains prophase I arrest in mouse oocytes through regulation of the MOS-MAPK pathway. *Biol Reprod*. 2012;87(1):11, 1-2. doi: 10.1095/biolreprod.112.099390. PubMed PMID: 22539682; PMCID: PMC3406555.
35. Shoji S, Muto, Y., Ikeda, M., He, F., Tsuda, K., Ohsawa, N., Akasaka, R., Terada, T., Wakiyama, M., Shirozu, M., Yokoyama, S. The zinc-binding region (ZBR) fragment of Emi2 can inhibit APC/C by targeting its association with the coactivator Cdc20 and UBE2C-mediated ubiquitylation. *FEBS Open Bio*. 2014;4:689-703.
36. Schmidt A, Duncan PI, Rauh NR, Sauer G, Fry AM, Nigg EA, Mayer TU. *Xenopus* polo-like kinase Plx1 regulates XErp1, a novel inhibitor of APC/C activity. *Genes Dev*. 2005;19(4):502-13. Epub 2005/02/17. doi: 10.1101/gad.320705. PubMed PMID: 15713843; PMCID: PMC548950.
37. Shoji S, Yoshida N, Amanai M, Ohgishi M, Fukui T, Fujimoto S, Nakano Y, Kajikawa E, Perry AC. Mammalian Emi2 mediates cytostatic arrest and transduces the signal for meiotic exit via Cdc20. *EMBO J*. 2006;25(4):834-45. Epub 2006/02/04. doi: 10.1038/sj.emboj.7600953. PubMed PMID: 16456547; PMCID: PMC1383546.
38. Suzuki T, Suzuki, E., Yoshida, N., Kubo, A., Li, H., Okuda, E., Amanai, M., Perry, AC. Mouse Emi2 as a distinctive regulatory hub in second meiotic metaphase. *Development*. 2010;137(19):3281-91.

39. Bernhardt ML, Kim AM, O'Halloran TV, Woodruff TK. Zinc requirement during meiosis I-meiosis II transition in mouse oocytes is independent of the MOS-MAPK pathway. *Biol Reprod.* 2011;84(3):526-36. doi: 10.1095/biolreprod.110.086488. PubMed PMID: 21076080; PMCID: PMC3043131.
40. Bernhardt ML, Kong BY, Kim AM, O'Halloran TV, Woodruff TK. A zinc-dependent mechanism regulates meiotic progression in mammalian oocytes. *Biol Reprod.* 2012;86(4):114. Epub 2012/02/04. doi: 10.1095/biolreprod.111.097253. PubMed PMID: 22302686; PMCID: PMC3338659.
41. Riddle DL, Blumenthal T, Meyer BJ, Priess JR. Introduction to *C. elegans*. In: Riddle DL, Blumenthal T, Meyer BJ, Priess JR, editors. *C elegans II*. 2nd ed. Cold Spring Harbor (NY)1997.
42. Lints R, Hall, D.H. Reproductive system, germline 2009.
43. Bruinsma JJ, Jirakulaporn T, Muslin AJ, Kornfeld K. Zinc ions and cation diffusion facilitator proteins regulate Ras-mediated signaling. *Dev Cell.* 2002;2(5):567-78. PubMed PMID: 12015965.
44. Bruinsma JJ, Schneider DL, Davis DE, Kornfeld K. Identification of mutations in *Caenorhabditis elegans* that cause resistance to high levels of dietary zinc and analysis using a genomewide map of single nucleotide polymorphisms scored by pyrosequencing. *Genetics.* 2008;179(2):811-28. doi: 10.1534/genetics.107.084384. PubMed PMID: 18505880; PMCID: PMC2429876.
45. Davis DE, Roh HC, Deshmukh K, Bruinsma JJ, Schneider DL, Guthrie J, Robertson JD, Kornfeld K. The cation diffusion facilitator gene *cdf-2* mediates zinc metabolism in *Caenorhabditis elegans*. *Genetics.* 2009;182(4):1015-33. doi: 10.1534/genetics.109.103614. PubMed PMID: 19448268; PMCID: PMC2728845.
46. Dietrich N, Tan CH, Cubillas C, Earley BJ, Kornfeld K. Insights into zinc and cadmium biology in the nematode *Caenorhabditis elegans*. *Arch Biochem Biophys.* 2016;611:120-33. doi: 10.1016/j.abb.2016.05.021. PubMed PMID: 27261336.
47. Roh HC, Collier S, Deshmukh K, Guthrie J, Robertson JD, Kornfeld K. *ttn-1* encodes CDF transporters that excrete zinc from intestinal cells of *C. elegans* and act in a parallel negative feedback circuit that promotes homeostasis. *PLoS Genet.* 2013;9(5):e1003522. doi: 10.1371/journal.pgen.1003522. PubMed PMID: 23717214; PMCID: PMC3662639.
48. Roh HC, Collier S, Guthrie J, Robertson JD, Kornfeld K. Lysosome-related organelles in intestinal cells are a zinc storage site in *C. elegans*. *Cell Metab.* 2012;15(1):88-99. doi: 10.1016/j.cmet.2011.12.003. PubMed PMID: 2225878; PMCID: PMC4026189.
49. Roh HC, Dimitrov I, Deshmukh K, Zhao G, Warnhoff K, Cabrera D, Tsai W, Kornfeld K. A modular system of DNA enhancer elements mediates tissue-specific activation of transcription by high dietary zinc in *C. elegans*. *Nucleic Acids Res.* 2015;43(2):803-16. doi: 10.1093/nar/gku1360. PubMed PMID: 25552416; PMCID: PMC4333406.
50. Warnhoff K, Roh HC, Kocsisova Z, Tan CH, Morrison A, Crosswell D, Schneider DL, Kornfeld K. The Nuclear Receptor HIZR-1 Uses Zinc as a Ligand to Mediate Homeostasis in Response to High Zinc. *PLoS Biol.* 2017;15(1):e2000094. doi: 10.1371/journal.pbio.2000094. PubMed PMID: 28095401; PMCID: PMC5240932.
51. Lui DY, Colaiacovo MP. Meiotic development in *Caenorhabditis elegans*. *Adv Exp Med Biol.* 2013;757:133-70. doi: 10.1007/978-1-4614-4015-4_6. PubMed PMID: 22872477; PMCID: PMC3764601.

52. Kershner A, Crittenden SL, Friend K, Sorensen EB, Porter DF, Kimble J. Germline stem cells and their regulation in the nematode *Caenorhabditis elegans*. *Adv Exp Med Biol*. 2013;786:29-46. doi: 10.1007/978-94-007-6621-1_3. PubMed PMID: 23696350.
53. Yang Y, Han SM, Miller MA. MSP hormonal control of the oocyte MAP kinase cascade and reactive oxygen species signaling. *Dev Biol*. 2010;342(1):96-107. doi: 10.1016/j.ydbio.2010.03.026. PubMed PMID: 20380830; PMCID: PMC4077032.
54. SIngsong A. Every Sperm Is Sacred: Fertilization in *Caenorhabditis elegans*. *Developmental Biology*. 2001;230:101-9. doi: 10.1006/dbio.2000.0118.
55. Evans TC, Hunter, C.P. Translational control of maternal RNAs. In: Priess JR, Seydoux, Geraldine, editor. *WormBook*, ed The *C. elegans* Research Community, *Wormbook2005*.
56. McCarter J, Bartlett B, Dang T, Schedl T. Soma-germ cell interactions in *Caenorhabditis elegans*: multiple events of hermaphrodite germline development require the somatic sheath and spermathecal lineages. *Dev Biol*. 1997;181(2):121-43. Epub 1997/01/15. doi: 10.1006/dbio.1996.8429. PubMed PMID: 9013925.
57. Wolff ID, Tran MV, Mullen TJ, Villeneuve AM, Wignall SM. Assembly of *Caenorhabditis elegans* acentrosomal spindles occurs without evident microtubule-organizing centers and requires microtubule sorting by KLP-18/kinesin-12 and MESP-1. *Mol Biol Cell*. 2016;27(20):3122-31. Epub 2016/08/26. doi: 10.1091/mbc.E16-05-0291. PubMed PMID: 27559133; PMCID: PMC5063619.
58. Wignall SM, Villeneuve AM. Lateral microtubule bundles promote chromosome alignment during acentrosomal oocyte meiosis. *Nat Cell Biol*. 2009;11(7):839-44. doi: 10.1038/ncb1891. PubMed PMID: 19525937; PMCID: PMC2760407.
59. Muscat CC, Torre-Santiago KM, Tran MV, Powers JA, Wignall SM. Kinetochores-independent chromosome segregation driven by lateral microtubule bundles. *Elife*. 2015;4:e06462. Epub 2015/05/31. doi: 10.7554/eLife.06462. PubMed PMID: 26026148; PMCID: PMC4481507.
60. Fabritius AS, Ellefson ML, McNally FJ. Nuclear and spindle positioning during oocyte meiosis. *Curr Opin Cell Biol*. 2011;23(1):78-84. Epub 2010/08/17. doi: 10.1016/j.ceb.2010.07.008. PubMed PMID: 20708397; PMCID: PMC2994957.
61. McCarter J, Bartlett B, Dang T, Schedl T. On the control of oocyte meiotic maturation and ovulation in *Caenorhabditis elegans*. *Dev Biol*. 1999;205(1):111-28. doi: 10.1006/dbio.1998.9109. PubMed PMID: 9882501.
62. Oegema K, Hyman AA. Cell division. *WormBook*. 2006:1-40. doi: 10.1895/wormbook.1.72.1. PubMed PMID: 18050484; PMCID: PMC4780891.
63. Olson SK, Greenan G, Desai A, Muller-Reichert T, Oegema K. Hierarchical assembly of the eggshell and permeability barrier in *C. elegans*. *J Cell Biol*. 2012;198(4):731-48. doi: 10.1083/jcb.201206008. PubMed PMID: 22908315; PMCID: PMC3514041.
64. Stein KK, Golden A. The *C. elegans* eggshell. *WormBook*. 2015:1-35. doi: 10.1895/wormbook.1.179.1. PubMed PMID: 26715360.
65. Bembenek JN, Richie, C.T., Squirrell, J.M., Campbell, J.M., Eliceriri, K.W., Poteryaev, D., Spang, A., Golden, A., White, J.G. Cortical granule exocytosis in *C. elegans* is regulated by cell cycle components including separase. *Development*. 2007;134(21):3837-48.
66. Beyersmann D, Haase H. Functions of zinc in signaling, proliferation and differentiation of mammalian cells. *Biometals*. 2001;14(3-4):331-41. PubMed PMID: 11831463.

67. Haase H, Maret W. The Regulatory and Signaling Functions of Zinc Ions in Human Cellular Physiology. *Cellular and Molecular Biology of Metals*. 2010:181-212. doi: Doi 10.1201/9781420059984-C8. PubMed PMID: WOS:000281677300009.
68. Bohnsack BL, Hirschi KK. Nutrient regulation of cell cycle progression. *Annual review of nutrition*. 2004;24:433-53. doi: 10.1146/annurev.nutr.23.011702.073203. PubMed PMID: 15189127.
69. Zhang N, Duncan FE, Que EL, O'Halloran TV, Woodruff TK. The fertilization-induced zinc spark is a novel biomarker of mouse embryo quality and early development. *Sci Rep*. 2016;6:22772. doi: 10.1038/srep22772. PubMed PMID: 26987302; PMCID: PMC4796984.
70. Suzuki T, Yoshida N, Suzuki E, Okuda E, Perry AC. Full-term mouse development by abolishing Zn²⁺-dependent metaphase II arrest without Ca²⁺ release. *Development*. 2010;137(16):2659-69. doi: 10.1242/dev.049791. PubMed PMID: 20591924.
71. Suzuki T, Suzuki E, Yoshida N, Kubo A, Li H, Okuda E, Amanai M, Perry AC. Mouse Emi2 as a distinctive regulatory hub in second meiotic metaphase. *Development*. 2010;137(19):3281-91. doi: 10.1242/dev.052480. PubMed PMID: 20724447; PMCID: PMC2934736.
72. Tian X, Diaz FJ. Zinc depletion causes multiple defects in ovarian function during the periovulatory period in mice. *Endocrinology*. 2012;153(2):873-86. doi: 10.1210/en.2011-1599. PubMed PMID: 22147014; PMCID: PMC3275394.
73. Lints R, Hall, D.H. . Reproductive system, germline. *WormAtlas*. 2009.
74. Tian X, Anthony K, Neuberger T, Diaz FJ. Preconception zinc deficiency disrupts postimplantation fetal and placental development in mice. *Biol Reprod*. 2014;90(4):83. doi: 10.1095/biolreprod.113.113910. PubMed PMID: 24599289; PMCID: PMC4076385.
75. Tian X, Diaz FJ. Acute dietary zinc deficiency before conception compromises oocyte epigenetic programming and disrupts embryonic development. *Dev Biol*. 2013;376(1):51-61. doi: 10.1016/j.ydbio.2013.01.015. PubMed PMID: 23348678; PMCID: PMC3601821.
76. L'Hernault SW. Spermatogenesis. *WormBook*. 2006:1-14. doi: 10.1895/wormbook.1.85.1. PubMed PMID: 18050478; PMCID: PMC4781361.
77. Lints R, Hall, D.H. Male introduction. *WormAtlas*. 2009.
78. Corsi AK, Wightman, B., Chalfie, M. A transparent window into biology: A primer on *Caenorhabditis elegans*. *WormBook*, ed The *Caelegans* Research Community. 2015.
79. Kimble J, Crittenden SL. Controls of germline stem cells, entry into meiosis, and the sperm/oocyte decision in *Caenorhabditis elegans*. *Annu Rev Cell Dev Biol*. 2007;23:405-33. doi: 10.1146/annurev.cellbio.23.090506.123326. PubMed PMID: 17506698.
80. Wignall SM, Villeneuve AM. Lateral microtubule bundles promote chromosome alignment during acentrosomal oocyte meiosis. *Nature cell biology*. 2009;11(7):839-44. Epub 2009/06/16. doi: 10.1038/ncb1891. PubMed PMID: 19525937; PMCID: 2760407.
81. Wormbase. Strain N2 2016. Available from: http://www.wormbase.org/species/c_elegans/strain/N2-02--10.
82. Wormbase. fog-1 2016. Available from: http://www.wormbase.org/species/c_elegans/gene/WBGene00001481-0-9g-3.
83. Stiernagle T. Maintenance of *C. elegans*. *WormBook*. 2006:1-11. doi: 10.1895/wormbook.1.101.1. PubMed PMID: 18050451; PMCID: PMC4781397.

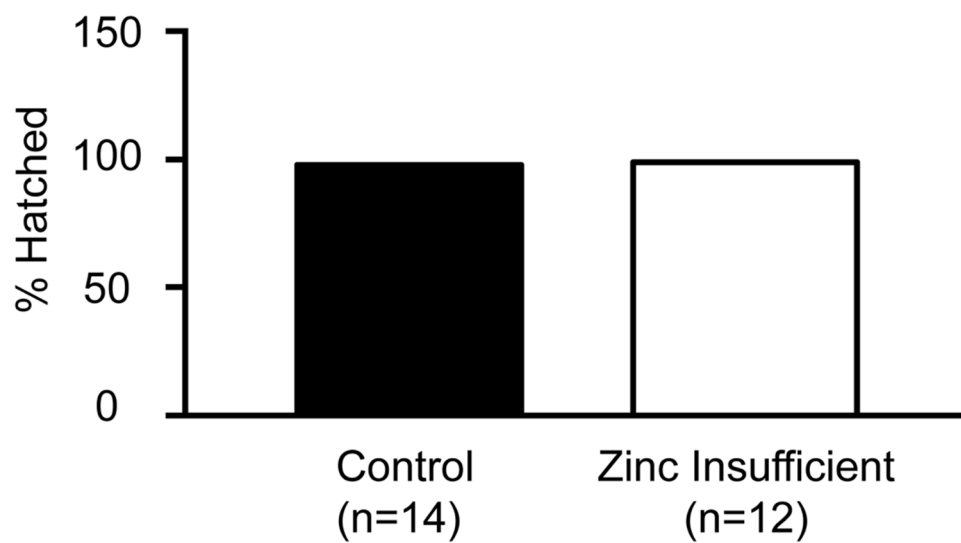
84. MacNeil LT, Watson E, Arda HE, Zhu LJ, Walhout AJ. Diet-induced developmental acceleration independent of TOR and insulin in *C. elegans*. *Cell*. 2013;153(1):240-52. doi: 10.1016/j.cell.2013.02.049. PubMed PMID: 23540701; PMCID: PMC3821073.
85. Lints R, Hall, D.H. Reproductive system, germ line. *WormAtlas*. 2009. doi: doi:10.3908/wormatlas.1.23
86. Lints R, Hall, D.H. Male reproductive system, germ line. *WormAtlas*. 2009. doi: 10.3908/wormatlas.2.16.
87. Zhang S, Kuhn JR. Cell isolation and culture. *WormBook*. 2013:1-39. doi: 10.1895/wormbook.1.157.1. PubMed PMID: 23430760; PMCID: PMC4781291.
88. Martell AE, Smith, R.M. NIST critical stability constants of metal complexes. Plenum, New York 1998.
89. Martell AE, Smith, R.M. NIST critical stability constants of metal complexes. NIST Standard Reference Database 46, v 50. Plenum, New York 1998.
90. Gonczy P, Schnabel H, Kaletta T, Amores AD, Hyman T, Schnabel R. Dissection of cell division processes in the one cell stage *Caenorhabditis elegans* embryo by mutational analysis. *J Cell Biol*. 1999;144(5):927-46. PubMed PMID: 10085292; PMCID: PMC2148205.
91. Hall H, Hunt P, Hassold T. Meiosis and sex chromosome aneuploidy: how meiotic errors cause aneuploidy; how aneuploidy causes meiotic errors - Commentary. *Curr Opin Genet Dev*. 2006;16(3):323-9. doi: 10.1016/j.gde.2006.04.011. PubMed PMID: WOS:000238350900018.
92. Hunt PA, Hassold TJ. Human female meiosis: what makes a good egg go bad? *Trends Genet*. 2008;24(2):86-93. doi: 10.1016/j.tig.2007.11.010. PubMed PMID: 18192063.
93. Bird A, Evans-Galea MV, Blankman E, Zhao H, Luo H, Winge DR, Eide DJ. Mapping the DNA binding domain of the Zap1 zinc-responsive transcriptional activator. *J Biol Chem*. 2000;275(21):16160-6. doi: 10.1074/jbc.M000664200. PubMed PMID: 10747942.
94. Bird AJ, Blankman E, Stillman DJ, Eide DJ, Winge DR. The Zap1 transcriptional activator also acts as a repressor by binding downstream of the TATA box in ZRT2. *EMBO J*. 2004;23(5):1123-32. doi: 10.1038/sj.emboj.7600122. PubMed PMID: 14976557; PMCID: PMC380977.
95. Bird AJ, McCall K, Kramer M, Blankman E, Winge DR, Eide DJ. Zinc fingers can act as Zn²⁺ sensors to regulate transcriptional activation domain function. *EMBO J*. 2003;22(19):5137-46. doi: 10.1093/emboj/cdg484. PubMed PMID: 14517251; PMCID: PMC204467.
96. Bird AJ, Swierczek S, Qiao W, Eide DJ, Winge DR. Zinc metalloregulation of the zinc finger pair domain. *J Biol Chem*. 2006;281(35):25326-35. doi: 10.1074/jbc.M600655200. PubMed PMID: 16829533.
97. Evans-Galea MV, Blankman E, Myszka DG, Bird AJ, Eide DJ, Winge DR. Two of the five zinc fingers in the Zap1 transcription factor DNA binding domain dominate site-specific DNA binding. *Biochemistry*. 2003;42(4):1053-61. doi: 10.1021/bi0263199. PubMed PMID: 12549926.
98. Frey AG, Bird AJ, Evans-Galea MV, Blankman E, Winge DR, Eide DJ. Zinc-regulated DNA binding of the yeast Zap1 zinc-responsive activator. *PLoS One*. 2011;6(7):e22535. doi: 10.1371/journal.pone.0022535. PubMed PMID: 21799889; PMCID: PMC3142189.
99. Herbig A, Bird AJ, Swierczek S, McCall K, Mooney M, Wu CY, Winge DR, Eide DJ. Zap1 activation domain 1 and its role in controlling gene expression in response to cellular zinc status. *Mol Microbiol*. 2005;57(3):834-46. doi: 10.1111/j.1365-2958.2005.04734.x. PubMed PMID: 16045625.

100. Wu CY, Roje S, Sandoval FJ, Bird AJ, Winge DR, Eide DJ. Repression of sulfate assimilation is an adaptive response of yeast to the oxidative stress of zinc deficiency. *J Biol Chem*. 2009;284(40):27544-56. doi: 10.1074/jbc.M109.042036. PubMed PMID: 19656949; PMCID: PMC2785683.
101. Gilston BA, Wang S, Marcus MD, Canalizo-Hernandez MA, Swindell EP, Xue Y, Mondragon A, O'Halloran TV. Structural and mechanistic basis of zinc regulation across the *E. coli* Zur regulon. *PLoS Biol*. 2014;12(11):e1001987. doi: 10.1371/journal.pbio.1001987. PubMed PMID: 25369000; PMCID: PMC4219657.
102. Homa ST, Carroll J, Swann K. The role of calcium in mammalian oocyte maturation and egg activation. *Hum Reprod*. 1993;8(8):1274-81. Epub 1993/08/01. PubMed PMID: 8408526.
103. Homa ST. Calcium and meiotic maturation of the mammalian oocyte. *Mol Reprod Dev*. 1995;40(1):122-34. Epub 1995/01/01. doi: 10.1002/mrd.1080400116. PubMed PMID: 7702866.
104. Tosti E. Calcium ion currents mediating oocyte maturation events. *Reprod Biol Endocrinol*. 2006;4:26. Epub 2006/05/11. doi: 10.1186/1477-7827-4-26. PubMed PMID: 16684344; PMCID: PMC1475868.
105. Dean KM, Qin Y, Palmer AE. Visualizing metal ions in cells: an overview of analytical techniques, approaches, and probes. *Biochim Biophys Acta*. 2012;1823(9):1406-15. Epub 2012/04/24. doi: 10.1016/j.bbamcr.2012.04.001. PubMed PMID: 22521452; PMCID: PMC3408866.
106. Maret W. Zinc in Cellular Regulation: The Nature and Significance of "Zinc Signals". *Int J Mol Sci*. 2017;18(11). Epub 2017/11/01. doi: 10.3390/ijms18112285. PubMed PMID: 29088067.
107. Jamnongjit M, Hammes SR. Oocyte maturation: the coming of age of a germ cell. *Semin Reprod Med*. 2005;23(3):234-41. Epub 2005/08/02. doi: 10.1055/s-2005-872451. PubMed PMID: 16059829; PMCID: PMC1482430.
108. Tischer T, Hormanseder R, Mayer TU. The APC/C inhibitor XErp1/Emi2 is essential for *Xenopus* early embryonic divisions. *Science*. 2012;338(6106):520-4.
109. Hester J, Hanna-Rose W, Diaz F. Zinc deficiency reduces fertility in *C. elegans* hermaphrodites and disrupts oogenesis and meiotic progression. *Comp Biochem Physiol C Toxicol Pharmacol*. 2017;191:203-9. Epub 2016/09/25. doi: 10.1016/j.cbpc.2016.09.006. PubMed PMID: 27663471.
110. Mendoza AD, Woodruff TK, Wignall SM, O'Halloran TV. Zinc availability during germline development impacts embryo viability in *Caenorhabditis elegans*. *Comp Biochem Physiol C Toxicol Pharmacol*. 2017;191:194-202. Epub 2016/09/25. doi: 10.1016/j.cbpc.2016.09.007. PubMed PMID: 27664515; PMCID: PMC5210184.
111. Barton MK, Kimble J. fog-1, a regulatory gene required for specification of spermatogenesis in the germ line of *Caenorhabditis elegans*. *Genetics*. 1990;125(1):29-39. PubMed PMID: 2341035; PMCID: PMC1204007.
112. Stiernagle T. Maintenance of *C.elegans*. The *C.elegans* Research Community2006. Available from: wormbook.org.
113. Shaham S. Methods in Cell Biology. 2006. In: The *C.elegans* Research Community, Worm Book [Internet].
114. Vogt S. MAPS: A set of software tools for analysis and visualization of 3D X-ray fluorescence data sets. *Journal de Physique IV (proceedings)*. 2003;104:635-8. doi: 10.1051/jp4:20030160.

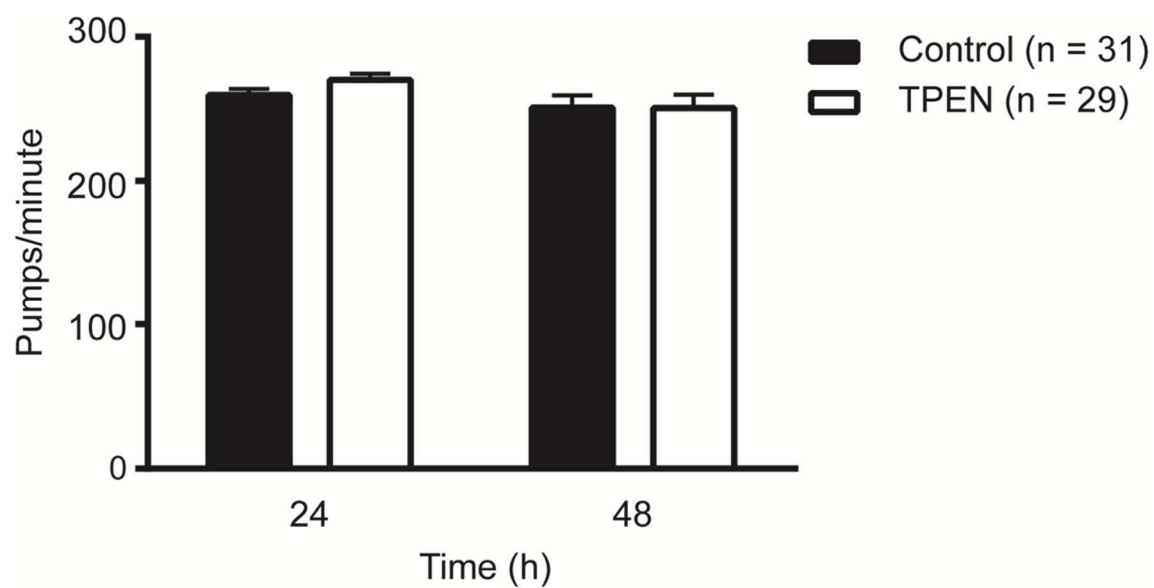
115. Kim ES, L.GAbel, C.V.,Fang-Yen, C. Long-term imaging of *Caenorhabditis elegans* using nanoparticle-mediated immobilization. *PLoS One*. 2013;8(e53419).
116. Schindelin J, Arganda-Carreras I, Frise E, Kaynig V, Longair M, Pietzsch T, Preibisch S, Rueden C, Saalfeld S, Schmid B, Tinevez JY, White DJ, Hartenstein V, Eliceiri K, Tomancak P, Cardona A. Fiji: an open-source platform for biological-image analysis. *Nat Methods*. 2012;9(7):676-82. doi: 10.1038/nmeth.2019. PubMed PMID: 22743772; PMCID: PMC3855844.
117. Schneider CA, Rasband WS, Eliceiri KW. NIH Image to ImageJ: 25 years of image analysis. *Nat Methods*. 2012;9(7):671-5. Epub 2012/08/30. PubMed PMID: 22930834; PMCID: PMC5554542.
118. Merzin M. Applying stereological method in radiology. Volume measurement.: University of Tartu; 2008.
119. Frederickson C. Imaging zinc: old and new tools. *Sci STKE*. 2003;2003(182):pe18. Epub 2003/05/15. doi: 10.1126/stke.2003.182.pe18. PubMed PMID: 12746547.
120. Johnston WL, Dennis JW. The eggshell in the *C. elegans* oocyte-to-embryo transition. *Genesis*. 2012;50(4):333-49. doi: 10.1002/dvg.20823. PubMed PMID: 22083685.
121. Johnston WL, Krizus A, Dennis JW. The eggshell is required for meiotic fidelity, polar-body extrusion and polarization of the *C. elegans* embryo. *BMC Biol*. 2006;4:35. doi: 10.1186/1741-7007-4-35. PubMed PMID: 17042944; PMCID: PMC1635065.
122. Johnston WL, Krizus A, Dennis JW. Eggshell chitin and chitin-interacting proteins prevent polyspermy in *C. elegans*. *Curr Biol*. 2010;20(21):1932-7. doi: 10.1016/j.cub.2010.09.059. PubMed PMID: 20971008.
123. Marlow FL. Maternal Control of Development in Vertebrates: My Mother Made Me Do It! San Rafael (CA)2010.
124. van den Heuvel S. Cell-cycle regulation. *Wormbook*. 2005.
125. Spike CA, Coetzee D, Nishi Y, Guven-Ozkan T, Oldenbroek M, Yamamoto I, Lin R, Greenstein D. Translational control of the oogenic program by components of OMA ribonucleoprotein particles in *Caenorhabditis elegans*. *Genetics*. 2014;198(4):1513-33. Epub 2014/09/28. doi: 10.1534/genetics.114.168823. PubMed PMID: 25261697; PMCID: PMC4256769.
126. Kong J, Lasko P. Translational control in cellular and developmental processes. *Nat Rev Genet*. 2012;13(6):383-94. Epub 2012/05/10. doi: 10.1038/nrg3184. PubMed PMID: 22568971.
127. Jadhav S, Rana M, Subramaniam K. Multiple maternal proteins coordinate to restrict the translation of *C. elegans* nanos-2 to primordial germ cells. *Development*. 2008;135(10):1803-12. Epub 2008/04/18. doi: 10.1242/dev.013656. PubMed PMID: 18417623; PMCID: PMC2573031.
128. Kaymak E, Ryder SP. RNA recognition by the *Caenorhabditis elegans* oocyte maturation determinant OMA-1. *J Biol Chem*. 2013;288(42):30463-72. Epub 2013/09/10. doi: 10.1074/jbc.M113.496547. PubMed PMID: 24014033; PMCID: PMC3798510.
129. Petroski MD, Deshaies RJ. Function and regulation of cullin-RING ubiquitin ligases. *Nat Rev Mol Cell Biol*. 2005;6(1):9-20. Epub 2005/02/03. doi: 10.1038/nrm1547. PubMed PMID: 15688063.
130. Vasudevan S, Starostina NG, Kipreos ET. The *Caenorhabditis elegans* cell-cycle regulator ZYG-11 defines a conserved family of CUL-2 complex components. *EMBO Rep*. 2007;8(3):279-86. Epub 2007/02/17. doi: 10.1038/sj.embor.7400895. PubMed PMID: 17304241; PMCID: PMC1808032.

131. Liu J, Vasudevan S, Kipreos ET. CUL-2 and ZYG-11 promote meiotic anaphase II and the proper placement of the anterior-posterior axis in *C. elegans*. *Development*. 2004;131(15):3513-25. Epub 2004/06/25. doi: 10.1242/dev.01245. PubMed PMID: 15215209.
132. Sonnevile R, Gonczy P. Zyg-11 and cul-2 regulate progression through meiosis II and polarity establishment in *C. elegans*. *Development*. 2004;131(15):3527-43. Epub 2004/06/25. doi: 10.1242/dev.01244. PubMed PMID: 15215208.
133. DeRenzo C, Reese KJ, Seydoux G. Exclusion of germ plasm proteins from somatic lineages by cullin-dependent degradation. *Nature*. 2003;424(6949):685-9. Epub 2003/08/02. doi: 10.1038/nature01887. PubMed PMID: 12894212; PMCID: PMC1892537.
134. Feng H, Zhong W, Punkosdy G, Gu S, Zhou L, Seabolt EK, Kipreos ET. CUL-2 is required for the G1-to-S-phase transition and mitotic chromosome condensation in *Caenorhabditis elegans*. *Nat Cell Biol*. 1999;1(8):486-92. Epub 1999/12/10. doi: 10.1038/70272. PubMed PMID: 10587644.
135. Wormbase. par-2 2017. Available from: http://www.wormbase.org/species/c_elegans/par-2/WBGene00003917.
136. Wormbase. pie-1 2017. Available from: http://www.wormbase.org/species/C_elegans/pie-1/WBGene00004027.
137. Zhang L, Maddox AS. Anillin. *Curr Biol*. 2010;20(4):R135-6. Epub 2010/02/25. doi: 10.1016/j.cub.2009.12.017. PubMed PMID: 20178751.
138. Piekny AJ, Glotzer M. Anillin is a scaffold protein that links RhoA, actin, and myosin during cytokinesis. *Curr Biol*. 2008;18(1):30-6. Epub 2007/12/26. doi: 10.1016/j.cub.2007.11.068. PubMed PMID: 18158243.
139. Maddox AS, Habermann B, Desai A, Oegema K. Distinct roles for two *C. elegans* anillins in the gonad and early embryo. *Development*. 2005;132(12):2837-48. Epub 2005/06/03. doi: 10.1242/dev.01828. PubMed PMID: 15930113.
140. Dorn JF, Zhang L, Paradis V, Edoh-Bedi D, Jusu S, Maddox PS, Maddox AS. Actomyosin tube formation in polar body cytokinesis requires Anillin in *C. elegans*. *Curr Biol*. 2010;20(22):2046-51. Epub 2010/11/09. doi: 10.1016/j.cub.2010.10.030. PubMed PMID: 21055941.
141. Somma MP, Fasulo B, Cenci G, Cundari E, Gatti M. Molecular dissection of cytokinesis by RNA interference in *Drosophila* cultured cells. *Mol Biol Cell*. 2002;13(7):2448-60. Epub 2002/07/23. doi: 10.1091/mbc.01-12-0589. PubMed PMID: 12134082; PMCID: PMC117326.
142. Naim V, Imarisio S, Di Cunto F, Gatti M, Bonaccorsi S. *Drosophila* citron kinase is required for the final steps of cytokinesis. *Mol Biol Cell*. 2004;15(11):5053-63. Epub 2004/09/17. doi: 10.1091/mbc.E04-06-0536. PubMed PMID: 15371536; PMCID: PMC524772.
143. Gai M, Camera P, Dema A, Bianchi F, Berto G, Scarpa E, Germena G, Di Cunto F. Citron kinase controls abscission through RhoA and anillin. *Mol Biol Cell*. 2011;22(20):3768-78. Epub 2011/08/19. doi: 10.1091/mbc.E10-12-0952. PubMed PMID: 21849473; PMCID: PMC3192857.
144. Wormbase. mrck-1 2017. Available from: <http://www.wormbase.org/species/C.elegans/mrck-1/WBGene00006437>.
145. Chen Z, Wang Y, Zhai YF, Song J, Zhang Z. ZincExplorer: an accurate hybrid method to improve the prediction of zinc-binding sites from protein sequences. *Mol Biosyst*. 2013;9(9):2213-22. Epub 2013/07/19. doi: 10.1039/c3mb70100j. PubMed PMID: 23861030.

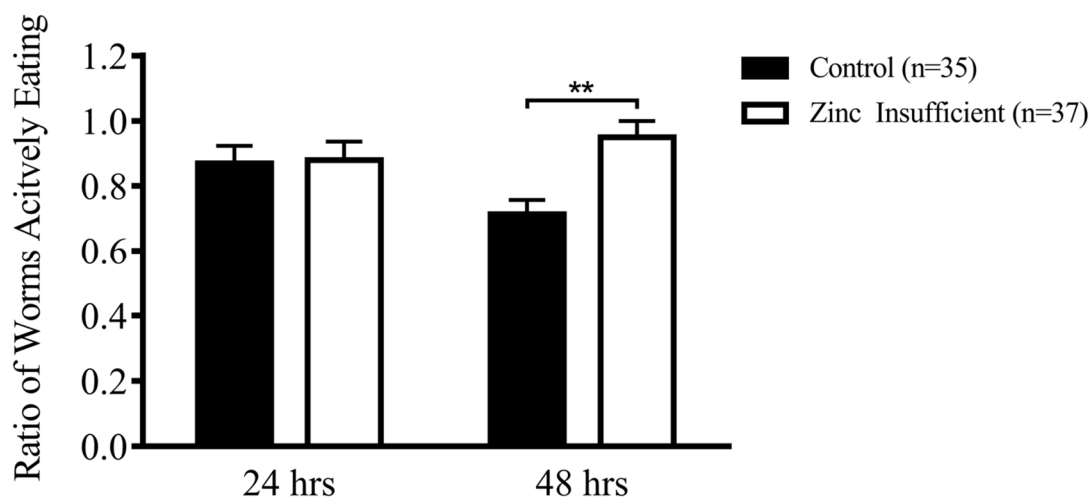
**APPENDIX A: SUPPLEMENTARY IMAGES: ZINC AVAILABILITY DURING
GERMLINE DEVELOPMENT IMPACTS OOCYTE DEVELOPMENT**



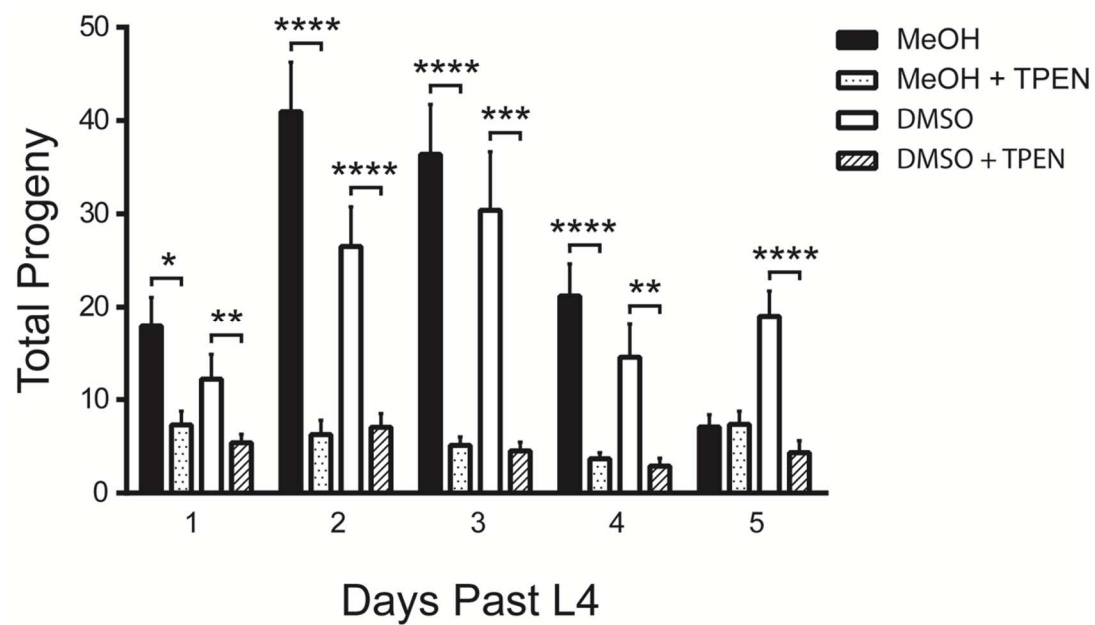
A.1 Zinc insufficiency does not impact hatching ability. Both the control and zinc insufficient conditions show that all embryos hatch.



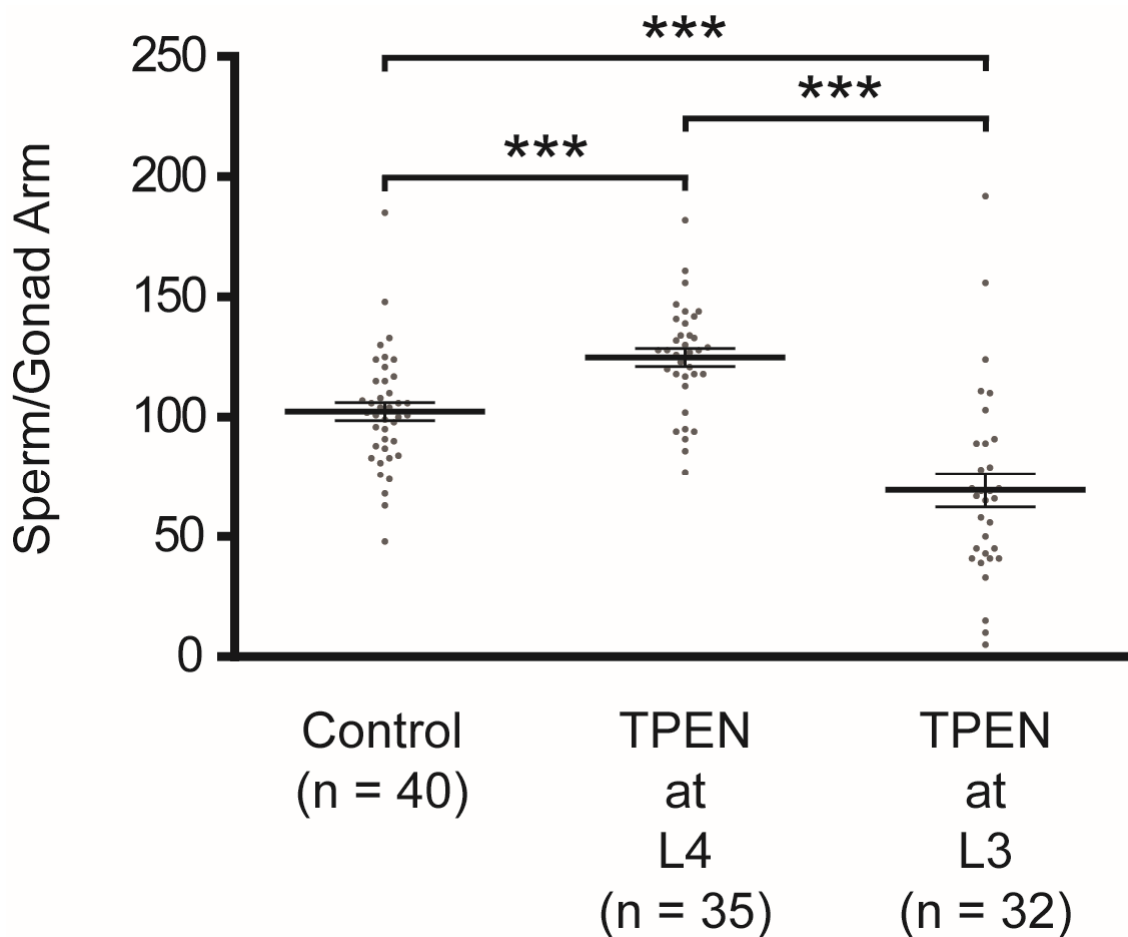
A.2. Zinc insufficiency does not impair eating ability. Young adults were observed for the number of pharyngeal contractions for 30 seconds each. There was no statistical difference between the control group (n=31) and the TPEN treated group (n=29) ($p=0.9$).



A.3. Worms do not avoid bacteria on TPEN treated plates. Young adults were observed for presence or absence on the OP50 lawn in control conditions (n=35) and TPEN treated conditions (n=37). There was no statistical difference on day 1 between the groups, but on day 2 the TPEN group tended to remain on the food more than the control (p=0.0074).

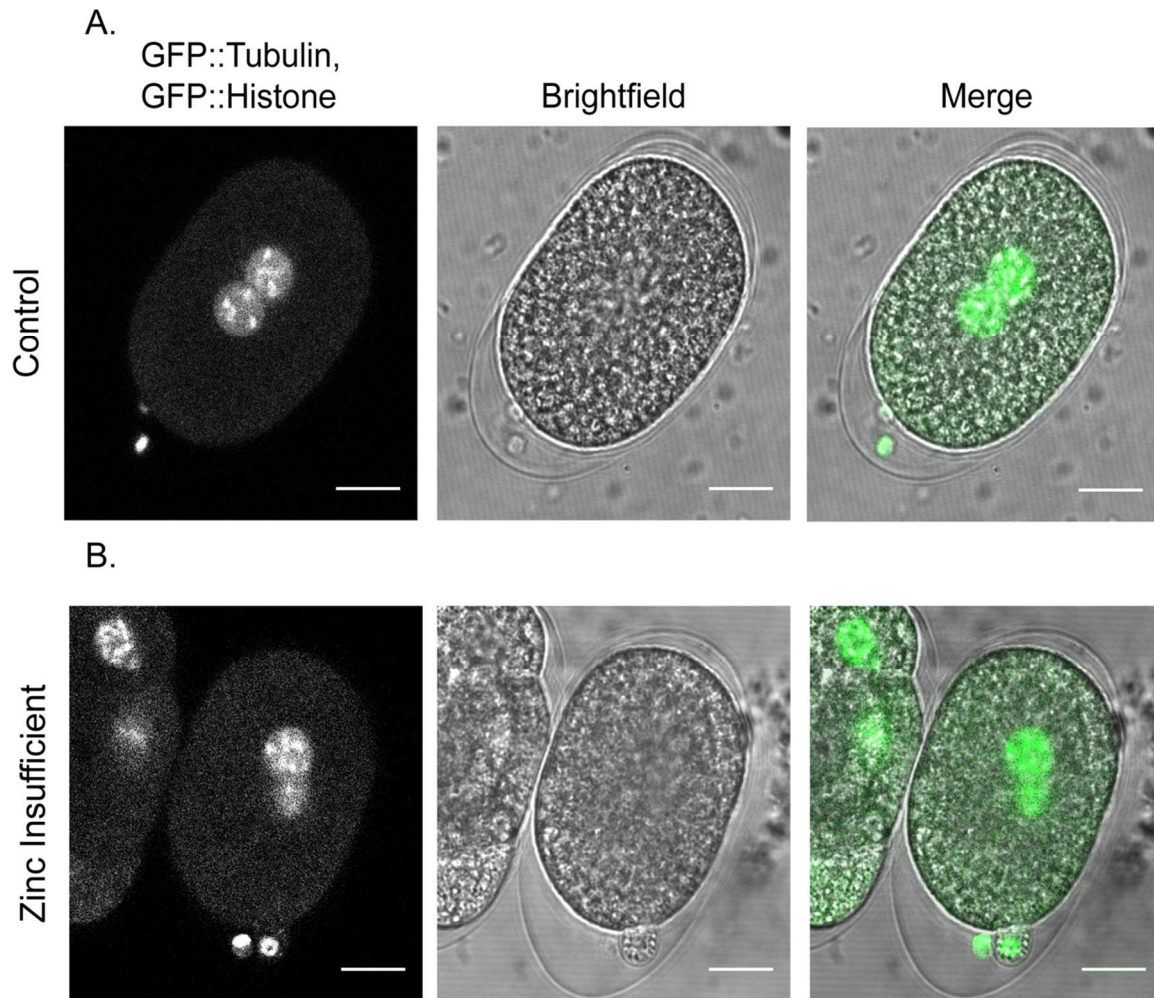


A.4. Killed bacteria still provide bioavailable nutrients. Brood size was quantified on bacteria that had been killed by Kanamycin, UV irradiation and heat exposure (75°C for 1 hour). Zinc

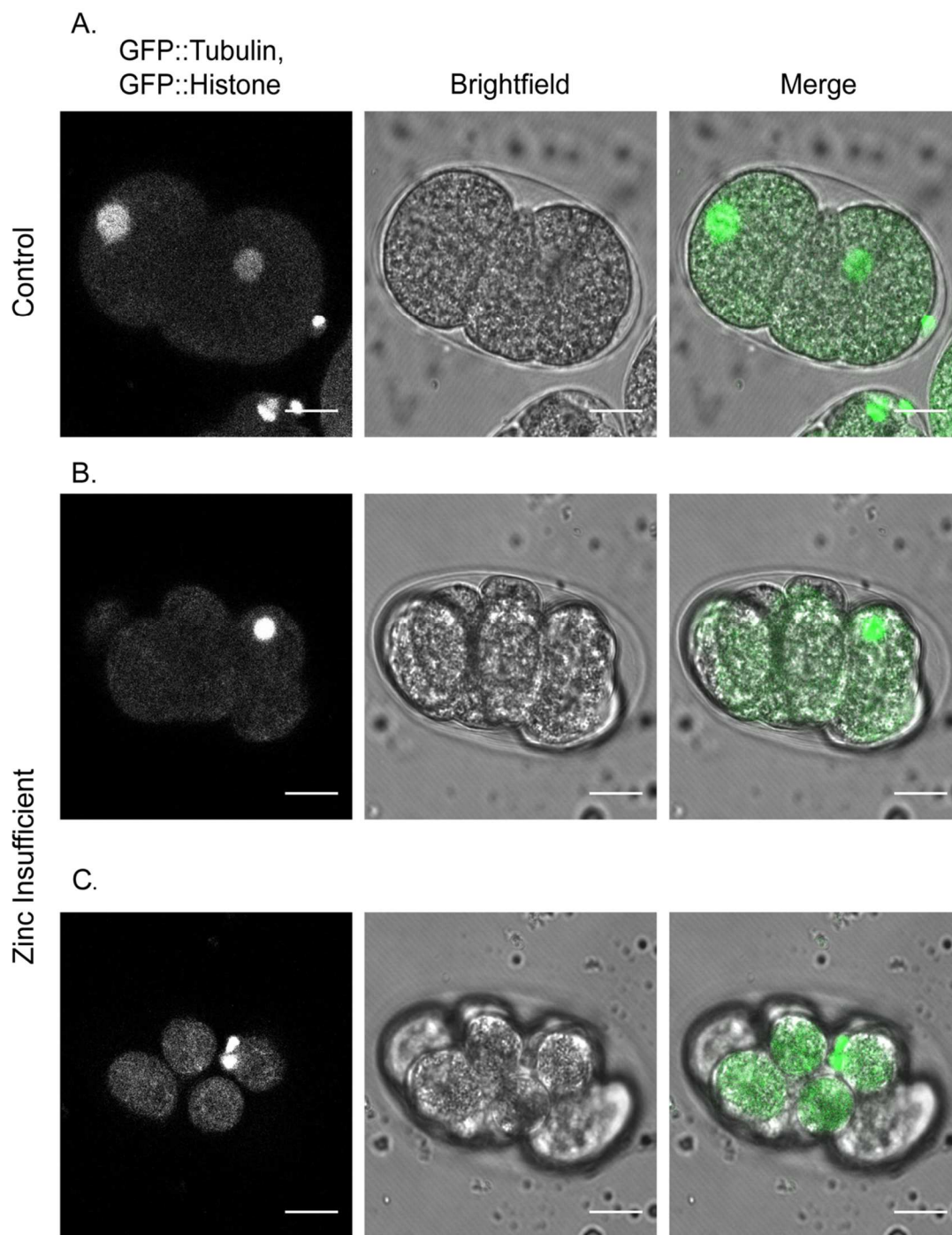


insufficient worms still yield a reduced number of progeny compared to controls.

A.5. Zinc insufficiency exerts a mild sperm impact. Sperm counts fluctuated depending on the time of TPEN exposure. When L3 worms were exposed to TPEN before sperm was created, a small drop (~20%) in sperm count occurred ($p < 0.0001$). When L4 worms were exposed to TPEN when sperm was almost finished developing, the sperm count increased slightly ($p < 0.0001$).

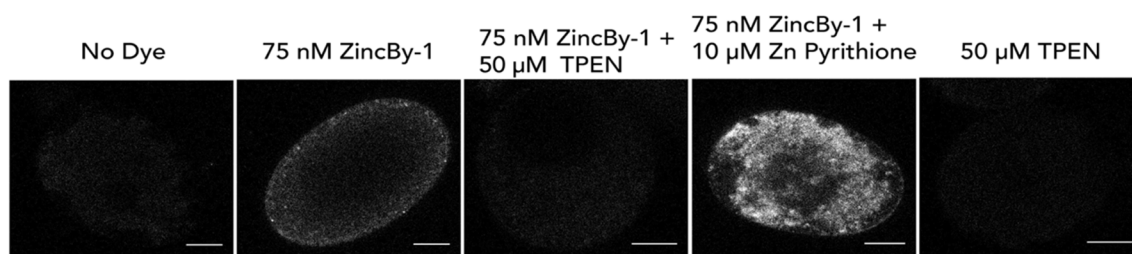


A.6. Zinc insufficient zygotes may overcome polar body extrusion errors. The control zygote extruded the second polar body appropriately during Telophase II (A). A zinc insufficient zygote failed to extrude the second polar body during Telophase II. During pronuclear migration, the zygote pinched off a small portion of the cytoplasm containing the second polar body and the zygote achieved the 2-cell stage (B).

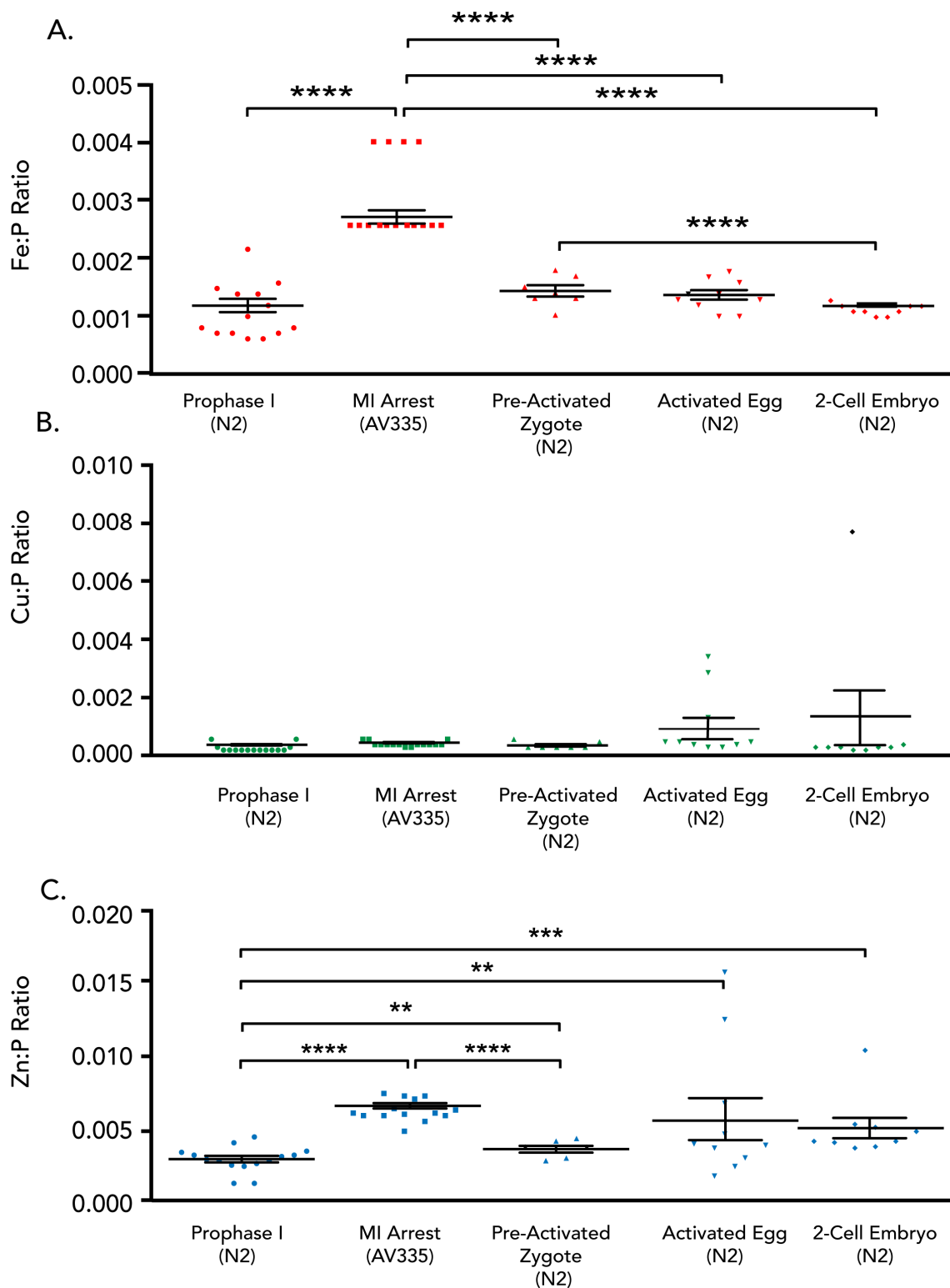


A.7. Zinc insufficient zygotes may experience polar body retraction. A zinc insufficient zygote successfully extruded both polar bodies. During pronuclear migration, both were pulled back into the cytoplasm, and the zygote arrested (B, C), while the control zygote successfully extruded both polar bodies and completed pronuclear migration (A). Both images for B and C were captured at the same time-point, in separate planes.

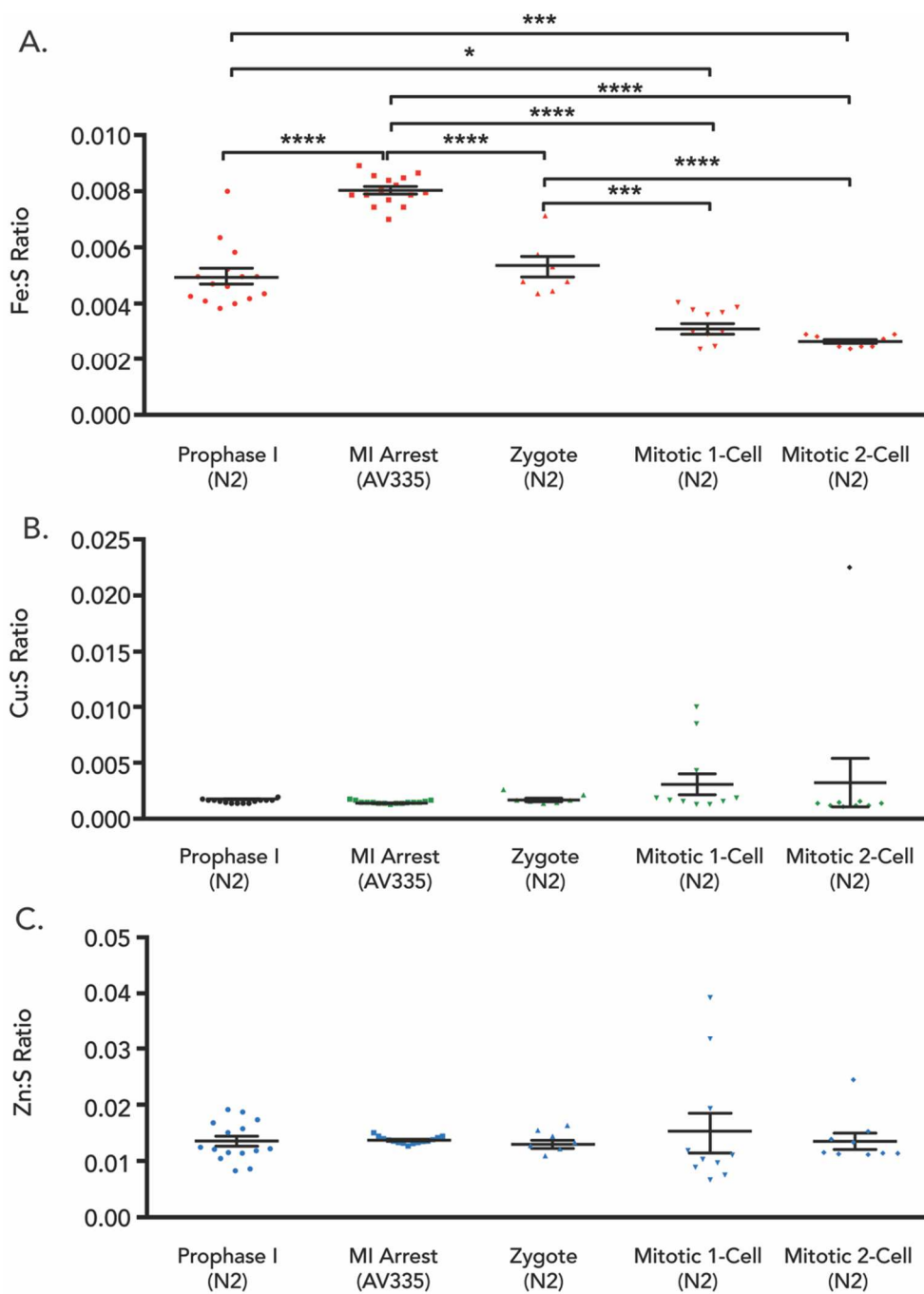
**APPENDIX B: SUPPLEMENTARY IMAGES: ZINC FLUXES REGULATE MEIOTIC
PROGRESSION IN MATURING *C. ELEGANS* OOCYTES**



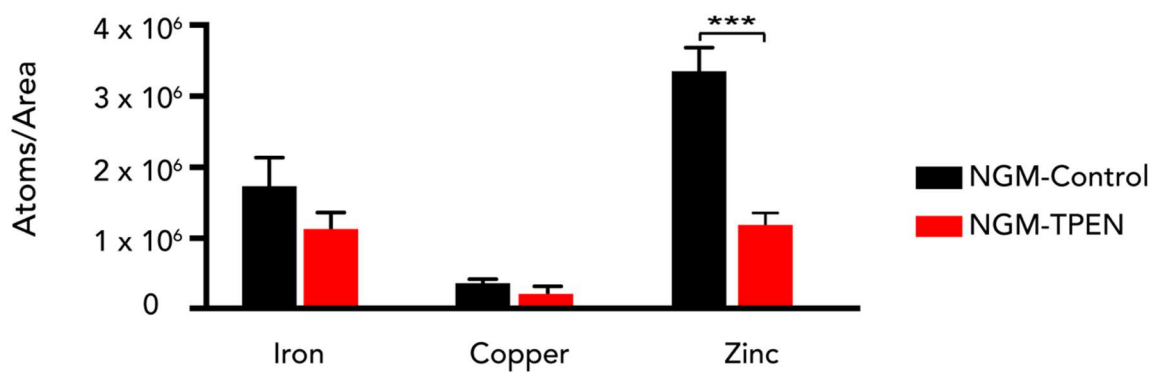
B.1. Test for zinc specificity by ZincBy-1 of isolated fog-1(q253) 1 oocytes. Oocytes that were not exposed to ZincBy-1 show no fluorescence, 75 nM ZincBy-1 shows dye penetration. After initial exposure of ZincBy-1, fluorescence was challenged with 50 μ M TPEN which diminished the fluorescence intensity to that comparable of the control and 50 μ M TPEN alone. Adding 10 μ M Zinc Pyrithione increased fluorescence as detected by ZincBy-1.



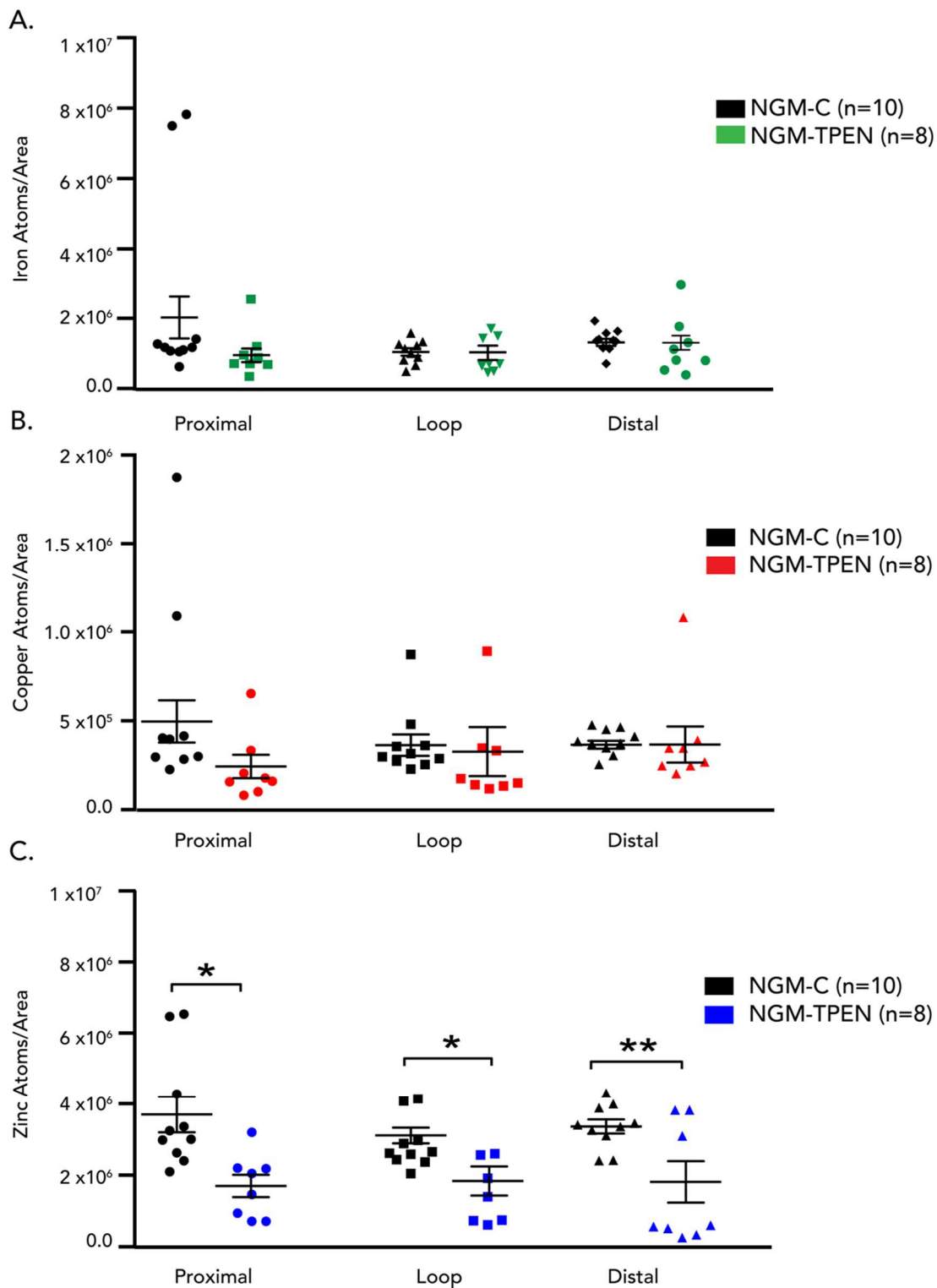
B.2. Fe:P ratios show that MI arrested zygotes contain statistically significant more Fe to P than other stages of meiotic progression. The Zygote stage was significantly higher than the 1-Cell, and 2-Cell stages A). Cu:P and Zn:P did not show significant differences between meiotic stages (B,C).



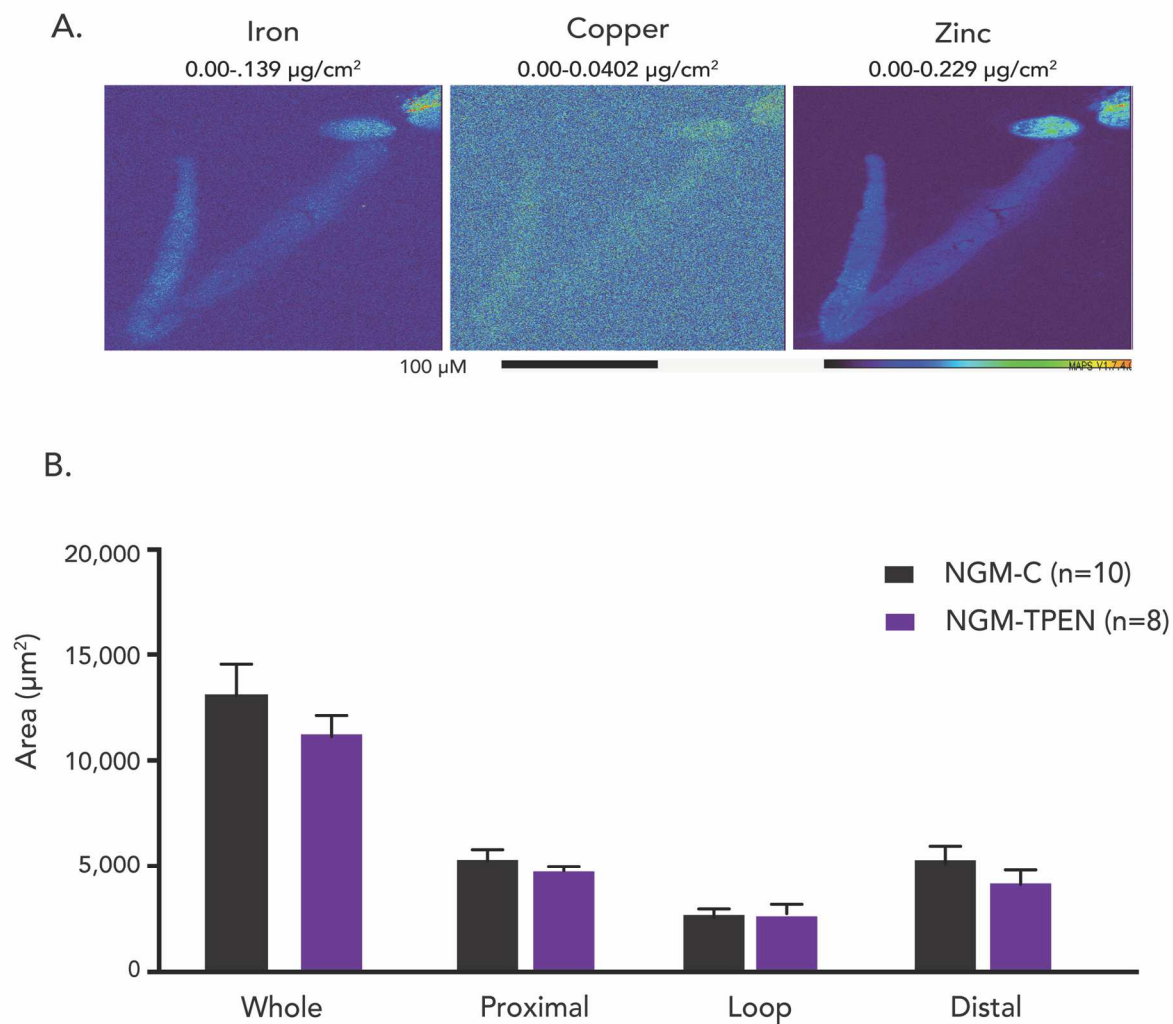
B.3 . Fe:S ratios show significant differences between several meiotic stages (A). Both Cu: and Zn:S ratios remained level throughout meiotic progression (B,C).



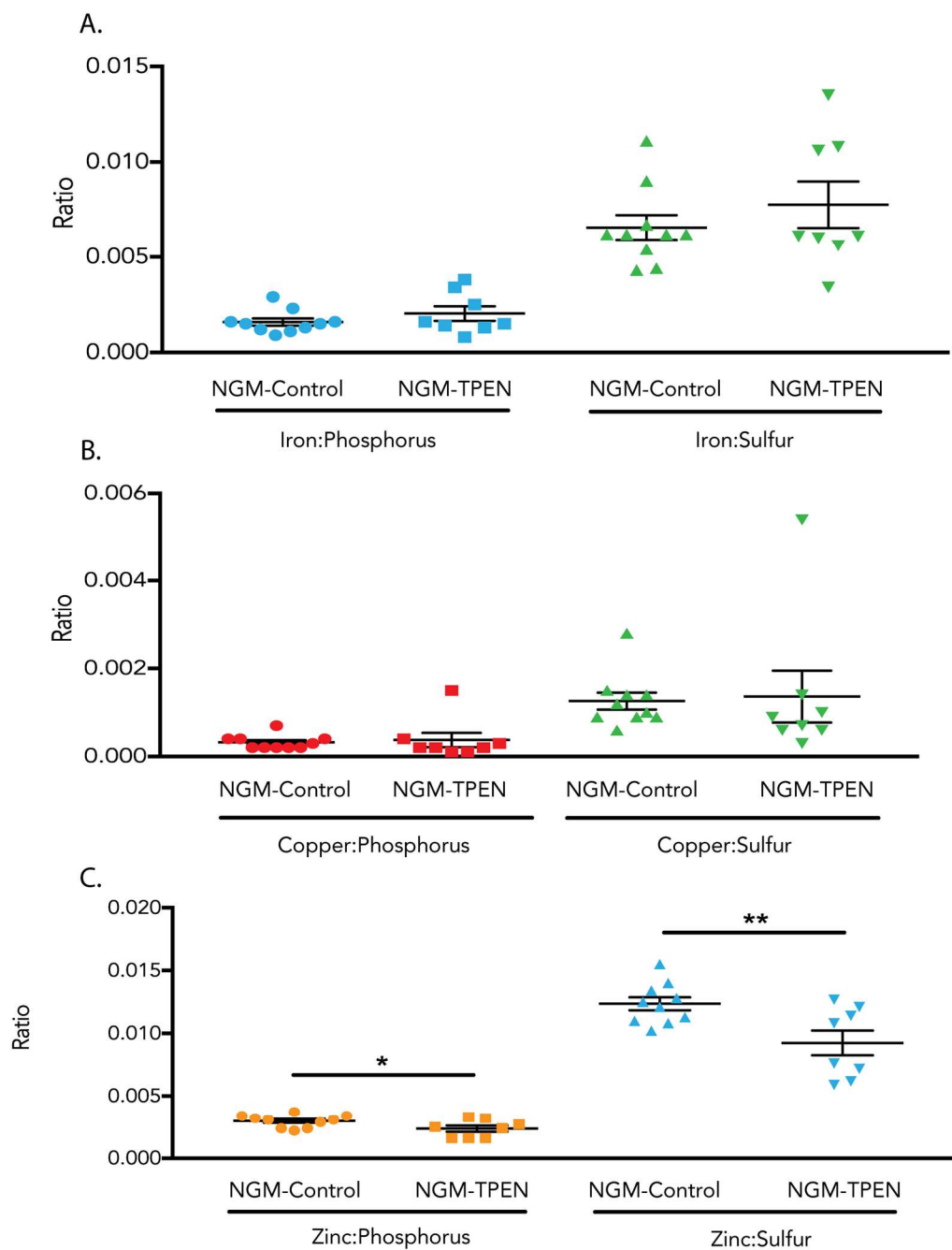
B.4. Total Fe, Cu and Zn contents in whole, isolated gonads from NGM-Control and NGM-TPEN groups. Analysis is calculated by atoms/area.



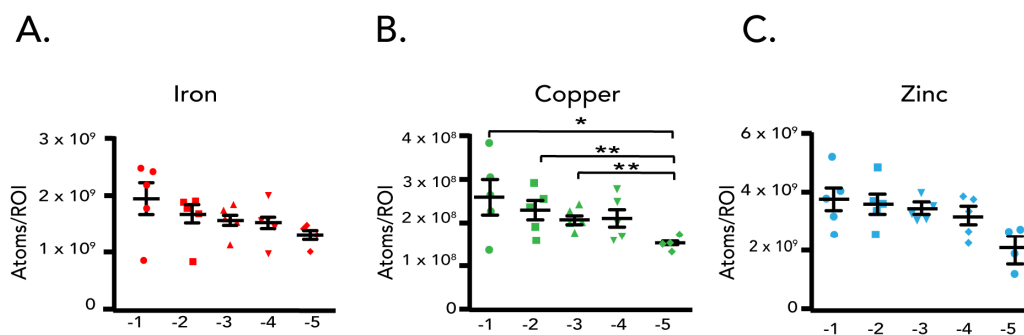
B.5. Analysis of total Fe, Cu and Zn the whole gonad (ROI/area). TPEN does not significantly reduce total Fe, and Cu in any gonad region (A, B). TPEN also sequesters zinc significantly in all regions (C).



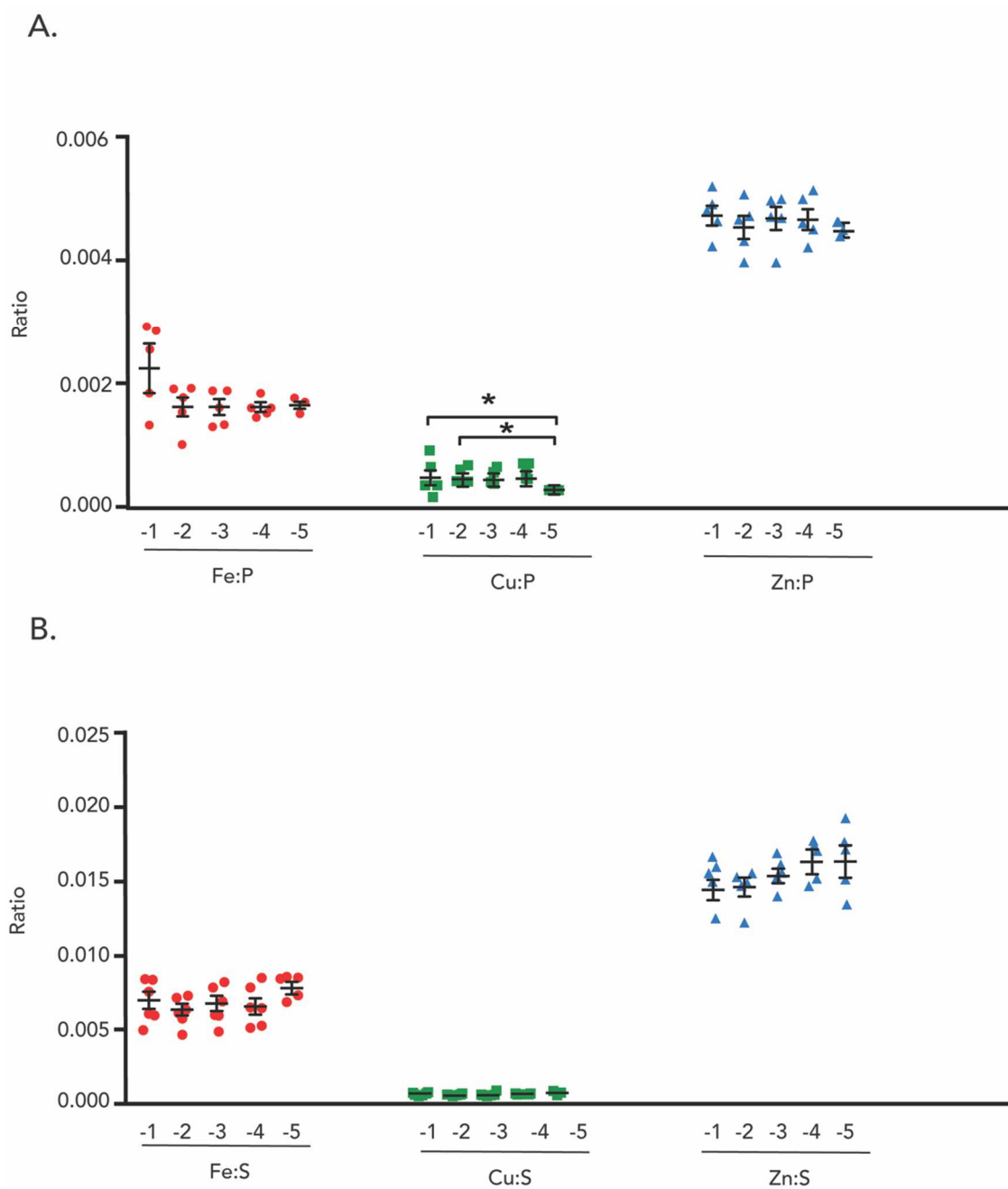
B.6 XFM maps display Fe, Cu, and Zn throughout the dissected gonad in the NGM-TPEN group (A). The area for each gonad in NGM-Control and NGM-TPEN groups were measured in whole, distal, loop, and proximal regions, and showed no statistical differences between groups (B).



B.7. Fe:P and Fe:S ratios were not statistically significant between NGM-Control and NGM-TPEN groups. Cu:P, and Cu:S ratios were also not statistically significant between NGM-Control and NGM-TPEN groups (A, B). Zn:P ratios were significantly different between NGM-Control and NGM-TPEN groups, as were Zn:S ratios (C).



B.8. Total Fe, Cu, and Zn atoms/ROI in individual oocytes all show steady increase in content as oocytes mature. The -5 oocyte showed statistical difference compared to the -3 through -1 oocytes in Cu.

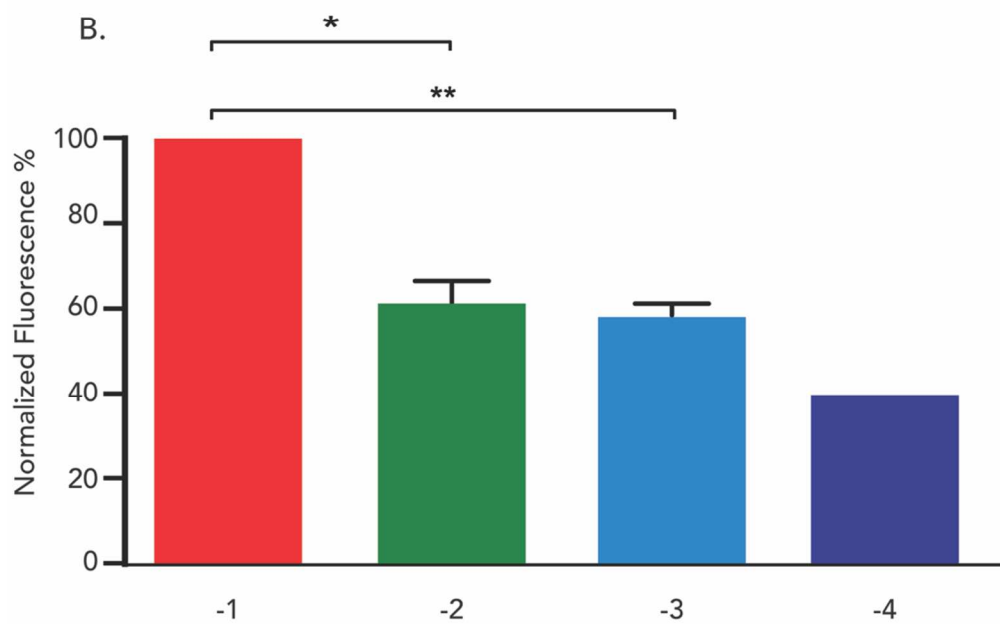
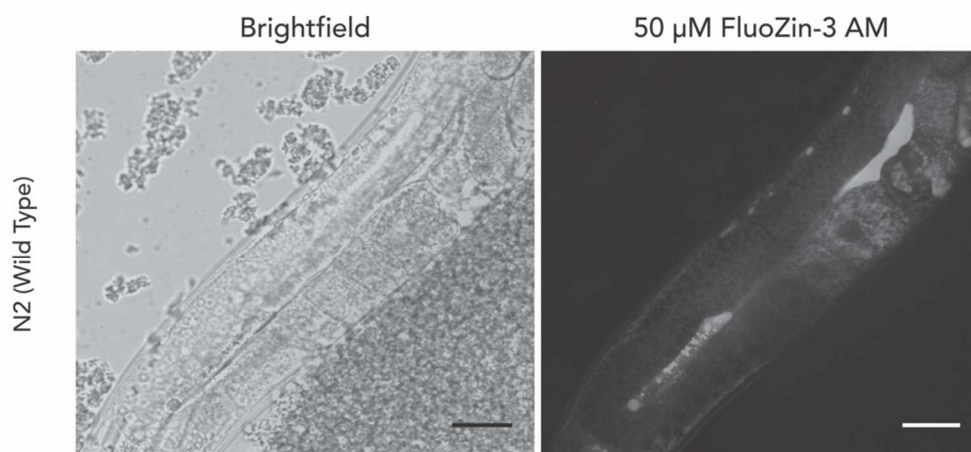


B.9. Fe:P ratios in individual oocytes are statistically significant from oocyte to oocyte, whereas Cu:P and Zn:P are not (A). Fe:S ratios in individual oocytes are statistically significant from oocyte to oocyte, as are the Cu:S ratios. As oocytes decrease in maturity, Zn:S ratios increase and the -5 oocyte is statistically different from the others (B).



B.10. Test for Zn specificity by 75 nM ZincBy-1 in isolated gonads. Gonads isolated in egg buffer alone do not display ZincBy-1 fluorescence. Gonads isolated in ZincBy-1 displays zinc fluorescence. Gonads isolated in 75 nM ZincBy-1 followed by 50 μ M TPEN addition eliminated the ZincBy-1 signal. Gonads isolated in 75 nM ZincBy-1 followed by 10 μ M Zn Pyritione incubation produced an increased fluorescence signal. Gonads isolated in 50 μ M TPEN alone did not produce fluorescence

A.



B.11. FluoZin-3 AM fluorescence distribution in gonads from live N2 adults. FluoZin-3 AM detected labile Zn in oocytes (A). The fluorescence intensity was normalized in oocytes (B).

APPENDIX C: FUTURE DIRECTIONS

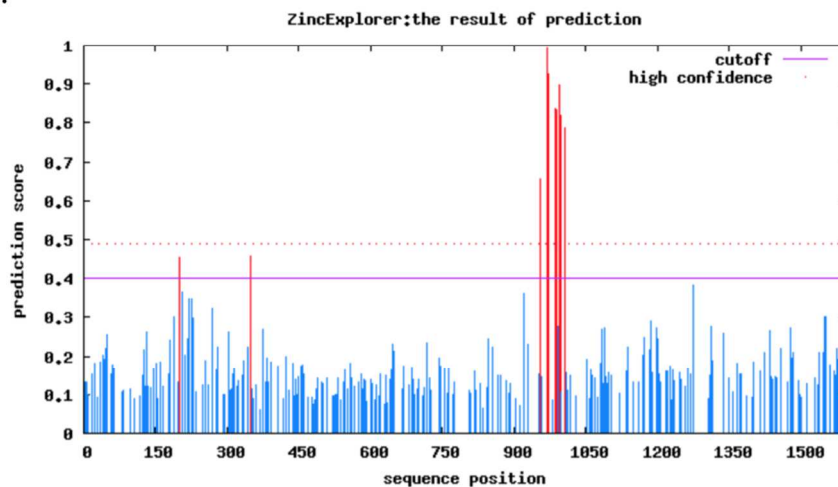
A.

```

MAEPPPDDSDAPVRLKLTLENIYMDGPSKKEPALSFEITLIDSLICLYDECCNSTLRKEKCIAEFVSESVKTVISKAKKRLRSR
DDFEVLKVIKGFAGFEVAVVRMRGVGEIYAMKILNKWEMVKRAETACFRERDVLVYGDERRWITNLHYAFQDEKNLYFVM
DYYIGGDMLTLLSKFVDHIPESSMAKFYIAEMVLAIDSLIRLGYVHRDVKPDNVLLDMQGHIRLADFGSCLRILADGSVAS
NVAVGTPDYISPEILRAMEIDGRGRYKGECDWWSLGIEMYEMLYGTPPFYSERLVDTYKIMS HQDMLDFPDDEIDWVVSE
EAKDLIRQLICSSDVRFRGNLSDFQLIPFFEIGIDWNTIRDSNPPYVPEVSSP EDTSNF DVLVCEDDFTPCETQPPVLA
AFTGNHLFPVGFYSYTHGSLLS DARS L T DEIRAIAQR CQGDALMEKSVJGFMVLENEKAE LVQKLKEAQTIIAQHVAEN
PRSEEDRNYESTTAAQLKDEIQILNKRLDEEALAQQQKPKDEIVAEESEKCLKELKERKQLVMEKSEIQRELDNDHLD
QVLVEKATVVQQRDDMQAELADVGDLSLLEKDSVKRLQDEAEKAKKQVADFEDEKLKEIETE KIALIKKQEEVTEIARKSV
ETDDHLS E VVAAKNTIASLQATNEERETEIKKLLKQRMDEERASHTAQSEQEMKQLEAHYE RAQKMLQDNVEQMNVENRG
LRDEIEKLSQQMAALPRGGLNEQQLHEIFNWVSEEKATREEMENLTKRITGEVSESKNNSPLTTSNYIQNTPSGWGSRM
NNVARKGLDLQRQLQAEIDAKLKLKAE LKNSQEYL TSAARLDDEKRMASLMRE VAMLKQOKNIESSD SAFSSTMGR
GDLMI MNNDYEMSNSLMRQEMISRQSTPSYENAILLHDDHQVPKRVDLRYKQKPKMTASGIFSPVSI SAMERG HNFER
MKIKTPTKCGHCTSIILIGLDRQGLFESQCYAGHVS CAERVSQSFPVPEEERRPLGIDPTRGVGTAYEGLVKT PRAGGVR
KGWQTAYVVCDFKLYLDCTVDRONKMDVKNEIRLVLDMRDPDFTVCGVSEADVIHAQKGDIPKIFRVTTQILNSSS
EYSSSSKFYTLFMAETEEERKRWVVALSELKTLRRSKLADRKAFLVKEVFDVTTLPSIRVAQCCAIIDRSKIVIGFSDH
GLYIEISRQLLIPVGGEEKENKQRCVETVEYDEAEQLMMIVGPAKDRHVRIVPSAALDCRDLKWKIVNDTKGCHLLAVG
TNNPGRGAGFFAVAFKKSVTIFQIDRSERKHKKWKDLAMPCTPQSIAIFNGRLYVGFHSFRSWSLVGV DSSPVGSGDAS
GAVLQHISLVNMDTSLQFLNQQTSYEAKLIVNVPVGPSPDEYLLVFNMIGLYVNE MGRSRLEPVMFPPTQAKYFAYHEPYL
CVFSENEVDIFNVTLAEVWQTINLRSAPLSGDGILSTCLCNDSPIFVLLQNVLQDQDSIEVPVNLASGSTDEGRKVTRRK
FTFRTIGKDDRSASERRSHIQISTSPDFMHIVHMGPAVME LQQNFIDLQSNHSH TSSDKDSLNRSVNND

```

B.



C.3. Predicted zinc finger sites from the MRCK-1 protein sequence in *C. elegans*. The protein MRCK-1 protein sequence shows 1590 amino acids, high prediction of amino acids in positions H956,C969, C972,C986, H994, C997, and C1005 (highlighted in red).

TABLES

	Prophase I (N2)			MI Arrest (AV335)			Zygote (N2)			1-Cell (N2)			2-Cell (N2)		
	Mean	SEM	N	Mean	SEM	N	Mean	SEM	N	Mean	SEM	N	Mean	SEM	N
P	8.87×10^{11}	6.76×10^{10}	15	7.79×10^{11}	2.19×10^{10}	15	5.09×10^{12}	7.29×10^{11}	7	2.40×10^{12}	8.88×10^{11}	10	2.72×10^{12}	9.97×10^{11}	9
Fe	1.10×10^9	1.72×10^8	15	2.56×10^9	5.42×10^7	15	7.35×10^9	6.64×10^8	7	3.57×10^9	1.51×10^9	10	3.23×10^9	1.24×10^9	9
Cu	2.43×10^8	2.76×10^7	15	3.19×10^8	1.36×10^7	15	1.79×10^9	1.96×10^8	7	1.75×10^9	5.05×10^8	10	1.95×10^9	1.08×10^9	9
Zn	2.72×10^9	2.68×10^8	15	4.61×10^9	1.13×10^8	15	2.19×10^{10}	3.81×10^9	7	1.45×10^{10}	4.66×10^9	10	1.51×10^{10}	5.29×10^9	9

Table. 3.1. Total P, Fe, Cu, and Zn atoms during meiotic maturation in N2 wild type animals and AV335 Metaphase I arrested animals.

	(-1)			(-2)			(-3)			(-4)			(-5)		
	Mean	SEM	N												
P	8.07×10^{11}	6.76×10^{10}	5	8.30×10^{11}	5.43×10^{10}	5	7.67×10^{11}	3.13×10^{10}	5	6.50×10^{11}	6.31×10^{10}	5	5.30×10^{11}	7.31×10^{10}	5
Fe	1.97×10^9	3.19×10^8	5	1.60×10^9	2.18×10^8	5	1.46×10^9	1.36×10^8	5	1.36×10^9	1.75×10^8	5	9.54×10^8	1.41×10^8	5
Cu	2.59×10^8	3.85×10^7	5	2.28×10^8	2.37×10^7	5	2.00×10^8	1.38×10^7	5	1.94×10^8	2.74×10^7	5	1.18×10^8	9.96×10^6	5
Zn	3.83×10^9	4.44×10^8	5	3.67×10^9	3.86×10^8	5	3.54×10^9	1.28×10^8	5	3.40×10^9	3.63×10^8	5	2.18×10^9	4.22×10^8	5

Table 3.2. Total P, Fe, Cu, and Zn atoms in individual oocytes in wild type animals.

Species	Common Name	Influx			Efflux		
		Beginning Stage	Ending Stage	% Increase	Beginning Stage	Ending Stage	% Decrease
<i>X.laevis</i>	African Clawed Frog	Stage I oocyte	Stage VI oocyte	34	-	-	-
<i>M. musculus</i>	Mouse	GV	MII	50	MI	2-Cell	20
<i>C. elegans</i>	Nematode	(-1) Oocyte Prophase I	Zygote	470	Zygote	2-Cell	31
<i>D. rerio</i>	Zebra Fish	Stage I oocyte	Stage III oocyte	350	-	-	-
<i>L. pictus</i>	Sea Urchin	Fertilization	pleuteus	600	-	-	-

Table 3.3. Zinc influx and efflux in some metazoan species

Adelita D. Mendoza

7333 N Ridge Blvd. #104 • Chicago, IL 60645
 Phone: 720-938-0140 • E-Mail: adelitamendoza2016@u.northwestern.edu

Education

Ph.D. Biological Sciences, Northwestern University, Evanston, IL	December 2017
B.A. Molecular, Cellular and Developmental Biology (MCDB), University of Colorado Boulder, Boulder, CO	2010
B.A. Environmental, Populations and Organismic Biology (EPOB), University of Colorado Boulder, Boulder, CO	2004

Research Experience

Doctoral Candidate

O'Halloran Laboratory, Northwestern University

- *Doctoral Thesis project: Investigations into Zinc Regulation of Germline Development in Caenorhabditis elegans* (in collaboration with the Wignall Laboratory at Northwestern University). Spearheaded investigations into zinc effects on germline production, oocyte viability and fertilization in *Caenorhabditis elegans*. These discoveries required a mastery of cross-disciplinary techniques in live-animal handling and maintenance, cell biology, fluorescence microscopy, analytical chemistry and X-ray physics. Results produced a publication in *Comparative Biochemistry & Physiology Part C, Toxicology*. 2012-current

Professional Research Assistant

Garcia Laboratory, University of Colorado Anschutz Medical Campus

- Research Technician position in a cancer cytogenetics laboratory involving the design and execution of Fluorescence In Situ Hybridization (FISH) studies in human tissue sections and cell lines for several genes implicated in cancer development 2009-2011

Summer Cancer Fellow

Garcia Laboratory, University of Colorado Anschutz Medical Campus

2008-2009

- Summer Intern position studying the role of heterogeneity in the Insulin-like Growth Factor Receptor 1(IGF1R) in Non-Small Cell Lung Carcinoma (NSCLC)

Publications

- **Mendoza AD**, Woodruff TK, Wignall SM, O'Halloran TV. *Zinc availability during germline development impacts embryo viability in *Caenorhabditis elegans**. Comparative Biochemistry and Physiology Part C, Toxicology and Pharmacology. 2017;191:194-202. doi: 10.1016/j.cbpc.2016.09.007. PubMed PMID: 27664515; PMCID: PMC5210184.
- Minuti G, Cappuzzo F, Duchnowska R, Jassem J, Fabi A, O'Brien T, **Mendoza AD**, Landi L, Biernat W, Czartoryska-Arlukowicz B, Jankowski T, Zuziak D, Zok J, Szostakiewicz B, Foszczynska-Kloda M, Tempinska-Szalach A, Rossi E, Varella-Garcia M. *Increased MET and HGF gene copy numbers are associated with trastuzumab failure in HER2-positive metastatic breast cancer*. British Journal of Cancer. 2012;107(5):793-9. doi: 10.1038/bjc.2012.335. PubMed PMID: 22850551; PMCID: PMC3425981.
- Dziadziuszko R, Merrick DT, Witta SE, **Mendoza AD**, Szostakiewicz B, Szymanowska A, Rzyman W, Dziadziuszko K, Jassem J, Bunn PA, Jr., Varella-Garcia M, Hirsch FR. *Insulin-like growth factor receptor 1 (IGF1R) gene copy number is associated with survival in operable non-small-cell lung cancer: a comparison between IGF1R fluorescent in situ hybridization, protein expression, and mRNA expression*. Journal of Clinical Oncology. 2010;28(13):2174-80. doi: 10.1200/JCO.2009.24.6611. PubMed PMID: 20351332; PMCID: PMC2860435.
- **Mendoza AD**, Sue A, Gleber S, Vine D, Antipova O, Vogt, S, Woodruff TK, Wignall SM, O'Halloran TV. *The *C.elegans* Reproductive Tract is a Map of Dynamic Zinc Activity*, Manuscript In Preparation

Presentations

- **A.D. Mendoza**, C. Schiffer, S. Cheung, S. Vogt, S.M. Wignall, T.V. O'Halloran, *Zinc Dynamics Regulate Germline Development in *Caenorhabditis elegans**, 2016 Denver X-Ray Conference, Rosemont, IL. Selected for oral presentation.
- **A.D. Mendoza**, C. Schiffer, S. Cheung, S. Vogt, S.M. Wignall, T.V. O'Halloran, *Zinc Dynamics Regulate Germline Development in *Caenorhabditis elegans**, 2016 Chicago Area SACNAS Symposium, Evanston IL. Selected for oral presentation.
- **A.D. Mendoza**, T.K. Woodruff, S.M. Wignall, T.V. O'Halloran, *Zinc Regulation of *Caenorhabditis elegans* Reproduction: Insights Provided by XFM*, 2016 APS Brown Bag Meeting, Argonne National Laboratory. Invited speaker.

- **A.D. Mendoza**, C. Schiffer, S. Cheung, S.M. Wignall, T.V. O'Halloran, *Zinc Dynamics of Germline Development in Caenorhabditis elegans*, 2015 SACNAS National Conference, Washington D.C. Selected for oral presentation.
- **A.D. Mendoza**, *Utilizing Caenorhabditis elegans to Investigate Zinc Regulation in the Maturing Oocyte*, 2014 Reproductive Research Updates for the Center for Reproductive Science, Northwestern University. Selected for oral presentation.
- S.A. Garwin, **A.D. Mendoza**, F.E. Duncan, E.L. Que, R. Bleher, T.K. Woodruff, T.V. O'Halloran *Characterizing the Metallome of Oocytes and Embryos in Multiple Species using X-ray Fluorescence Microscopy* 2013 Biological Applications of X-Ray Fluorescence Microscopy Workshop, Northwestern University. Poster presentation.
- **A.D. Mendoza**, M.Skokan, M.Theodoro, R. Dziadziuszko, M. Varella-Garcia, F. Hirsch *Insulin-like growth factor receptor 1(IGF1R): Genomic Status in Non-Small Cell Lung Cancer (NSCLC)* 2010 Society for the Advancement for Chicanos & Native Americans in Science (SACNAS) National Conference, Anaheim CA, 2009 American Association for Cancer Research, Denver, CO and the 2009 Society for the Advancement for Chicanos & Native Americans in Science (SACNAS) Rocky Mountain Regional Conference, Denver, CO. Poster presentation.

Research Grants

- Ruth L. Kirchenstein NIH NRSA to Promote Diversity in Health-Related Research, 2014-2017
Grant Number: F31GM112478, funded for 3 years at \$36,038.00/year
- Chicago Biomedical Consortium (CBC) Scholarship Program 2014-2016
Grant Number: A2011-00985, funded for 2 years at \$4,000/year
- T32 Carcinogenesis Training Grant 2013-2014
Grant Number: T32CA09560, funded for 1 year at \$27,032.00

Specialized Coursework

- **Writing a successful NIH F31 course, Northwestern University** Spring 2013
Attended a 2-day course targeted toward graduate students preparing to write an F31 NIH NRSA.
- **Grantsmanship for the Research Professional** Winter 2013
Attended a 1-day course offered through Northwestern University designed up help grant writers compose successful grants to the NIH & NSF funding agencies

Competitive Applications for Laboratory Experiments

- 160

• **Lattice Light Sheet Microscopy (LLSM), Janelia Research Campus, Ashburn VA-** Awarded time to conduct experiments on the LLSM at the Advanced Imaging Center to track labile zinc distribution in maturing *C. elegans* oocytes. The application passed a two-tiered, peer-review process. 2016
- **X-Ray Fluorescence Microscopy (XFM), Advanced Photon Source, Argonne National Laboratory, Lemont, IL-** Awarded time to conduct experiments at the 2-ID-E beamline at the APS synchrotron to map and quantify total zinc content in the *C. elegans* reproductive tract. The application passed a review process to be awarded beam time. 2013-2014

Teaching Experience

- **Teaching Assistant, Advanced Cell Biology** 2013
 Ran a recitation style course involving in-depth review of primary literature in cell biology and discussion. I also proctored and graded exams, and homework assignments,
- **Laboratory Teaching Assistant, Cellular Processes Laboratory** 2013
 Ran three laboratory sections with undergraduate assistants. Provided explanation of the scientific method, ran experiments, graded homework assignments and lab exams, and assisted the laboratory coordinator.
- **Instructor for Science, Engineering & Math Sophomore Internship, Ronald E. McNair Post-Baccalaureate Achievement Program** 2009
 Course instructor for new STEM students in the McNair program. The course was designed to expose students to scientific culture and encourage them to pursue a career in research science
- **Teaching Assistant, Ronald E. McNair Post-Baccalaureate Achievement Program Sophomore Transitions Course** 2008
 Involved in curriculum development, teaching of scientific method, and how to search for mentors/get into labs

Awards & Funding

- Travel Award, The Whole Scientist 2017
- Robert L. Snyder Student Travel Award 2016
- Student Poster Award, X-Ray Fluorescence Microscopy Workshop 2013
- Community Building Grant sponsored by The Graduate School, co-authored for SACNAS activities 2012-current

- Initiative for Maximizing Student Development Fellowship 2011-2013 161
- Honorable Mention for Poster Presentation- SACNAS Rocky Mountain Regional Conference, Denver CO 2009
- NIH/HHMI Scholars Program for Diversity in the Biosciences 2009
- Graduate Experience for Multicultural Students (GEMS) 2008
- University of Colorado Student Cancer Research Fellowship Program 2008

Affiliations/Memberships

- President & Co-founder, Northwestern University Society for the Advancement of Chicanos and Native Americans in Science (SACNAS) Student Chapter- 2012-2017
 - Established a student chapter, outlined our chapter mission, and established initial connections with The Graduate School staff at Northwestern University.
 - Networked with other student groups, and designed programming intended to enhance leadership skills and provide career-enhancing opportunities for chapter members.
 - Strengthened relationships with The Graduate School, multiple graduate student programs including IBiS, DGP, NUIN, & MSTP.
 - Recruited for Northwestern University at the National SACNAS conference annually.
 - Trained incoming officers
 - Maintain strong relationships with the four other Chicago area SACNAS chapters and together we host an annual research and career symposium.
- Student member, Society for the Advancement of Chicanos & Native Americans in Science (SACNAS) 2005-current

Service

- Student organizer, 1st and 2nd Annual Chicago Area SACNAS Symposium- Served as a lead graduate student in planning and executing a 1-day symposium at Northwestern University. 2015 & 2016
- Art & Science Fair, student volunteer- As part of a SACNAS and Jugando con la Ciencia student group collaboration, I participated as a judge for the art competition and facilitated kid-friendly science experiments at the Evanston Public Library 2016

- 162
- HERStory, student leader- As part of a SACNAS and Jugando con la Ciencia student group collaboration, I participated in the planning and execution of an event to bring middle and high school aged girls to the Field Museum in Chicago to learn about the contributions of female scientists and to get them thinking about pursuing a science career, 2016
 - Northwestern University International Student Brown Bag Lunch, invited speaker- I gave a talk to International graduate students about how intersectionalities play out in scientific culture in the United States. 2015
 - Continuing Umbrella of Research Experience (CURE) program & Summer Undergraduate Research Opportunities Program (SROP), panel speaker- Spoke with undergraduate students in the CURE program about how to prepare a successful application to graduate school, and shared my experience as a graduate student and areas of success. 2013-2016
 - Introduction to Graduate Education at Northwestern, panel speaker- Spoke to rising juniors & seniors who are interested in pursuing a PhD about graduate student life at Northwestern and key behaviors for success. 2014 & 2016
 - Bridge Program at Roosevelt University, panel speaker- Spoke with undergraduate students at Roosevelt University about how to prepare a successful application to graduate school, and shared my experience as a graduate student. 2012 & 2013
 - Physical Sciences Weekend Academy (PSWA), volunteer- Helped high school girls design an experiment that studied the effects of drugs on breast cancer. Fall 2012

Mentorship

- Cody Schiffer, Sophomore in Weinberg College of Arts & Sciences- Trained Mr. Schiffer in worm handling protocols and assisted him with his summer project studying how zinc impacts successful fertilization in *Caenorhabditis elegans* 2014
- Sandy Cheung, Junior in Weinberg College of Arts & Sciences- Trained Ms. Cheung in cell culture protocols, cell line maintenance and reading primary literature. Provided direction as she began her summer project involving studying the effects of sequestering zinc on cell cycle progression in multiple myeloma. During the academic year, she transitioned to studying how zinc affects oocyte production in *Caenorhabditis elegans* 2013-2014
- Hira Khatri, Niles West High School, Skokie Illinois- Mentored Ms. Khatri in *C. elegans* worm handling and helped her design a project to test the effect of drugs on ALS. 2012

- Samina Kassam, Niles West High School, Skokie Illinois- Mentored Ms. Kassam in *C. elegans* worm handling and assisted with project design on testing chemicals that induce Parkinson's disease symptoms in *C. elegans*.

References

Thomas V. O'Halloran

t-ohalloran@northwestern.edu

847-491-5060

Sadie Wignall

s-wignall@northwestern.edu

(847) 467-0386

Teresa K. Woodruff

tkw@northwestern.edu

312-503-2503